Studies on High Performance Microscale Electrophoresis Using Online Sample Concentration Techniques

Takayuki Kawai

2012

Contents

Chapter 1.

General Introduction

1-1. Capillary Electrophoresis

Electrophoresis is a separation method based on the different migration rate of charged species in an applied dc electric field. Capillary electrophoresis (CE) is an electrophoretic technique using a capillary as a separation field with an application of the high voltage [1–4]. In CE, several advantages are obtained such as high resolution (plate number of up to 1,000,000), short analysis time (a few minutes), and small sample consumption (several nano-liters), compared with high performance liquid chromatography (HPLC) generally employed for many separation analyses. Since HPLC consumes large amount of organic solvents and expensive columns, CE also takes advantages in terms of the cost and damage to the environment.

To analyze various kinds of analytes including non-charged compounds by CE, several separation modes have been developed, such as capillary zone electrophoresis (capillary ZE; CZE), electrokinetic chromatography (EKC) [5–7], affinity CE (ACE) [8,9], capillary gel electrophoresis (capillary GE; CGE) [10–12], isotachophoresis (ITP) [13–15], and capillary isoelectric focusing (capillary IEF; CIEF) [16–18]. Brief explanations are provided in the following paragraphs except for ITP. Detailed explanation of ITP is given in the Section 1-4.

In the most basic separation mode, CZE, analytes are separated in a buffered electrolyte based on the difference in the electrophoretic velocity, which depends on the

charge-to-size ratio of the analytes. It should be noted that cationic, neutral, and anionic compounds can be simultaneously detected due to an electroosmotic flow (EOF), which is derived from the electric double layer generated on the capillary surface. In generally employed fused silica capillary with a negatively charged surface, a fast EOF toward the cathode is generated except in the low pH solution, so that analytes are detected in the order of cationic, neutral, and anionic compounds.

In the most popular EKC technique, micellar EKC (MEKC), ionic surfactants are added into the electrolyte to form micelles as a pseudo-stationary phase (PSP) in the separation field. In the typical MEKC analysis of neutral compounds employing anionic surfactant like sodium dodecyl sulfate (SDS) [5,6], the electrophoretic velocity of the analyte is increased only while incorporated into the micelle. Hence, neutral analytes can be separated based on the difference in the distribution ratio into the micelle. In cyclodextrin (CD) EKC and CD-modified CZE (CDCZE), similarly, chiral compounds are optically resolved according to the difference in the interaction strength between CD and enantiomers [7].

ACE can provide a specific separation by utilizing the affinity interaction between the biological analytes and affinity ligands added in the electrolyte. ACE is also used to measure the binding affinity involving biomolecules such as antigen-antibody, receptor-ligand, complementary nucleic acids, aptamer-ligands, and drug-protein [8]. ACE experiments are usually performed by analyzing the effect of the concentration of the affinity ligands on the electrophoretic mobility of the analytes. From the kinetic plot, the binding constant can be evaluated with the theoretical consideration.

CGE is a quite efficient separation technique for the analyses of biomacromolecules such as proteins and nucleic acids. In CGE, charged analytes

electrophoretically migrate inside the gels, where molecular sieving action retards the migration of the analytes according to the molecular size, resulting in the separation in the order of molecular weight. In the recent CGE analyses, not only gels such as poly(acrylamide) and agarose but also electrolytes containing linear polymers such as hydroxypropyl methylcellulose and poly(ethyleneoxide) are employed to obtain the molecular sieving effects [10–12]. It is well known that the high resolution of CGE has been contributing to the sequencing of DNA especially in the human genome project.

In CIEF, the amphoteric compounds such as peptides and proteins are focused at respective positions corresponding to their isoelectric points (p*I*s). Hence, the CIEF separation is based on the difference not in the electrophoretic velocity, but in the focusing position. In CIEF, carrier ampholytes with different p*I*s are added into the electrolyte to form a pH gradient in the capillary, where analytes are focused at the same pH zone as its p*I*. CIEF is not only a separation mode but also an online sample concentration technique, so that both high sensitivity and high resolution are achieved.

Although the high resolution and rapid analysis time are provided in CE as mentioned above, HPLC is still used as a standard separation method. One reason is that the concentration sensitivity in CE is poor due to the short optical path length and the small sample injection volume. The analytical reproducibility is also poor in terms of the migration time and peak height/area, because the EOF tends to be unstable and the sample injection in the nano-liter range by pressure is difficult to be precisely controlled. Biomolecules including proteins and saccharides are sometimes adsorbed onto the inner surface of the capillary via electrostatic and/or hydrophobic interaction, reducing the analytical performance in CE. These have been the most significant disadvantages of CE, preventing the wide penetration of CE into many analytical fields. In the following

Sections 1-3 and 1-4, some strategies to improve the drawbacks are described.

1-2. Microchip Electrophoresis

Recently, many researchers have been intensively studying the integration of many analytical processes, such as chemical reaction, purification, separation, and detection, into a single microchip, which is called micro total analysis system (μTAS) [19–21]. The microchannel is often fabricated by the "soft" lithography technique [22,23] on a polymer substrate such as poly(dimethylsiloxane) (PDMS) and poly(methyl methacrylate) (PMMA). Compared with glass, silica, and silicon microchips fabricated by the "hard" lithography with an etching process [23], polymer microchips take advantages for the disposable use in terms of the material cost, rapid and easy fabrication, and easy bonding of fabricated lids and flat substrates. By the progress of μTAS, the present analysis with complicated and cumbersome procedures is expected to be rapid, easy, automatic, and low-cost, so that home clinical diagnosis and on-site environmental analysis are expected to be realized.

Electrophoretic separation on the microchannel is called microchip electrophoresis (MCE) and has been studied as a separation part of μTAS [24–26]. Compared with CE, the features of MCE such as shorter analysis time and smaller sample consumption are considered quite suitable for realizing μTAS separation. As in the case of CE, moreover, the similar separation modes, such as ZE, MEKC, ACE, GE, ITP, and IEF, are available for analyzing wide variety of analytes, supporting the versatility of MCE. It should be noted, however, that the separation performance in MCE is usually lower than that in CE due to the shorter effective separation length and that the concentration sensitivity is

also low in MCE due to the same reason mentioned in the Chapter 1-1.

Not to reduce the resolution in MCE with a short effective separation length, a few tens pico-liters of the sample must be injected as a quite narrow band, which is hundreds-fold smaller than in CE. However, such small-volume sample injection by pressure is not as easy as in CE because of the low hydrodynamic resistance from the short channel. Hence, electrokinetic sample injection such as the pinched injection (PI) and gated injection (GI) is mainly employed in MCE [27–30]. In both techniques, a cross-type channel microchip is usually utilized with four reservoirs for BGS (B), sample (S), sample waste (SW), and BGS waste (BW) at the end of each channel (Figures 1-1 and 1-2). Sample injection into the separation channel is performed by precisely controlling the voltage at the four reservoirs.

In the case of PI, the sample is first introduced into the intersection along the flow from S to SW, which is pinched with the two flows from B to SW and from BW to SW (Figure 1-1b). These flows are then changed to those from B to S, from B to BW, and from B to SW to introduce only the intersectional part of the sample solution into the separation channel (Figure 1-1c).

In GI, the sample is introduced into the intersection along the flow from S to SW with preventing the sample influx into the separation channel with the flows from B to BW (Figure 1-2b). The flows are changed for a second to those from S to SW and from S to BW by stopping the flow from B to BW, where a small amount of sample is injected into the separation channel (Figure 1-2c). The flow regulation was then turned back for the separation (Figure 1-2d).

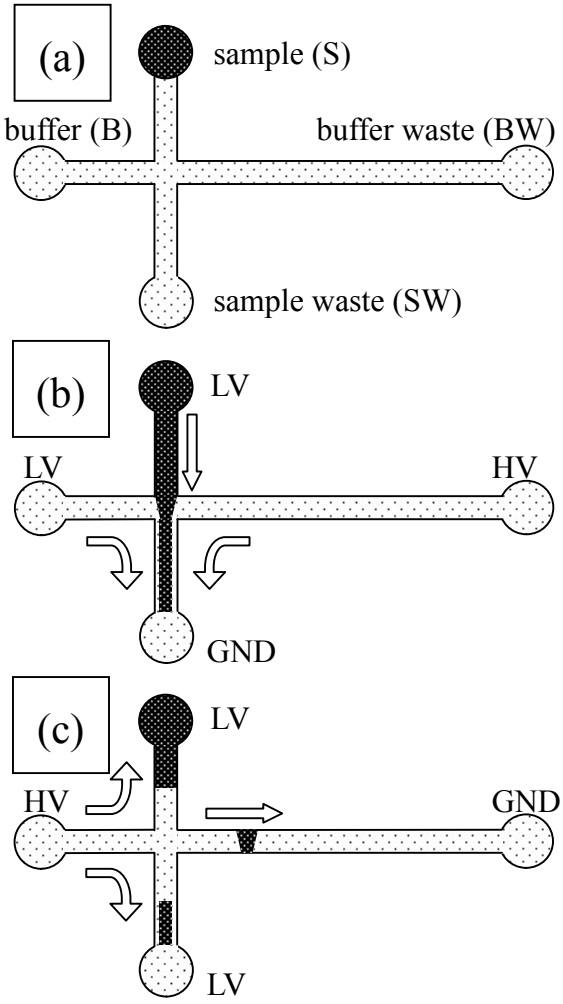

Figure 1-1. Schematic diagram of PI. (a) initial condition, (b) sample loading, and (c) injection and separation of the sample. HV, LV, GND represent high voltage, low voltage, and ground, respectively.

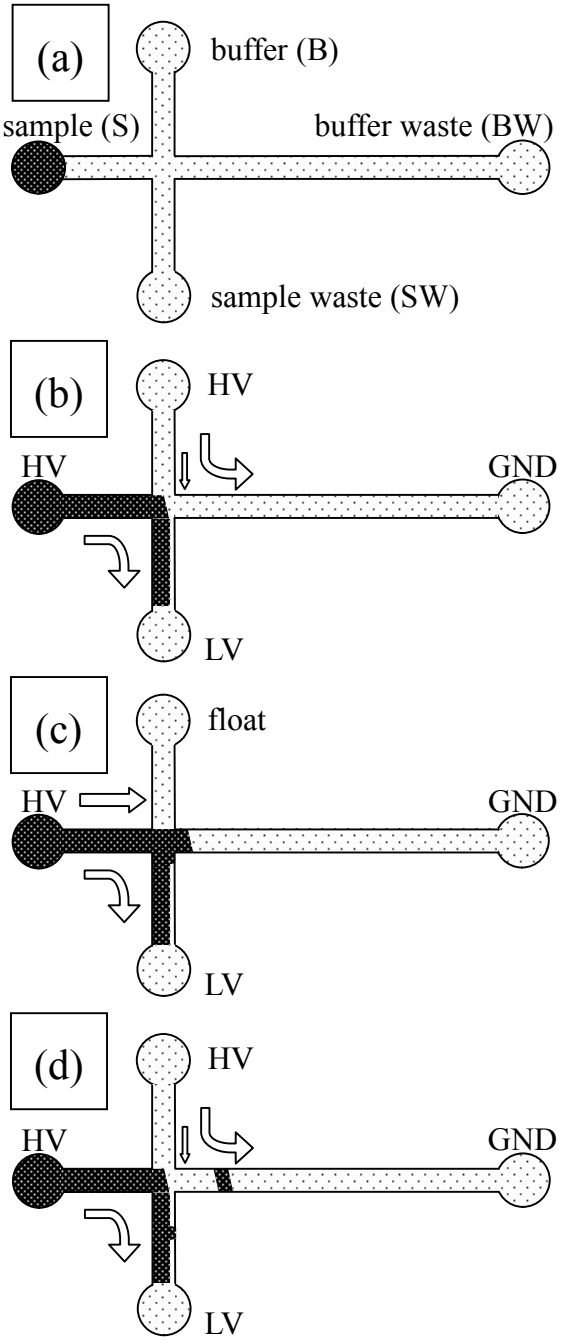

Figure 1-2. Schematic diagram of GI. (a) initial condition, (b) sample loading, (c) sample injection, and (d) sample separation.

Although the small-volume sample introduction is available by PI or GI, there are several disadvantages in MCE: the sample composition can be changed by the electrokinetic injection according to the electrophoretic velocity of the analytes; the complicated voltage regulation over four channel for a few steps is required, which often causes the poor throughput and low analytical reproducibility; extremely small-volume sample injection reduces the concentration sensitivity; biomolecules are easily adsorbed onto the internal channel surface of the polymer microchip via the hydrophobic and/or electrostatic interaction, causing the reduction in the analytical performance; the area-consuming cross-channel geometry is not suitable for high throughput analysis on a highly integrated channel chip. Thus, these drawbacks have been seriously desired to be improved. In the Chapters 1-3 and 1-4, several techniques to improve the analytical performance in MCE are introduced.

In MCE integrated with other functions such as the sample purification, reaction, and concentration, the design of the microchip tends to be complicated. Since these functional sections are connected with each other, it is often difficult to operate each function independently. Thus, the entire microchip must be controlled to avoid the interference of each function as in the case of sample introduction by PI and GI. Hence, the more functions are integrated in a single microchip, the more complicated fluidic control is required, resulting that quite time-consuming and bothersome optimization is needed. Therefore, the operation not only of MCE, but also of any functional parts should be as simple and easy as possible in μTAS.

1-3. Surface Modification Techniques

In CE/MCE, there have been serious problems derived from the unstable surface condition such as less reproducible detection time due to the unstable EOF velocity and band broadening by the sample adsorption onto the inner surface. To improve the drawbacks, in general, the characteristic of the inner surface of the capillary/ microchannel has been changed by the surface modification techniques mainly with functionalized polymers and surfactants [31–33]. There are mainly two types of surface modifiers: hydrophilic neutral one for the stable suppression of EOF and suppression of non-specific sample adsorption by the hydrophobic interaction; charged one for the continuous generation of fast EOF and suppression of the sample adsorption by electrostatic interaction. There are also mainly two techniques to stabilize modifiers on the capillary/microchannel surface, the covalent and non-covalent modifications. Since polymers are covalently linked with the capillary/microchannel surface in the covalent modification, the coating is usually quite robust and durable. However, one or a few chemical reactions are required, so that the coating procedure tend to be complicated and cumbersome. In the non-covalent modification, on the other hand, polymers or surfactants are physically immobilized on the surface. Thus, the modification can be carried out only by flushing the modifier solution in the capillary/microchannel. However, these modifications tend to be easily desorbed due to the weak adsorptivity onto the surface, resulting in the less durability. To improve the poor durability, dynamic coating methods have been often employed, where the modifiers are added into the electrolyte to maintain the coating.

Surface Modification Techniques in CE

In CE, a fused silica capillary is usually employed owing to its optical transparency. The silica surface is negatively charged due to the dissociated silanol groups so that the fast EOF toward cathode is generated except in the low pH solution. The EOF velocity is often unstable especially in the pH around the pK_a of silanol group (~5.0), resulting in less reproducible migration time. Hence, the EOF should be continuously fast or suppressed. Meanwhile, some proteins are known to be adsorbed onto the silica surface with the hydrophobic and/or electrostatic interactions, causing the serious band broadening. To regulate the EOF velocity and to prevent the sample adsorption, the capillary is often modified with neutral polymers/surfactants, such as poly(vinyl alcohol) (PVA) [34,35], linear poly(acrylamide) (LPA) [36,37], poly(vinyl pyrrolidone) [38], and cellulose derivatives [39,40]. Since the zeta potential is reduced by coating the neutral polymers, the EOF is efficiently suppressed. Sample adsorption via the hydrophobic and electrostatic interactions is also minimized according to the hydrophilic and neutral surface. Charged modifiers such as poly(ethyleneimine) (PEI) and dextran sulfate are also employed to provide a stably fast EOF [41,42]. Since the reversed EOF toward the cathode is generated in the capillary coated with cationic modifiers, the analytes are detected in the order of anionic, neutral, and cationic analytes, which takes the advantage in the rapid analysis of anionic compounds. In the charged polymer coatings, the sample adsorption is also prevented due to the electrostatic repulsion between the analytes and the surface so that the surface charges should have the same sign as those of the analytes.

Surface Modification Techniques in MCE

In MCE, various kinds of materials have been utilized for the microchip substrates such as silica, glass, PDMS, PMMA, and so on [22,23]. In terms of required cost and time to produce a chip, polymers have been mainly employed. However, the polymer surface is usually so hydrophobic that many biomolecules are often nonspecifically adsorbed. Since μTAS often focuses on the analysis of biomolecules like proteins and nucleic acids, it is quite important to suppress the sample adsorption in MCE. Compared with silica and glass, moreover, the surface with low and volatile zeta potential generates slower and unstable EOF, resulting in more serious requirements to modify the microchannel surface. In a microchip, the introduction/removal of modifier solutions into/from the complicated channel network are often carried out by a microsyringe via small reservoirs (several millimeters i.d.), which are quite cumbersome and often causing channel clogs by a microdusts and microcrystals. Thus, rapid, simple, and easy methods like the dynamic coating techniques are suitable for disposable microchips, whereas robust and durable coatings like covalent modification are preferable for a repetitive use. As with CE, similar surface modification techniques have been developed in MCE with employing charged modifiers such as PEI [43] and dextran sulfate [44], and neutral modifiers such as PVA [45] and LPA [46]. Although there have been many reports on the surface modification associated with the EOF regulation and suppression of the sample adsorption, the detailed information such as EOF rates against the ionic strength (I) and sample adsorption degree against pH have not often been provided both in CE/MCE. Moreover, the lab-to-lab reproducibility is quite poor in MCE employing the laboratory-built instrument. Thus, it is important to recheck the practical performance of the noted modification technique.

1-4. Online Sample Concentration Techniques

As discussed in the previous sections, the concentration sensitivity in CE/MCE is quite poor. Hence, many researchers have been studying the sensitivity improvement, mainly by using high-sensitive detectors [47,48] and/or online sample concentration techniques [49,50]. In terms of detectors, several sensitive detectors are employed instead of the conventional UV absorption detector such as laser-induced fluorescence (LIF) [51], mass spectrometry (MS) [52,53], electrochemical detector [54,55], and thermal lens microscope [56]. In these detection schemes, however, samples are usually required to be derivatized and/or expensive detector instruments are necessary, increasing in the total analysis time and cost.

On the other hand, several online sample concentration techniques have been developed due to its wide applicability to many detection systems. There are mainly two kinds of online sample concentration techniques: one is electrophoretic concentration regulating the migration rate and the other is non-electrophoretic sample enrichment like solid phase extraction (SPE) [57,58]. In this section, the electrophoretic concentration techniques are mainly introduced due to its simple operation procedure: introduction of sample to the capillary/microchannel as a long plug, followed by the voltage application. Except for ITP and focusing techniques like IEF, fundamentally, the concentration is based on the decrease in the relative migration velocity of the analytes to the concentration boundary between the sample matrix (SM) and background solution (BGS). That is, fast approaching analytes to the boundary are stacked when the moving velocity becomes slow on the boundary (Figure 1-3). Thus, the SM is fundamentally different from the BGS in terms of pH, conductivity, and additives to

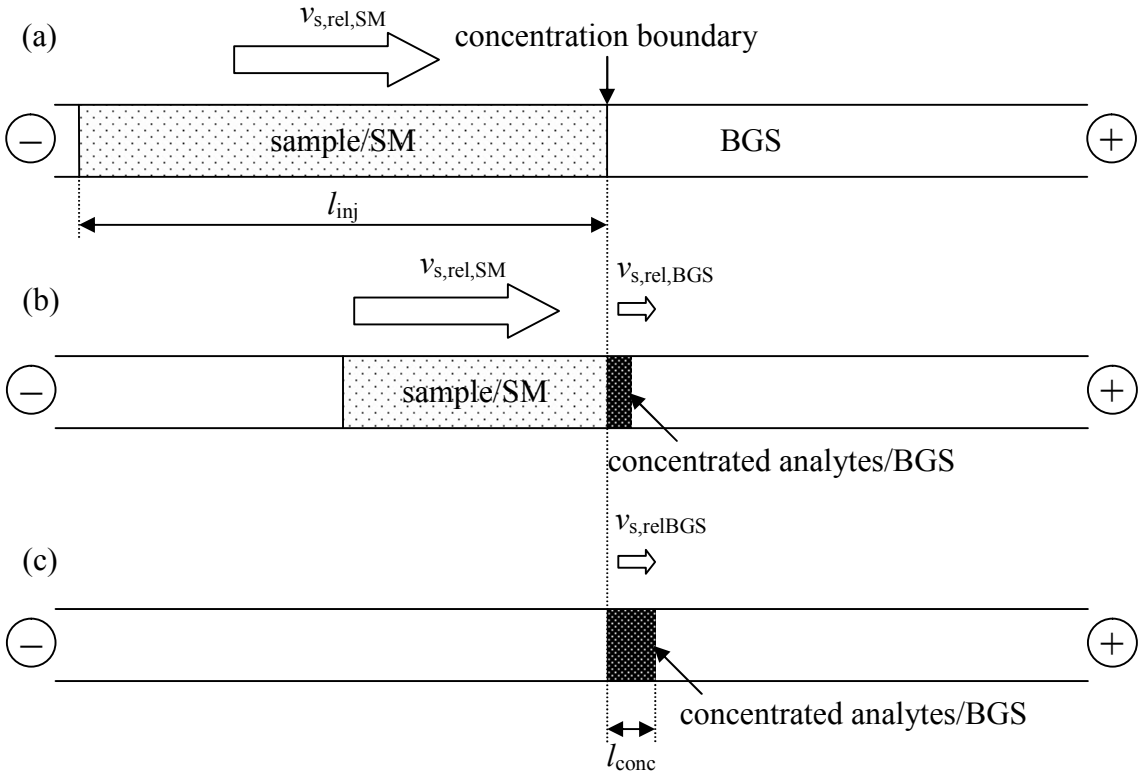

Figure 1-3. Schematic diagram of a general online concentration techniques $v_{s,SM}$ and $v_{s,BGS}$ are the migration velocities of the analyte in the SM and BGS, respectively, relative to the concentration boundary. l_{inj} and l_{conc} represent the lengths of the injected sample plug and concentrated sample plug, respectively.

make the migration rates changed. When the sample diffusion is neglected, the sensitivity enhancement factor (SEF) is determined just by the ratio of the lengths of the injected sample plug and the concentrated sample plug (l_{inj} and l_{conc}, respectively) as the following equation:

$$\mathrm{SEF} = \frac{l_{inj}}{l_{conc}} = \frac{v_{s,rel,SM}}{v_{s,rel,BGS}} \tag{1-1}$$

where $v_{s,rel,SM}$ and $v_{s,rel,BGS}$ are the migration velocities of the analyte in the SM and BGS, respectively, relative to the concentration boundary. Since the boundary and the analyte actually move independently, it is important to simplify the situation by focusing on the relative velocity of the analyte to the boundary when considering online sample

concentration techniques. In the following paragraphs, brief explanations about several online sample concentration techniques are introduced mainly focusing on those in CE except for IEF already explained in the Section 1-1.

Field-amplified Sample Stacking and Related Techniques

One of the most fundamental sample concentration techniques in CE/MCE is field amplified sample stacking (FASS) [59,60] for the analyses of charged analytes. In FASS, an analyte dissolved in a SM with a lower conductivity (σ) is injected as a long plug between the BGS with higher σ in the capillary/microchannel. After the voltage application, the electric field strength (E) in the SM is amplified compared to that in the BGS according to the difference in σ. Hence, the analyte electrophoretically migrates faster in the SM (Figure 1-4a). After penetrating into the BGS with the reduced E, the velocity of the analyte becomes so slow that it is accumulated around the SM/BGS boundary, or concentrated (Figure 1-4b). After the sample concentration, the focused analyte is separated by ZE in the BGS (Figure 1-4c). Since the concentration boundary moves only by the EOF, $v_{s,rel,SM}$ and $v_{s,rel,BGS}$ are equal to $\mu_{ep}E_{SM}$ and $\mu_{ep}E_{BGS}$, respectively, where μ_{ep} is electrophoretic mobility of the analyte. Thus, SEF is theoretically calculated as follows.

$$\mathrm{SEF} = \frac{E_{\mathrm{SM}}}{E_{\mathrm{BGS}}} = \frac{\sigma_{\mathrm{BGS}}}{\sigma_{\mathrm{SM}}} \tag{1-2}$$

It should be noted that large amount of sample can not be injected in FASS. This is because the electrophoretic separation in the BGS becomes quite poor due to reduced E in the BGS by the long SM zone occupying the most of the applied voltage.

There are several kinds of related techniques of FASS such as field amplified sample injection (FASI) [61,62], large-volume sample stacking (LVSS) [63,64], LVSS

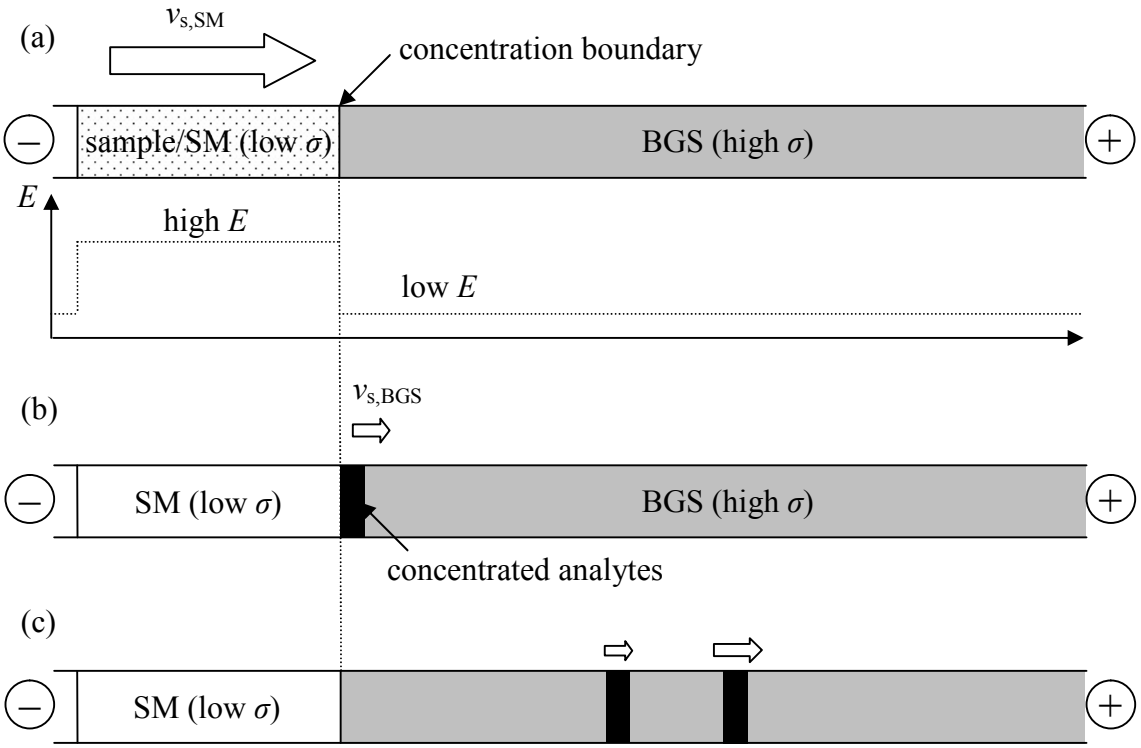

Figure 1-4. Schematic diagram of FASS. (a) fast electrophoretic migration under the high electric field strength in the SM, (b) concentration by the decrease in the migration rate under the low electric field strength in the BGS, (c) sample separation by ZE in the BGS.

with an EOF pump (LVSEP) [65,66], and so on. In FASI, the sample in the μL–mL range can be electrokinetically injected from the inlet vial/reservoir into the capillary/ microchannel with the FASS sample concentration. In LVSS, large-volume sample up to the whole capillary/microchannel volume is injected into the capillary by pressure. Since the introduced long SM zone decreases the effective separation length and the electric field strength in the separation field, the remaining SM must be removed immediately after the concentration. The SM removal has been carried out by a pressure application and EOF regulation. In the case using the EOF as a pump to remove the SM in LVSS, both the sample concentration and SM removal are simultaneously carried out

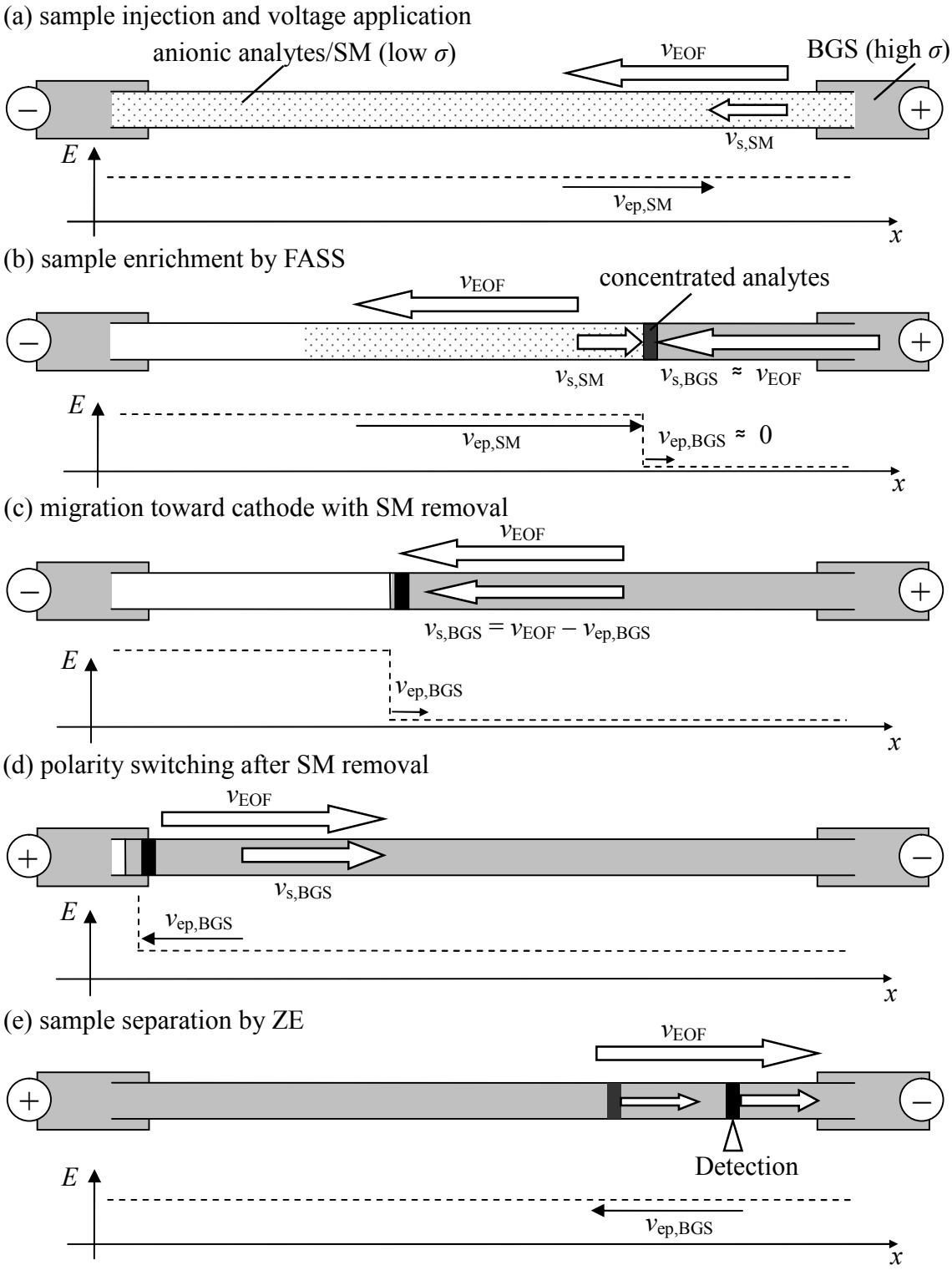

Figure 1-5. LVSS analysis of anionic sample with the polarity switching. v_{ep}, v_{EOF} and v_s mean the electrophoretic velocities of the analyte, the EOF velocity, and apparent velocity of the analyte, respectively.

only by applying a constant voltage. However, the voltage must be often reversed immediately after the concentration because the fast EOF flushes the concentrated analytes out of the inlet capillary end (Figure 1-5). He and Lee reported the elimination of the polarity switching by suppressing the EOF in the separation stage by using an acidic buffer as the BGS [65]. This kind of LVSS technique is named LVSEP, where up to the entirely introduced sample in the capillary is efficiently concentrated and separated. In the FASS-related techniques, however, it should be noted that the conductivity of the sample solution must be low. Hence, sample desalination techniques such as gel filtration and SPE should be coupled with LVSS and LVSEP.

Sweeping and Transient-Trapping

As a driving force to reduce the relative velocity of the analyte, an interaction between the analyte and PSP like an SDS micelle has also been employed. One of the most popular concentration techniques is sweeping developed by Quirino and Terabe [67,68], which can concentrate a hydrophobic neutral analyte on the SM/BGS boundary. In sweeping, an analyte dissolved in the SM without micelle is introduced as a long plug between the BGS containing micelle, where a neutral analyte itself does not migrate electrophoretically (Figure 1-6a). Instead, the charged micelle migrates electrophoretically and penetrates into the SM zone, where the micelle uptakes the analyte with keeping migration velocity because the size of the micelle-analyte complex is almost the same as that of the micelle (Figure 1-6b). From the relative point of view from the SM/BGS boundary, thus, the analyte penetrating in the micelle zone starts migrating with almost the same velocity of the boundary, so that it is concentrated on the boundary (Figure 1-6c). After the concentration, the analyte is separated by MEKC

in the BGS (Figure 1-6d). Since the concentration boundary moves with $v_{ep,mc}$ and the neutral analyte does not electrophoretically migrate in the SM but starts migrating in the BGS with $kv_{ep,mc}/(1+k)$, $v_{s,rel,SM}$ and $v_{s,rel,BGS}$ are equal to $v_{ep,mc}$ and $v_{ep,mc}/(1+k)$, respectively [6], where k is the retention factor of the analyte in the MEKC mode. Thus, the SEF is theoretically calculated as follows.

$$\mathrm{SEF} = k + 1 \tag{1-3}$$

Although up to 5,000-fold sensitivity increases have been reported in the application of

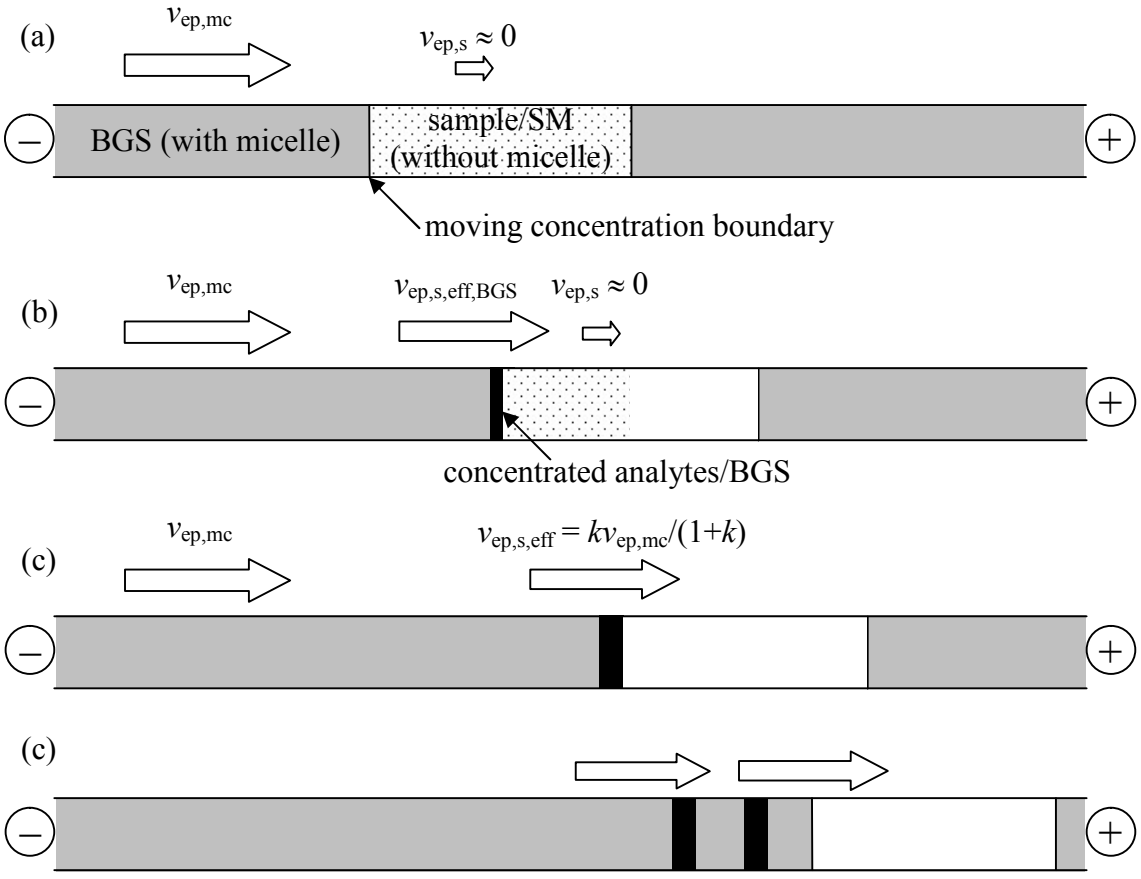

Figure 1-6. Schematic explanation of sweeping employing an anionic micelle. (a) fast migrating micelle penetrating in the sample solution, (b) sample concentration by the increase in the migration rate of the neutral analyte distributed in the micelle, (c) complete sample concentration, and (d) sample separation by MEKC. $v_{ep,mc}$, $v_{ep,s}$, and $v_{ep,s,eff}$ represent the electrophoretic velocities of the micelle and sample, and effective electrophoretic velocity of the analyte in the BGS, respectively.

sweeping [67], the resolution is often reduced because the effective separation length is shortened according to the increase in the sample injection volume. Moreover, it is difficult to combine the sweeping technique with MS detection due to the presence of the surfactant in the BGS.

To realize both high sensitivity and high resolution, Sueyoshi *et al.* have developed transient trapping (tr-trapping) [69] in MCE, where only a short plug of a micelle solution (MCS) is introduced between the sample plug and the BGS without the micelle. The analyte is first focused on the SM/MCS boundary by the "trapping" mechanism similar to that of sweeping. The short MCS plug becomes broadened and the micelle concentration is also decreased due to the molecular diffusion and different migration velocities of the SDS monomer and micelle, resulting in the insufficient retention of the analyte on the concentration boundary. Hence, the focused analyte is "released" in the reverse order of their hydrophobicity according to the gradual decrease in the micelle concentration on the boundary. In addition to the release timing, the hydrophobic analyte is separated by MEKC in the MCS zone with a gradient of micelle concentration, resulting in the higher separation performance than that of conventional MEKC. Actually, up to 580-fold sensitivity improvements and high resolution are achieved within 5 s in the analysis of sulforhodamine B and sulforhodamine 101 in MCE. Moreover, only a short plug of micelle solution is required, that means tr-trapping has a potential to be well coupled with MS detection. In tr-trapping, however, the applicable analytes have been limited to highly hydrophobic ones. Hence, the extension of the applicability to hydrophilic analytes is required in tr-trapping for the practical use.

Dynamic pH Junction, ITP, and Transient ITP

Dynamic pH junction developed by Britz-McKibbin and Chen is a sample stacking technique based on the change of the electrophoretic mobility caused by the pH change [70,71]. In dynamic pH junction, SM/BGS with low/high pH are usually employed, respectively, mainly for the analysis of amphoteric analytes. After the voltage application, the analyte migrating toward cathode penetrates into high pH zone, where it is negatively charged by the pH increase to start migrating fast toward the anode. Hence, the analytes are swept by the dynamically moving pH junction so that the sample band is sharpened. After the concentration, they are separated by ZE in the high pH BGS. Although up to 4,000-fold sensitivity increases have been reported, the resolution is reduced due to the reduction in the effective separation length in exchange for the increase in the sample injection volume.

ITP is known not only as a separation mode in CE/MCE but also as an online sample concentration technique [10–12]. A brief explanation of ITP is provided here in the case of the anion analysis. The sample is injected between leading/terminal electrolytes (LE/TE) containing anionic components with larger/smaller electrophoretic mobility than those of the analytes, respectively. After the voltage application, each analyte migrates with its unique velocity to be separated into spatially continuous zones between LE and TE in the order of faster electrophoretic migration. The electric field strength in each zone is automatically changed according to the Kohlrausch regulating function [72] so that the migration rate of each species becomes identical to keep the electric neutrality of each zone. Since the electric field strength is determined only by the electrophoretic mobility of the analyte, the bandwidth of each zone is automatically changed to the certain sample concentration giving the determined electric field strength.

The lower the original sample concentration is, therefore, the relatively higher concentration efficiency is provided. However, the concentrated analytes are detected as sequential trapezoidal peaks so that the data should be differentiated against time to provide separated peaks. Moreover, the focused bands become quite narrow when the original sample concentration is low, making it difficult to distinguish each zone even after the data processing.

To solve these drawbacks, Foret *et al.* have developed transient ITP (tITP) [73], where samples are separated by ZE after the ITP concentration. In a typical case, the sample and LE are introduced into the capillary as plugs between the TE as the BGS. After the ITP concentration between LE and TE, the TE in front of the LE plug penetrates into the LE zone and then into sample zone, where ITP condition is broken triggering sample separation by ZE. Similarly, there are several ways to introduce the sample, LE, and TE for tITP. It should be noted that tITP is a kind of the partial filling technique as with tr-trapping described in the next section, indicating that the partial application of online concentration techniques has a potential for the development of high performance CE/MCE analysis.

Online Sample Concentration Techniques in MCE

In the case of MCE, several online concentration techniques originally developed in CE have been applied to MCE such as FASS [74], sweeping [75], tITP [76], and IEF [77]. Moreover, several other on-chip concentration techniques have been developed such as SPE [78,79], size filtration [80,81], and electrokinetic trapping [82,83]. In SPE, analytes are adsorbed on the hydrophobic, hydrophilic, or ion exchange columns prepared on the microchip. After the column washing, analytes are eluted and then

introduced into the separation channel for the MCE analysis. Although up to 1,000-fold sensitivity increases have been reported, cumbersome column preparation process is required for SPE. In size filtration, a membrane filter with small pore size, such as silica [80] and poly(acrylamide) gel [81], is prepared on the microchannel. Macromolecules such as DNA and proteins can not pass through the membrane, so that they are concentrated on the membrane. In electrokinetic trapping, a nanochannel is fabricated on the microchip, where the electrical double layer is overlapped to each other. An ionic analyte with the same sign of zeta potential of the nanochannel surface can not penetrate into the overlapped layer, resulting in the concentration around the channel junction. Although efficient sample concentrations have been achieved with these techniques, it should be noted that the channel fabrication and experimental operation usually became much more complicated to regulate the integrated functions precisely. For example, in a tITP analysis, a triple-T channel with five reservoirs was employed with complicated voltage regulation of five channels for four steps [76]. In the case of size filtration, a high-cost and less reproducible membrane filter was employed in a triple-T channel, where the voltage regulation was also complicated as six-channels for three-steps [82].

Although many online concentration techniques have been developed in CE/MCE with good sensitivity increases as mentioned above, in most cases there are two serious disadvantages, reduction in the separation performance and complication of experimental procedure. Hence, simple-operation and high-performance online concentration techniques like LVSEP are required in CE/MCE. In MCE, moreover, the complication of channel geometry and fluidic control is also the major disadvantage of online sample concentration techniques. As with CE, thus, it is quite important and invaluable to develop simple-operation and high-performance online concentration

techniques in a simple microchannel network.

1-5. Purpose and Contents of this Thesis

As discussed in the previous sections, many researchers have reported the improvement of the sensitivity and reproducibility in CE/MCE by employing online sample concentration and surface modification techniques, respectively. However, CE/MCE still has not acquired the position of the standard analytical method. In terms of the online sample concentration, these sensitivity improvements were usually carried out with sacrificing the separation performance and simplicity of analytical procedure. The loss of analytical performance and cumbersome optimization of experimental conditions have been preventing many analysts from employing CE/MCE, resulting in the persistence for the conventional techniques like HPLC with low performance and high cost. Hence, it should be quite invaluable to develop novel CE/MCE techniques realizing high resolution, high sensitivity, and simple experimental procedure simultaneously. In this thesis, the author mainly focuses on LVSEP with high sensitivity, high resolution, and simple experimental procedure. Since the sample injection into the entire capacity/microchannel is allowed without loss of resolution, no optimization of sample injection condition is required. Moreover the voltage control, a constant voltage application, is quite simple, so that the total analytical procedure is expected to be quite simple. Thus, the author expected the LVSEP-CE/MCE to be the next-generation electrophoresis. In this thesis, applications of LVSEP to CE/MCE are first investigated with a deep theoretical consideration. Application of LVSEP to several separation modes and extension of target analytes to cations were then carried out to extend the

applicability of LVSEP to many analytical situations. The author also focused on tr-trapping. Although tr-trapping requires a cumbersome partial-filling procedure, the exceeding separation performance and the high-speed analysis are expected to extend the maximum performance of CE/MCE. Thus, a high performance analysis employing tr-trapping was also investigated as a progressive approach for the ultra performance CE/MCE.

In the Chapter 2, the application of LVSEP to the MCE analysis of oligosaccharides is investigated. In the conventional PI-MCE, there are several disadvantages such as complicated voltage regulation (four channels for two steps), less integratable cross-channel geometry, and low concentration sensitivity. Hence, LVSEP is focused on to overcome the drawbacks. LVSEP has been first developed in CE, where the whole capillary of the sample is well concentrated and separated with good resolution without polarity switching. In the conventional LVSEP-CE analysis, an acidic buffer is employed to suppress the EOF of bare fused silica capillary in the separation stage. To confirm the versatile applicability, however, electrolytes with a wide pH range should be usable in the separation stage and the sample adsorption should be suppressed for the analysis of biomolecules. Hence, the development of LVSEP using a PVA-coated microchannel was investigated in this chapter. First, the mechanism of LVSEP using an EOF-suppressed capillary/microchannel was studied because it has never been clarified. Second, the separation performance was considered both theoretically and experimentally in terms of the maintained effective separation length, or the inversion position of the sample migration. Finally, the LVSEP-MCE analysis of oligosaccharides including glycans from a glycoprotein was carried out to demonstrate its high performance.

In the Chapter 3, the application of LVSEP to the CE analysis of oligosaccharides is studied. In terms of the injectable sample volume and effective separation length, LVSEP-CE with longer column is superior to LVSEP-MCE so that higher sensitivity and resolution are expected to be provided. Although there have been several reports on LVSEP-CE, they lack in the point of view for the real sample analysis such as the conductivity of the SM, the maintained effective separation length, and the starting time of separation stage. To develop high performance analytical system for oligosaccharide analysis in CE, which is applicable for a real sample analysis, the property of LVSEP in CE was investigated in detail, where the author employs a PVA-coated capillary with a sufficient suppression of the EOF and sample adsorption. Finally, the LVSEP-CE analysis of oligosaccharides including glycans from three glycoproteins was carried out.

In the Chapter 4, the application of LVSEP to separation modes other than CZE is described. For various kinds of analytes, the applicability of LVSEP to most separation modes should be confirmed. Although the separation performance might be decreased in applying LVSEP, there has been no report considering the resolution in LVSEP coupled with separation modes other than CZE. To study the effect of the separation modes on resolution, therefore, LVSEP was coupled with three chiral separation modes CDCZE, CDEKC, and CD-modified MEKC (CDMEKC) as the model cases. Of course, the development of high-performance chiral analysis in CE is quite valuable for drug screening, metabolomic research, and clinical diagnosis. As in the chapter 3, the practical use of LVSEP-CDCZE in a PVA-coated capillary was also investigated by employing a C_{18} SPE column to remove unnecessary salts in the SM. Finally, a drug component spiked in urine was analyzed in LVSEP-CDCZE to demonstrate the practical utility of LVSEP-CDCZE in a clinical diagnosis.

In the Chapter 5, the applicability of LVSEP-CZE is extended to cationic analytes. Conventionally, the LVSEP has been applicable only to the analyses of anionic species because cationic analytes are flushed out by the EOF from the cathodic capillary end. To prevent the sample efflux, it is required to reverse the EOF. In this study, inner surface of the capillary was modified with slightly positive-charged polymers to obtain the EOF basically suppressed but enhanced only in the low *I* SM. The EOF property was investigated in the three capillaries: one physically coated with polymer mixture of PVA and poly(allylamine) with thermal stabilization; one covalently modified with a copolymer synthesized from 3-(methacryloylamino)propyltrimethylammonium chloride and acrylamide; and one physically coated with dimethyldioctadecylammonium bromide and polyoxyethylene stearate. Finally, the LVSEP-CZE analysis of aromatic amines was carried out to investigate the analytical performance.

In the final Chapter 6, the application of tr-trapping for the analysis of hydrophilic amino acids is described. Tr-trapping has been originally developed as a high performance analytical tool mainly for highly hydrophobic compounds. Hence, the hydrophilic amino acids were labeled with a hydrophobic fluorophore to be well concentrated and separated in tr-trapping process. Optimization of the labeling reagent and analytical conditions such as the injection volume of micelle solution and sample solution was carried out in the tr-trapping-CE analysis of valine, isoleucine, leucine, and phenylalanine. Finally, the tr-trapping-MCE analysis of lysine and histidine was also performed to achieve rapid, highly sensitive, and high-resolution analysis.

1-6. References

[1] Monnig C. A.; Kennedy, R. T. *Anal. Chem.* **1994**, *66*, 280–314.

[2] Karger, B. L.; Cohen, A. S.; Guttman, A. *J. Chromatogr.* **1989**, *492*, 585–614.

[3] Watzig, H.; Degenhardt, M.; Kunkel, A. *Electrophoresis* **1998**, *19*, 2695–2752.

[4] Douglas A. S.; James, F. H.; Stanley, R. G. *Principles of Instrumental Analysis*, **2007**, *6*, 867–884.

[5] Terabe, S.; Otsuka, K.; Ichikawa, K.; Tsuchiya, A.; Ando, T. *Anal. Chem.* **1984**, *56*, 111–113.

[6] Terabe, S.; Otsuka, K.; Ando, T. *Anal. Chem.* **1985**, *57*, 834–841.

[7] Jakubetz, H.; Juza, M.; Schurig, V. *Electrophoresis* **1997**, *18*, 897–904.

[8] Schou, C.; Heegaard, H. H. N. *Electrophoresis* **2006**, *27*, 44–59.

[9] Liu, X.; Dahdouh, F.; Salgado, M.; Gomez, A. F. *J. Pharm. Sci.* **2009**, *98*, 394–410.

[10] Dolník, V. *J. Biochem. Biophys. Meth* **1999**, *41*, 103–119.

[11] Hu, S.; Michels, A. D.; Fazal, A. M.; Ratisoontorn, C.; Cunningham, L. M.; Dovichi, J. N. *Anal. Chem.* **2004**, *76*, 4044–4049.

[12] Righetti, G. P.; Gelfi, C.; D'Acunto, R. M. *Electrophoresis* **2002**, *23*, 1361–1374.

[13] Timerbaev, R. A.; Hirokawa, T. *Electrophoresis* **2006**, *27*, 323–340.

[14] Gebauer, P.; Boček, P. *Electrophoresis* **2002**, *23*, 3858–3864.

[15] Gebauer, P.; Malá, Z.; Boček, P. *Electrophoresis* **2011**, *32*, 83–89.

[16] Rodriguez-Diaz, R.; Wehr, T.; Zhu, M. *Electrophoresis* **1997**, *18*, 2134–2144.

[17] Kilár, F. *Electrophoresis* **2003**, *24*, 3908–3916.

[18] Silvertand, L. H. H.; Toraño, S. J.; Bennekom, W. P.; Jong, G. J. *J. Chromatogr. A* **2008**, *1204*, 157–170.

[19] Reyes, R. D.; Iossifidis, D.; Auroux, P.-A.; Manz, A. *Anal. Chem.* **2002**, *74*, 2623–2636.

[20] Auroux, P.-A.; Iossifidis, D.; Reyes, R. D.; Manz, A. *Anal. Chem.* **2002**, *74*, 2637–2652.

[21] West, J.; Becker, M.; Tombrink, S.; Manz, A. *Anal. Chem.* **2008,** *80*, 4403–4419.

[22] McDonald, C. J.; Duffy, C. D.; Anderson, R. J.; Chiu, T. D.; Wu, H.; Schueller, J. A. O.; Whitesides, M. G. *Electrophoresis* **2000**, *21*, 27–40.

[23] Ziaie, B.; Baldi, A.; Lei, M.; Gu, Y.; Siegel, A. R. *Adv. Drug Del. Rev.* **2004**, *56*, 145–172.

[24] Dolník, V.; Liu, S.; Jovanovich, S. *Electrophoresis* **2000**, *21*, 41–54.

[25] Bruin, J. M. G. *Electrophoresis* **2000**, *21*, 3931–3951.

[26] Pumera, M. *Electrophoresis* **2006**, *27*, 244–256.

[27] Jacobson, S. C.; Hergenroder, R.; Koutny, L. B.; Warmack, R. J.; Ramsey, J. M. *Anal. Chem.* **1994**, *66*, 1107–1113.

[28] Fu, L.-M.: Yang, R.-J. Lee, G.-B. *Anal. Chem.* **2003**, *75*, 1905–1910.

[29] Harrison, D. J.; Manz, A.; Fan, Z.; Lüdi, H.; Widmers, H. M. *Anal. Chem.* **1992**, *64*, 1926–1932.

[30] Manz, A.; Harrison, J. D.; Verpoorte, M. J. E.; Fettinger, C. J.; Paulus, A.; Lüdi, H.; Widmer, M. H. *J. Chromatogr. A* **1992**, *593*, 253–258.

[31] Hovarth, J.; Dolník, V. *Electrophoresis* **2001**, *22*, 644–655.

[32] Dolník, V. *Electrophoresis* **2004**, *25*, 3589–3601.

[33] Zhou, J.; Ellis, V. A.; Voelcker, H. N. *Electrophoresis* **2010**, *31*, 2–16.

[34] Gllges, M.; Kleemlss, M.H.; Schomburg, G. *Anal. Chem.* **1994**, *66*, 2038–2046.

[35] Belder, D.; Deege, A.; Husmann, H.; Kohler, F.; Ludwig, M. *Electrophoresis* **2001**,

22, 3813–3818.

[36] Cobb, A. K.; Dolník, V.; Novotny, M. *Anal. Chem.* **1990**, *62*, 2478–2483.

[37] Gelfi, C.; Curcio, M.; Righetti, G. P.; Sebastiano, R.; Citterio, A.; Ahmadzadeh, H.; Dovichi, J. N. *Electrophoresis* **1998**, *19*, 1677–1682.

[38] Srinivasan, K.; Pohl, C.; Avdalovic, N. *Anal. Chem.* **1997**, *69*, 2798–2805.

[39] Busch, M. H. A.; Kraak, J. C.; Poppe, H. *J. Chromatogr. A* **1995**, *695*, 287–296.

[40] Huang, M.; Plocek, J.; Novotny, V. M. *Electrophoresis*, **1995**, *16*, 396–401.

[41] Erim, F. B.; Cifuentes, A.; Poppe, H.; Kraak, C. J. *J. Chromatogr A* **1995**, *708*, 356–361.

[42] Katayama, H.; Ishihama, Y.; Asakawa, N. *Anal. Chem.* **1998**, *70*, 5272–5277.

[43] Kitagawa, F.; Kubota, K.; Sueyoshi, K.; Otsuka, K. *Sci. Technol. Adv. Mater.* **2006**, *7*, 558–565.

[44] Liu, Y.; Fanguy, J. C.; Bledsoe, J. M.; Henry, C. S. *Anal. Chem.* **2000**, *72*, 5939–5944.

[45] Wu. D.; Luo, Y.; Zhou, X.; Dai, Z.; Lin, B. *Electrophoresis* **2005**, 2*6*, 211–218.

[46] Xiao, D.; Le, V. T.; Wirth, J. M. *Anal. Chem.* **2004**, *76*, 2055–2061.

[47] Swinney, K.; Bornhop, J. D. *Electrophoresis*, **2000**, *21*, 1239–1250.

[48] Mogensen, B. K.; Klank, H.; Kutter, P. J. *Electrophoresis*, **2004**, *25*, 3498–3512.

[49] Simpson Jr. L. S.; Quirino, P. J.; Terabe, S. *J. Chromatogr. A* **2008**, *1184*, 504–541.

[50] Sueyoshi, K.; Kitagawa, F.; Otsuka, K. *J. Sep. Sci*. **2008**, *31*, 2650–2666.

[51] Wu, S.; Dovichi, J. N. *J. Chromatogr.* **1989**, *480*, 141–155.

[52] Tsuji, K.; Baczynskyj, L.; Bronson, E. G. *Anal. Chem.* **1992**, *64*, 1864–1870.

[53] Kitagawa, F.; Otsuka, K. *J. Pharm. Biomed. Anal.* **2011**, *55*, 668–678.

[54] Baldwin, P. R. *Electrophoresis*, **2000**, *21*, 4017–4028.

[55] Lacher, A. N.; Garrison, E. K.; Martin, R. S.; Lunte, M. S. *Electrophoresis*, **2001**, *22*, 2526–2536.

[56] Kitagawa, F.; Tsuneka, T.; Akimoto, Y.; Sueyoshi, K.; Uchiyama, K.; Hattori, A.; Otsuka, K. *J. Chromatogr. A* **2006**, *1106*, 36–42.

[57] Strausbauch, M. A.; Xu, S. J.; Ferguson, J. E.; Nunez, M. E.; Machacek, D.; Lawson, G. M.; Wettsteina, J. P.; Landers, P. J. *J. Chromatogr. A* **1995**, *717*, 279–291.

[58] Hutchinson, P. J.; Macka, M.; Avdalovic, N.; Haddad, R. P. *J. Chromatogr. A* **2006**, *1106*, 43–51.

[59] Burgi, S. D.; Chien, R.-L. *Anal. Biochem.* **1992**, *202*, 306–309.

[60] Chien, R.-L.; Helmer, J. *Anal. Chem.* **1991**, *63*, 1354–1361.

[61] Chien, R.-L.; Burgi, S. D. *J. Chromatogr.* **1991**, *559*, 141–152.

[62] Monton, M.R.N.; Terabe, S. *J. Chromatogr. A* **2004**, *1032*, 203–211.

[63] Albert, M.; Debusschere, L.; Demesmay, C.; Rocca, J. L. *J. Chromatogr A* **1997,** *757*, 281–289.

[64] Zhu, L.; Lee, H. K. *Anal. Chem.* **2001**, *73*, 3065–3072.

[65] He, Y.; Lee, H. K. *Anal. Chem.* **1999**, *71*, 995–1001.

[66] Chun, M.-S.; Chung, D. S. *Anal. Chim. Acta* **2003**, *491*, 173–179.

[67] Quirino, J. P.; Terabe, S. *Science* **1998**, *282*, 465–468.

[68] Quirino, J. P.; Terabe, S. *Anal. Chem.* **1999**, *71*, 1638–1644.

[69] Sueyoshi, K.; Kitagawa, F.; Otsuka, K. *Anal. Chem.* **2008**, *80*, 1255–1262.

[70] Britz-McKibbin, P.; Chen, D. Y. D. *Anal. Chem.* **2000**, *72*, 1242–1252.

[71] Britz-McKibbin, P.; Bebault, M. G.; Chen D. Y. D. *Anal. Chem.* **2000**, *72*,

1729–1735.

[72] Hruška V.; Gaš, B. *Electrophoresis* **2007**, *28*, 3–14.

[73] Foret, F.; Szoko, E.; Karger, B. L. *J. Chromatogr.* **1992**, *608*, 3–12.

[74] Jacobson, S. C.; Ramsey, J. M. *Electrophoresis* **1995**, *16*, 481–486.

[75] Sera, Y.; Matsubara, N.; Otsuka, K.; Terabe, S. *Electrophoresis* **2001**, *22*, 3509–3513.

[76] Mohamadi, M. R.; Kaji, N.; Tokeshi, M.; Baba, Y. *Anal. Chem.* **2007**, *79*, 3667−3672.

[77] Hofmann, O.; Che, D.; Cruickshank, K. A.; Müller, U. R. *Anal. Chem.* **1999**, *71*, 678–686.

[78] Oleschuk, R. D.; Shultz-Lockyear, L. L.; Ning, Y.; Harrison, D. J. *Anal. Chem.* **2000**, *72*, 585 – 590.

[79] Ramsey, J. D.; Collins, G. E. *Anal. Chem.* **2005**, *77*, 6664–6670.

[80] Khandurina, J.; Jacobson, S. C.; Waters, L. C.; Foote, R. S.; Ramsey, J. M. *Anal. Chem.* **1999**, *71*, 1815–1819.

[81] Hatch, V. A.; Herr, E. A.; Throckmorton, J. D.; Brennan, S. J.; Singh, K. A. *Anal. Chem.* **2006,** *78*, 4976–4984.

[82] Dai, J.; Ito, T.; Sun, L.; Crooks, R. M. *J. Am. Chem. Soc.* **2003**, *125*, 13026–13027.

[83] Kim, S. M.; Burns, M. A.; Hasselbrink, E. F. *Anal. Chem.* **2006**, *78*, 4779–4785.

Chapter 2.

Microchip Electrophoresis of Oligosaccharides Using Large-volume Sample Stacking with an Electroosmotic Flow Pump in a Single Channel

2-1. Introduction

Electrophoretic analysis on a microfluidic device is called microchip electrophoresis (MCE) [1], which allows high-speed separation within a few minutes. Although conventional MCE analysis using the pinched injection (PI) technique [2] exhibits high separation performance, there is a serious problem concerning the low concentration sensitivity. To overcome the sensitivity problem, several online concentration techniques have been applied to MCE [3–7]. Although the sensitivity can be improved, these techniques often require a complicated voltage program (>four channels for >two steps) for fluidic control [3,4,7]. Since the large-volume sample is injected into the separation channel for the concentration, furthermore, the effective separation length is often reduced [3,5,6], resulting in poor reproducibility, low resolution and an inconvenient experimental procedure. Thus, the introduction of a novel approach to provide both high sensitivity and high resolution with a simple procedure has been strongly desired in MCE.

To realize the highly sensitive analysis with a simple injection scheme in MCE, the author focused on large-volume sample stacking with an electroosmotic flow pump (LVSEP) [8,9], which is an online sample concentration technique developed in

capillary electrophoresis (CE). LVSEP is one of the variations of the field-amplified sample stacking techniques [10] and exhibits efficient concentration and separation performance. A typical protocol of LVSEP is very simple: filling a bare fused silica capillary exhaustively with a low ionic strength sample solution (e.g., anionic analytes dissolved in deionized water), followed by applying a constant voltage between the inlet and outlet reservoirs filled with a high ionic strength background solution (BGS) containing acids. In the first concentration stage, anionic analytes are stacked around the sample/BGS boundary and move toward the cathode by the electroosmotic flow (EOF). In the second separation stage, the removal of the sample matrix (SM) and the introduction of the BGS into the capillary suppress the EOF, so that the analytes start to migrate toward the anode. Finally, they are separated according to the principle of capillary zone electrophoresis (CZE). In applying the LVSEP technique to MCE, therefore, only a sample injection throughout a "single" straight channel and application of a constant voltage between both ends of the single channel (two channels for one step) are required as with the conventional LVSEP-CZE, simplifying the experimental procedure and improving the detection sensitivity in MCE. Of course, the analysis time is dramatically reduced in MCE compared to conventional LVSEP-CZE. A highly integrated-array channel chip for LVSEP-MCE can be easily fabricated due to the straight channel geometry. Furthermore, the flexibility of the channel designs in MCE is useful in combining the LVSEP analysis with various analytical processes such as online enzymatic reaction [11], sample derivatization [12], two-dimensional separation [13], and so on. These characteristics of LVSEP-MCE are quite suitable for realizing the high-throughput, practical and integrated analysis systems.

The main aim of this study is the development of the LVSEP-MCZE technique to

analyze biomolecules. To suppress the sample adsorption and EOF, the microchannel surface was coated with poly(vinyl alcohol) (PVA). Although the author found that LVSEP could be applied to the PVA-coated microchannel as LVSEP-CZE reported by Chun and Chung [9], the mechanism of the SM removal by an "EOF pump" in an "EOF-suppressed" capillary/microchannel has not been clarified. Hence, the author investigated the mechanism based on EOF enhancement by low ionic strength SM (see the Appendix). Furthermore, a theoretical model of LVSEP in the coated microchannel is proposed to obtain important electrophoretic parameters such as the bandwidth and the inversion position of the concentrated analytes. To verify the proposed theoretical model, fluorescence imaging of LVSEP-MCZE processes was performed in a PVA-coated straight microchannel on a poly(dimethylsiloxane) (PDMS) substrate. Finally, LVSEP-MCZE was applied to the analyses of oligosaccharides. Oligosaccharides are suitable for the LVSEP analysis since they are usually derivatized with 8-aminopyrene-1,3,6-trisulfonic acid (APTS), which possesses three anionic groups, to obtain higher sensitivity in the CZE/MCZE analyses. Of course, oligosaccharides play very important roles in the living body such as cell recognition, cell communication, and cell proliferation [14], so it is very important to develop rapid and highly sensitive analytical methods. As far as the author knows, only a few reports on online concentration of oligosaccharides in CZE/MCZE have appeared. Kamoda *et al*. reported online concentration by head-column field-amplified sample stacking, where the sensitivity enhancements were limited to at most 360-fold [15–18]. Therefore, the development of the highly efficient concentration and high-throughput separation system on a microchip should contribute to the progress of glycomic research. In this paper, the author reports the LVSEP-MCZE analyses of the linear glucose ladder and

dendritic glycans released from a glycoprotein.

2-2. Experimental Section

Materials and Chemicals

Acetic acid, 2-[4-(2-hydroxyethyl)-1-pyperazinyl]ethanesulfonic acid (HEPES), and fluorescein were purchased from Nacalai Tesque (Kyoto, Japan), sodium cyanoborohydride, APTS, tetrahydrofuran (THF), bovine ribonuclease B and PVA (M_w = 80,000, 88% hydrolyzed) were purchased from Sigma-Aldrich (St. Louis, MO, USA), thiourea was purchased from Wako (Osaka, Japan), PDMS was purchased from Dow Corning Toray (Tokyo, Japan), the glucose ladder was purchased from J-Oil mills (Tokyo, Japan), peptide-*N*-glycosidase F (PNGase F) was purchased from Prozyme (San Leandro, CA, USA), and SU8-50 was purchased from MicroChem (Newton, MA, USA). Silicon wafers were supplied from Shin-etsu Chemical (Tokyo, Japan). All solutions were prepared with deionized water purified by using a Direct-Q system (Nihon Millipore, Japan) and filtered through a 0.45 μm pore membrane filter prior to use.

Apparatus

MCE experiments were performed on a fluorescence microscope (IX71, Olympus, Tokyo, Japan) as described previously [19]. Laser-induced fluorescence (LIF) detection was carried out at excitation and detection wavelengths of 488 and 520 nm, respectively. For the fluorescence imaging measurement, a 100 mW mercury lamp and a CCD camera (JK-TU53H, Toshiba, Tokyo, Japan) were used as the light source and detector,

respectively. The observed images were analyzed with Image J software.

Microchip Fabrication

A PDMS microfluidic device was fabricated by the conventional soft lithography technique [20]. The straight channel microchip had a single straight channel (50 μm width × 50 μm depth) with a total separation channel length of 80 or 40 mm. The cross-channel microchip consisted of three 5 mm long channels and a 40 mm long separation channel (50 μm width × 50 μm depth). The surface of the microchannel plate and a PDMS lid were activated by O_2 plasma. The activation was performed at a 75 W plasma power and a 15 mL/s oxygen flow for 10 s. Finally, direct bonding between the activated substrates was carried out.

Channel Coating

A PDMS microchip and fused silica capillary were coated with PVA [21]. In the MCZE analysis, 2% PVA was introduced into the microchannel immediately after the fabrication, and then left for 15 min. The solution was removed and the microchip was heated at 110 °C for 15 min. The injection of the PVA solution and the heating of the microchip were repeated three times, where the temperature at the third heating was 140 °C.

Sample Preparation

Oligosaccharides were released from bovine ribonuclease B with PNGase F enzyme using the methods reported previously [22]. For fluorescence labeling, oligosaccharides released from 200 μg ribonuclease B or 80 μg glucose ladder were

mixed with 5 μL of 0.1 M APTS in 15% acetic acid and 10 μL of 0.5 M $NaCNBH_3$ in THF. The mixture was kept at 55 °C for 2 h, followed by dilution with water to 50 μL. In the analysis of oligosaccharides from bovine ribonuclease B, the solution was desalted with a Centri-Spin-10 column (Princeton Separations, NJ, USA) to remove excess APTS and reagents used in the enzymatic reaction. In LVSEP-MCZE, these samples were diluted 2000-fold with water, whereas in the conventional MCZE using the PI technique (PI-MCZE), the samples were diluted 10-fold with the BGS.

Procedure

In determining the EOF velocity in the PVA-coated channel, an 80 mm long channel microchip was employed. The outlet reservoir and the channel were filled with 0.1–25 mM BGS, while the inlet reservoir was filled with 1 μM fluorescein dissolved in the BGS. The applied voltage and the temperature were set at 800 V and 25 °C, respectively. The moving process of the fluorescein/BGS boundary was traced by fluorescence imaging to calculate the apparent electrophoretic mobility. By subtracting the electrophoretic mobility of fluorescein determined in the CZE experiments, the EOF velocity in the coated channel was determined.

In LVSEP-MCZE, 40 mm and 80 mm long channel were employed in the fluorescence imaging of the concentration processes and the separation of oligosaccharides, respectively. A sample solution was introduced into the entire channel by using a syringe manually. The two reservoirs were filled with 3 μL of a 10 or 25 mM HEPES buffer. The electric field strength of 500 V/cm was applied through two platinum electrodes immersed in the two reservoirs. In the separation of oligosaccharides, the analytes were detected by the LIF scheme at the point of 5 mm

from the anodic channel end.

In the conventional PI-MCZE, a cross-channel PDMS microchip with a total separation length of 40 mm was used. There were four reservoirs at the end of each channel. Three reservoirs connected to the loading channel were for the BGS (B), sample (S), and sample waste (SW), whereas that to the separation channel was for the BGS waste (BW). In the first step of the PI, the applied voltages were 1.5, 1.5, and 2.5 kV at the S, B, and SW, respectively, while the BW was grounded. After 30 s, the voltage was switched to the separation mode with 1.0, 0.0, 1.0, and 2.5 kV for the S, B, SW, and BW, respectively. The detection was carried out at a distance of 5 mm from the BW reservoir.

2-3. Results and Discussion

Theoretical Model

In the conventional LVSEP, a large volume of the sample solution containing anionic analytes prepared in deionized water is introduced into the bare fused silica capillary, and then the separation voltage is applied to both ends of the capillary immersed in the acidic BGS. Since most of the capillary is filled with the low-ionic strength sample, a faster EOF removes the SM to the cathodic end. After the acidic BGS is introduced into most of the capillary, the EOF is suppressed by the protonation of silanol groups on the inner surface of the capillary. As the electrophoretic mobility of the anionic analyte becomes higher than the electroosmotic mobility, the stacked analytes migrate to the anode. In the conventional LVSEP technique, therefore, the EOF is temporarily suppressed only in the acidic BGS zone.

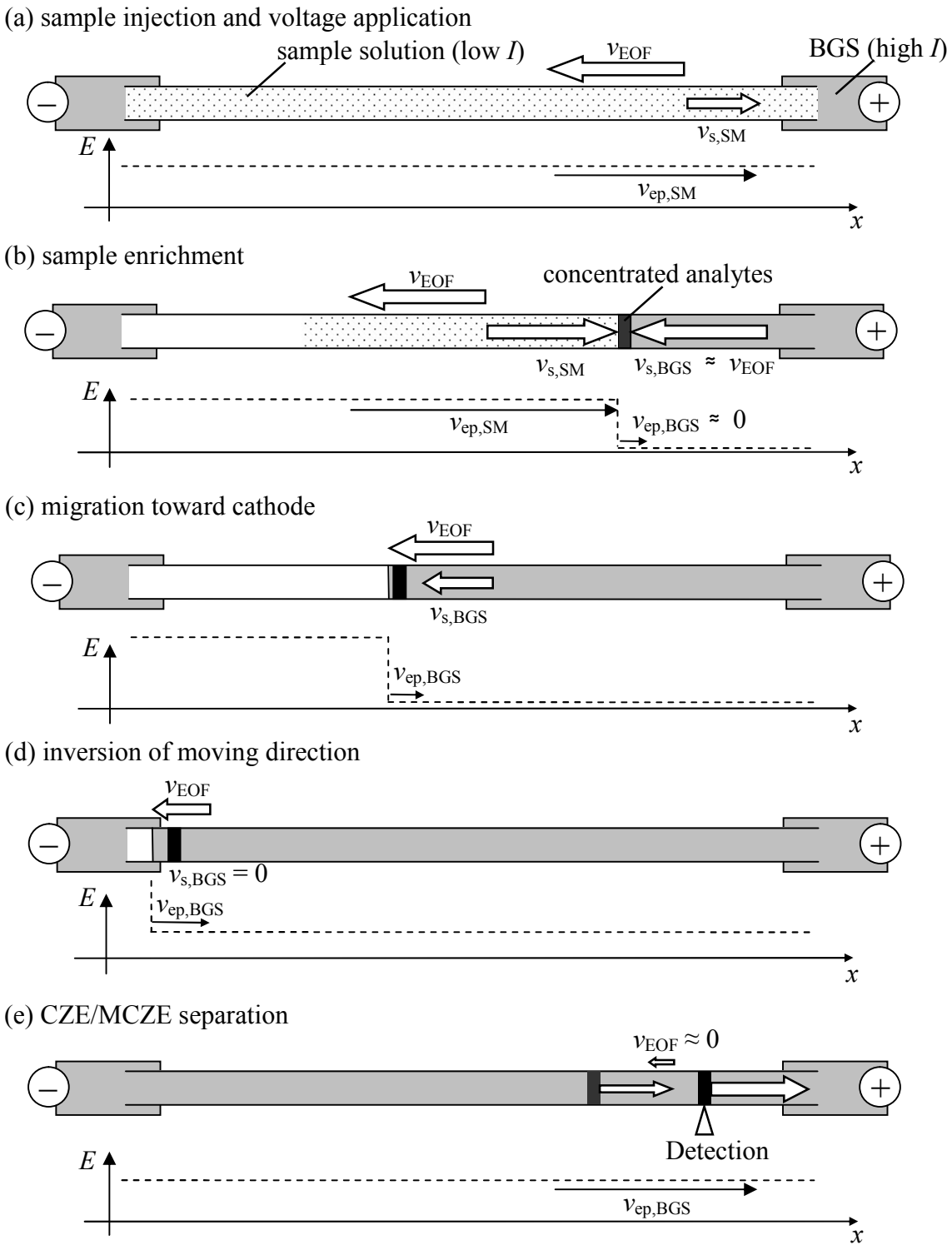

Figure 2-1. Concept of LVSEP in the EOF-suppressed capillary/microchannel. v_{ep}, v_{EOF} and v_s mean the electrophoretic velocity of the analyte, the EOF velocity, and apparent velocity of the analyte, respectively.

On the other hand, the LVSEP method in the PVA-coated capillary/microchannel proposed by the author is contrary to the conventional LVSEP; i.e., the EOF is temporarily enhanced only in the sample zone. The concept of LVSEP proposed by the author is shown in Figure 2-1. The PVA-coated channel is filled with a low ionic strength solution containing anionic analytes (Figure 2-1a). After application of the voltage, anionic analytes are concentrated at the SM/BGS boundary by the difference in the electric field strength between the two zones (Figure 2-1b). Both the focused analytes and the analyte-free SM zone move toward the cathode by the enhanced EOF (μ_{EOF} of ~4.4 × 10^{-4} $cm^2V^{-1}s^{-1}$) due to the low ionic strength of the solution (Figure 2-1c). As the BGS with a high ionic strength is introduced into the microchannel, the EOF velocity becomes slower (μ_{EOF} of ~1.0 × 10^{-5} $cm^2V^{-1}s^{-1}$). When most of the SM is removed from the cathodic end, the electric field in the BGS zone becomes higher. Hence, the electrophoretic velocity of the analyte exceeds the EOF velocity, resulting in the inversion of the moving direction of the analytes (Figure 2-1d). After the complete removal of the SM, the analytes are separated by zone electrophoresis during the anodic migration (Figure 2-1e). In the LVSEP system proposed by the author, therefore, the faster EOF in the sample zone should be necessary to remove the analyte-free SM (deionized water). However, PVA is known to be one of the most effective coatings to suppress the EOF. To clarify the mechanism of the EOF enhancement in the low ionic strength SM on the PVA-coated surface, EOF measurements were carried out (see the Appendix).

In the LVSEP technique, the inversion of the moving direction of the concentrated analytes is the most specific feature. By virtue of switching the migration direction around the cathodic end, loss of the effective separation length can be minimized. To

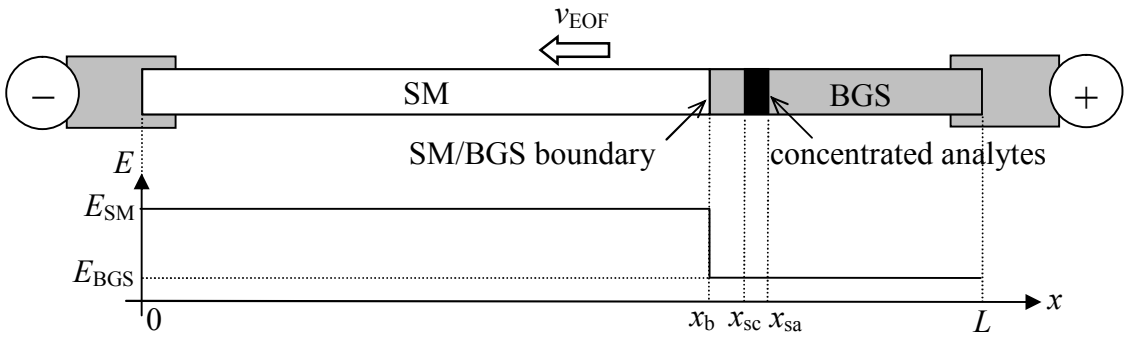

Figure 2-2. Schematic representation for the parameters used in the theoretical model. All positions are expressed as the distance from the cathodic channel end. Subscripts b, sc, and sa mean anodic side of the SM/BGS boundary and the cathodic and anodic sides of the concentrated analyte zone, respectively.

estimate the reversal point, a theoretical model of LVSEP was elaborated (Figure 2-2). Figure 2-2 shows the schematic of the longitudinal distribution of the electric field and the position of the SM/BGS boundary and the concentrated analyte zone in the microchannel. All positions are expressed by the distance from the cathodic end of the channel.

When the microchannel is filled with the BGS and sample solutions as shown in Figure 2-2, the quotient of the electric field strength in the two zones is proportional to γ:

$$E_{SM} = \gamma \times E_{BGS} \tag{2-1}$$

where E and γ are the electric field and the ratio of the conductivities (σ) of the SM and BGS ($\gamma = \sigma_{BGS}/\sigma_{SM}$), respectively. Since the distribution of the field strength depends on the length of the two zones, the applied voltage (V) can be expressed as follows:

$$V = x_b E_{SM} + (L - x_b) E_{BGS} \tag{2-2}$$

where L and x_b are the capillary length and the position of the SM/BGS boundary, respectively. Substituting Eq. (2-1) into Eq. (2-2) gives the field strengths in the BGS

and SM zones:

$$E_{\mathrm{SM}} = \frac{\gamma V}{(\gamma - 1)x_{\mathrm{b}} + L} \tag{2-3}$$

$$E_{\mathrm{BGS}} = \frac{V}{(\gamma - 1)x_{\mathrm{b}} + L} \tag{2-4}$$

It should be noted that the stacking of analytes changes the composition and the conductivity of the SM zone since the displacement of buffer ions between the two zones occurs according to the Kohlraush regulating function (KRF) [23]. However, further calculations are performed using the same simplified model as that used by Albert *et al.*, assuming that γ is approximated as constant during the whole LVSEP process [24].

As mentioned in the Appendix, the electrophoretic mobility of the anionic analyte (μ_{ep}) in the BGS is almost identical with that in the sample. Thus, the mobilities in the two zones ($\mu_{\mathrm{ep,BGS}}$ and $\mu_{\mathrm{ep,SM}}$) are expressed by μ_{ep}. From Eq. (2-4), the electrophoretic velocity of the analyte in the BGS zone ($v_{\mathrm{ep,BGS}}$) is given as follows:

$$v_{\mathrm{ep,BGS}} = \frac{\mu_{\mathrm{ep}} V}{(\gamma - 1)x_{\mathrm{b}} + L} \tag{2-5}$$

The overall electroosmotic velocity (v_{EOF}) can be calculated by averaging the local EOF velocities in the BGS and SM zones, which is proportional to the fraction of the zone length in the microchannel [25]:

$$v_{\mathrm{EOF}} = \frac{x_{\mathrm{b}}}{L} E_{\mathrm{SM}} \mu_{\mathrm{EOF,SM}} + \frac{(L - x_{\mathrm{b}})}{L} E_{\mathrm{BGS}} \mu_{\mathrm{EOF,BGS}} \tag{2-6}$$

Since $\mu_{\mathrm{EOF,BGS}}$ is enough small to be ignored in the PVA-coated channel, Eq. (2-6) can be approximated as follows:

$$v_{\mathrm{EOF}} \approx \frac{\gamma \mu_{\mathrm{EOF,SM}} V x_{\mathrm{b}}}{\{(\gamma - 1)x_{\mathrm{b}} + L\}L} \tag{2-7}$$

A plot of v_{EOF} *vs*. the fraction of the SM zone (x_{b}/L) is given in the Appendix.

To discuss the separation performance, the inversion position of the concentrated analytes should be calculated. For calculating the inversion point, the author estimated several parameters, e.g., x_b, x_{sa} and x_{sc}, as indicated in Figure 2-2. Detailed calculations are also provided in the Appendix. When the concentrated analytes start to move against the EOF, the SM plug length remaining in the channel/capillary ($x_{b,i}$) is expressed by the following simple equation:

$$x_{b,i} = \frac{-\mu_{ep} L}{\gamma \mu_{EOF,SM}} \tag{2-8}$$

In a typical experimental condition, e.g., $\gamma = 200$ and $\mu_{ep} \sim \mu_{EOF}$, 99.5% of the SM plug is removed before the inversion of the migration direction. However, $x_{b,i}$ is different from the inversion position of the concentrated zone since the concentrated analytes move electrophoretically for a short distance even in the low electric field in the BGS zone. Hence, the author calculated the distance by integrating $v_{ep,BGS}$ over time (see the Appendix). As a result, the concentrated bandwidth (w) and the inversion position of the concentrated analytes ($x_{sc,i}$) can be expressed as follows:

$$w = -\frac{\mu_{ep} L}{\gamma \mu_{EOF,SM}} \ln\left(-\frac{e\mu_{EOF,SM}}{\mu_{ep}}\right) \quad (\text{when } \mu_{EOF,SM} > -\mu_{ep}) \tag{2-9-1}$$

$$x_{sc,i} = -\frac{\mu_{ep} L}{\gamma \mu_{EOF,SM}} \ln \gamma \quad (\text{when } \mu_{EOF,SM} > -\mu_{ep}) \tag{2-10-1}$$

$$w = \frac{L}{\gamma} \quad (\text{when } \mu_{EOF,SM} \le -\mu_{ep}) \tag{2-9-2}$$

$$x_{sc,i} = -\frac{\mu_{ep} L}{\gamma \mu_{EOF,SM}} - \frac{\mu_{ep} L}{\gamma \mu_{EOF,SM}} \ln\left(-\frac{\gamma \mu_{EOF,SM}}{\mu_{ep}}\right) - \frac{L}{\gamma} \quad (\text{when } \mu_{EOF,SM} \le -\mu_{ep}) \tag{2-10-2}$$

At the inversion time, only 0.5% SM zone remains in the usual condition, but the remained zone is soon removed even by the reduced EOF. Therefore, the MCZE

separation stage starts immediately after the inversion of the analytes. Since the inversion position of the analytes can be approximated as the starting point of the MCZE separation, the prediction of the inversion position should be useful for discussing the separation efficiency of LVSEP-MCZE. The turning positions calculated by Eqs. (2-9) and (2-10) are compared by those estimated by the fluorescence imaging in the next section.

Fluorescence Imaging of LVSEP

In LVSEP-MCZE in the 40 mm long PVA-coated channel, the concentration behavior of fluorescein was observed by the fluorescence imaging technique. As shown in Figure 2-3, the moving concentration boundary was traced from the anodic channel end. After application of the voltage, the analyte was stacked from the anodic side. The concentrated analyte moved toward the cathode by the enhanced EOF (Figures 2-3a,b). The observed velocity of the stacked analytes remained almost constant until reaching near the cathodic end of the channel. When the analytes reached the channel position of 3–4 mm, the analytes decelerated drastically (Figures 2-3c,d), and then the moving direction of the concentrated analyte was inverted to the anode at the position of 2.3 mm (Figure 2-3e). After the turn, the analyte migrated with almost the same velocity until being removed out from the anodic channel end (Figure 2-3f). Such migration behavior was observed at HEPES concentrations ranging from 0 to 0.2 mM.

To verify the proposed model of LVSEP, two important parameters, μ_{EOF} and $x_{sc,i}$ are discussed (Table 2-1). Variation of μ_{EOF} in the PVA-coated microchannel was estimated at HEPES concentrations of 0–0.2 mM by analyzing the fluorescence images. As described in the previous section, v_{ep} of the stacked analyte in the early concentration

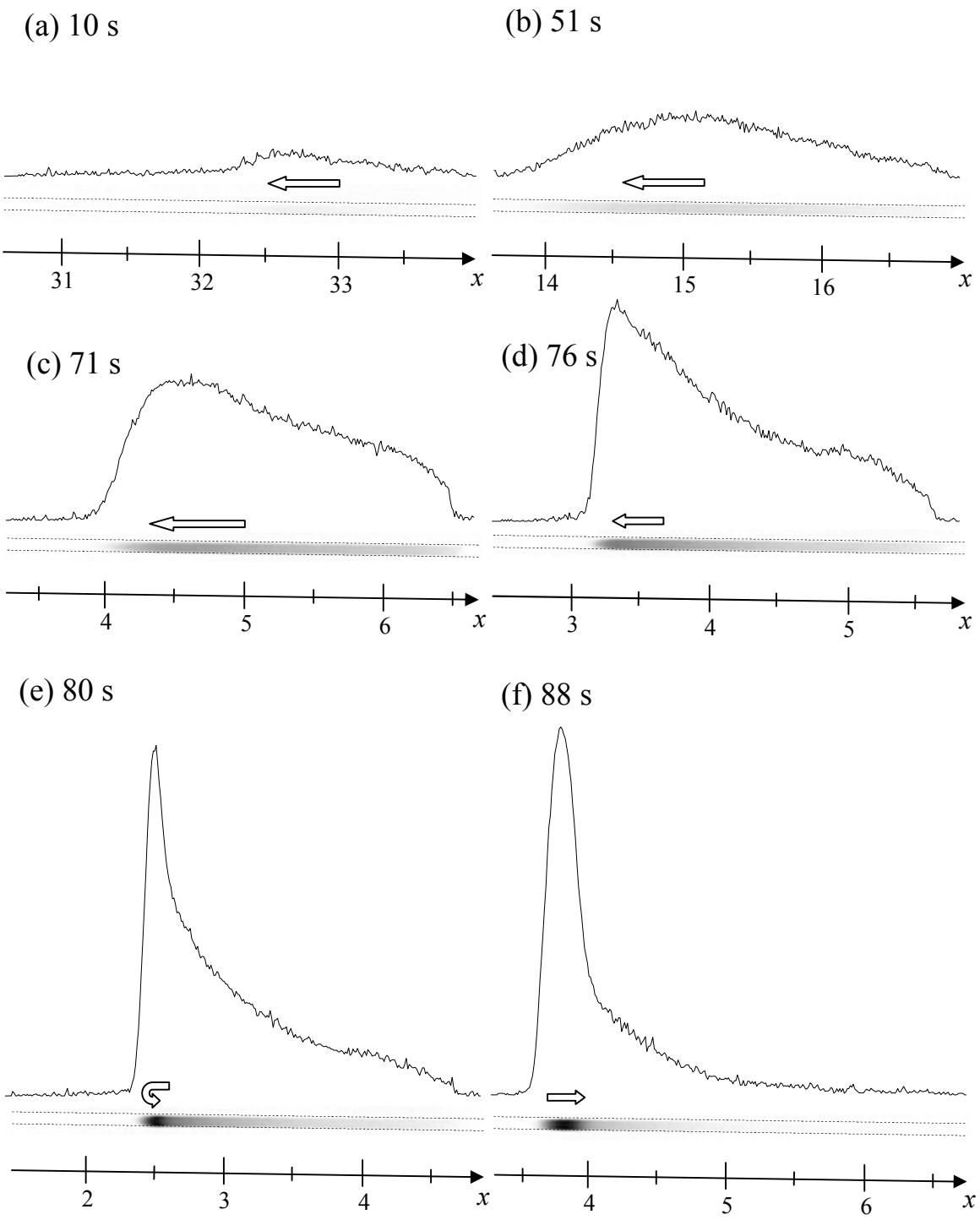

Figure 2-3. Fluorescence images and intensity profile of fluorescein concentrated by LVSEP-MCZE in 40 mm long straight channel. The abscissa axis gives the distance from the anodic channel end. The length of the arrow is proportional to the apparent velocity of the analyte zone.

stage was so low that the analyte moved at almost the same velocity as the EOF. Actually, the apparent mobility of fluorescein (μ_{app}) at the initial stage of the concentration was similar to μ_{EOF} determined experimentally. However, the velocity of the analytes toward the cathode was gradually increased as concentration proceeded (Figures 2-3a–c), indicating that much faster EOF occurred in the late concentration stage. This might be because some ion displacement caused an increase in the pH of the SM zone and/or the extremely high electric field in the SM zone raised the temperature.

The inversion position of the analyte was evaluated for further investigation of the mechanism of LVSEP. Both the experimentally observed and theoretically calculated inversion positions from the cathodic end ($L–x_{sc,i,obs}$ and $L–x_{sc,i,theo}$, respectively) are summarized in Table 2-1. The experimental results, $L–x_{sc,i,obs}$, agreed well with the theoretical prediction, $L–x_{sc,i,theo}$, at buffer concentrations of 0.05 and 0.1 mM in the sample solution. In the case of 0.2 mM HEPES, μ_{app} in the LVSEP process was larger than μ_{EOF}, which might cause the relatively larger difference between $L–x_{sc,i,theo}$ and $L–x_{sc,i,obs}$. At 0 mM, a significant difference between theoretical and observed inversion points appeared. This could be explained by the molecular diffusion and the parabolic flow caused by the EOF velocity difference in the BGS and SM zones. Actually, the parabolic flow profile was observed in the fluorescence imaging as shown in Figures 2-3c,d. Such boundary distortion and the molecular diffusion would generate the concentration gradient of the buffer components around the SM/BGS boundary. This concentration gradient around the inversion point reduced the apparent γ, which made $x_{b,i}$ larger, especially in the extremely diluted sample solution. Of course, the contamination of the sample solution with remaining HEPES in the microchip might change the γ value.

Although some differences between $x_{sc,i,theo}$ and $x_{sc,i,obs}$ were observed at HEPES concentrations of 0–0.2 mM, the inversion points predicted by the theoretical model corresponded well to the observed values with less than 5% error at HEPES concentrations of 0–0.2 mM, indicating the validity of the proposed LVSEP model. It should be emphasized that LVSEP gives a sufficient separation length with more than 94% of the whole channel length in the usual condition of γ >100. The LVSEP theory can be applied to conventional LVSEP in CE, which helps us to obtain a better understanding of the concentration processes.

Table 2-1. Electrophoretic parameters in the LVSEP analysis of fluorescein.

C_{SM} (mM)[a]	μ_{app}[c] (10^{-4}cm^{2}V^{-1}s^{-1})	μ_{EOF}[d] (10^{-4}cm^{2}V^{-1}s^{-1})	L–$x_{sc,i,obs}$ (mm)[e]	L–$x_{sc,i,theo}$ (mm)[f]
0[b]	3.7	4.4	76.9	80.0
0.05	2.7	2.5	76.0	77.7
0.1	2.2	2.1	75.1	75.3
0.2	2.2	1.8	73.5	70.4

[a] HEPES concentration of the sample solution.
[b] Sample solution was prepared with deionized water.
[c] Apparent mobility calculated from the velocity of fluorescein in the early concentration stage of the LVSEP-MCZE analysis.
[d] μ_{EOF} was calculated by subtracting the electrophoretic mobility of fluorescein from μ_{app}.
[e] Distance of the observed inversion position from the anodic channel end.
[f] Distance of the theoretically calculated inversion position from the anodic channel end.

LVSEP-MCZE Analyses of Oligosaccharides

As discussed in the Introduction, the application of LVSEP to the MCZE analysis is expected to overcome several drawbacks in conventional PI. Since a sample solution is injected into the entire channel in LVSEP-MCZE, the voltage control can be simplified from four channels for two steps to two channels for one step. It should be

noted that, when only a single drop (a few microliters) of the sample solution was put on the inlet reservoir, the sample was easily introduced into the entire microchannel via capillary force. This is due to the highly hydrophilic surface of the PVA coating on the channel. Such a simple injection process can save the sample volume to be analyzed. Consequently, low sensitivity is improved by the concentration effect with little loss of the effective separation length as demonstrated in the previous section.

To evaluate the analytical performance, LVSEP-MCZE and conventional PI-MCZE analyses of oligosaccharides were performed on the 80 mm long straight channel microchip and a cross-channel microchip with the 40 mm long separation channel, respectively. Linear glucose ladder and dendritic sugar chains obtained from bovine ribonuclease B were used as the model and real samples, respectively. When a bare PDMS microchip was employed, the oligosaccharides were seriously adsorbed onto the channel surface and could not be separated in the PI-MCZE analysis. Thus, the PVA-coated microchip was applied to suppress both the EOF and the sample adsorption. In the PI-MCZE analysis of the glucose ladder, G1–G10 were well separated, but longer oligomers than G10 could not be detected as shown in Figure 2-4a. On the other hand, G1–G20 were well concentrated and separated in the LVSEP-MCZE analysis (Figure 2-4b). It should be emphasized that the effect of the anionic electrolytes in the BGS on the concentration efficiency was not considerable but the conductivity of the BGS was significant. Among several buffer components (phosphate, acetate, HEPES, MES, and MOPS), the author found that 25 mM HEPES was optimal in the LVSEP-MCZE analysis of oligosaccharides. The sensitivity enhancement factor (SEF), which was calculated by comparing the peak height obtained in the LVSEP condition with that in the conventional PI-MCZE taking into account the dilution factor regardless of the

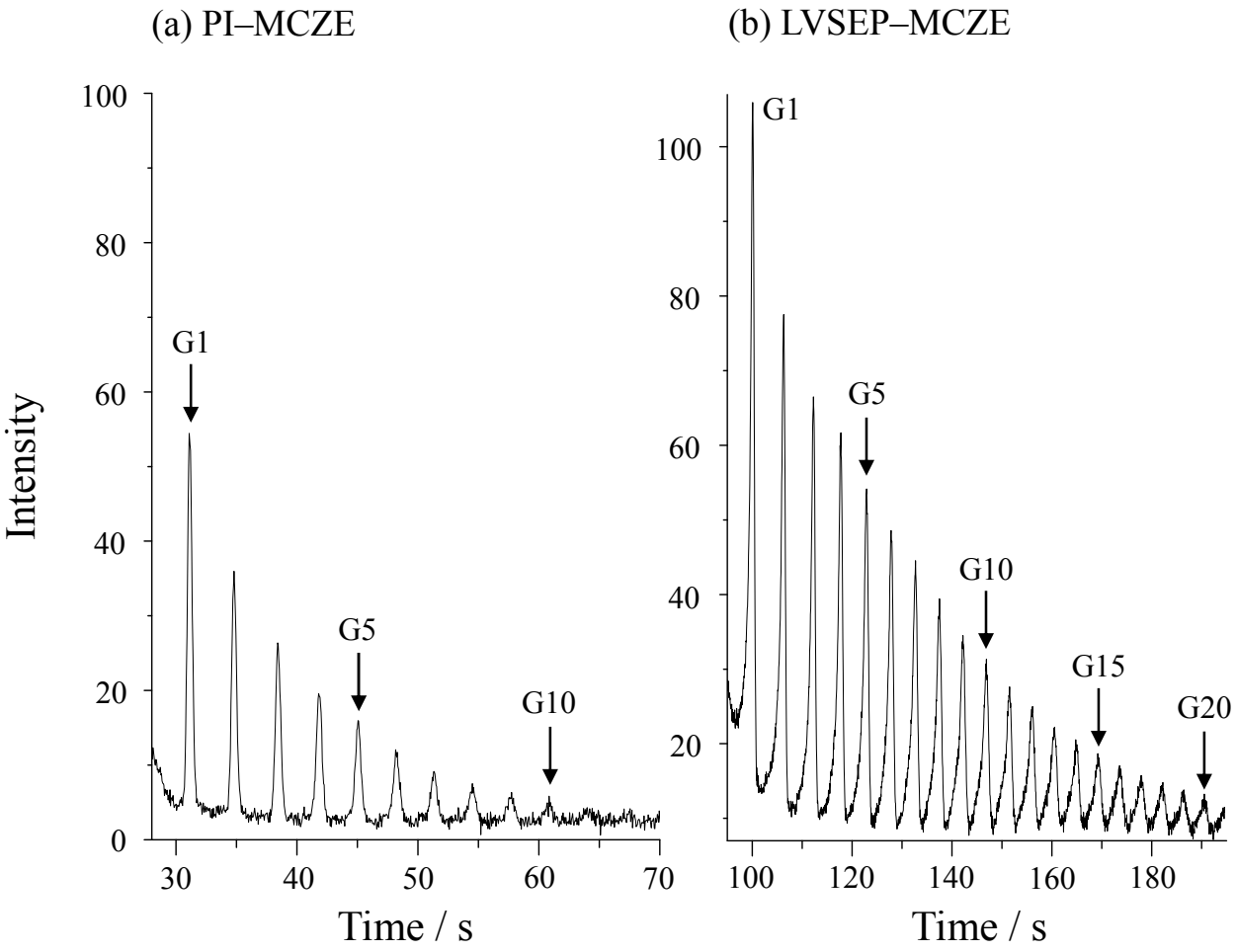

Figure 2-4. Electropherograms of glucose ladder obtained with (a) conventional PI-MCZE and (b) LVSEP-MCZE. Concentration of glucose ladder: (a) 160 ppb, (b) 320 ppt.

injection volume of the sample solution, was estimated to be 930–2,900.

In the analysis of the real sample, only M5 and M6 were detected in the PI-MCZE analysis (Figure 2-5a). On the other hand, M5–M9 could be detected and resolved in LVSEP-MCZE with the SEFs ranging from 1900 to 2200 (Figure 2-5b). As far as the author know, such high SEF values over 1000 have not been reported in previous papers on the online concentration of carbohydrates in CE [15–18]. In this experimental condition, the sample 200-fold-diluted with deionized water was employed in the LVSEP analysis. Interestingly, the undiluted oligosaccharide sample was also enriched

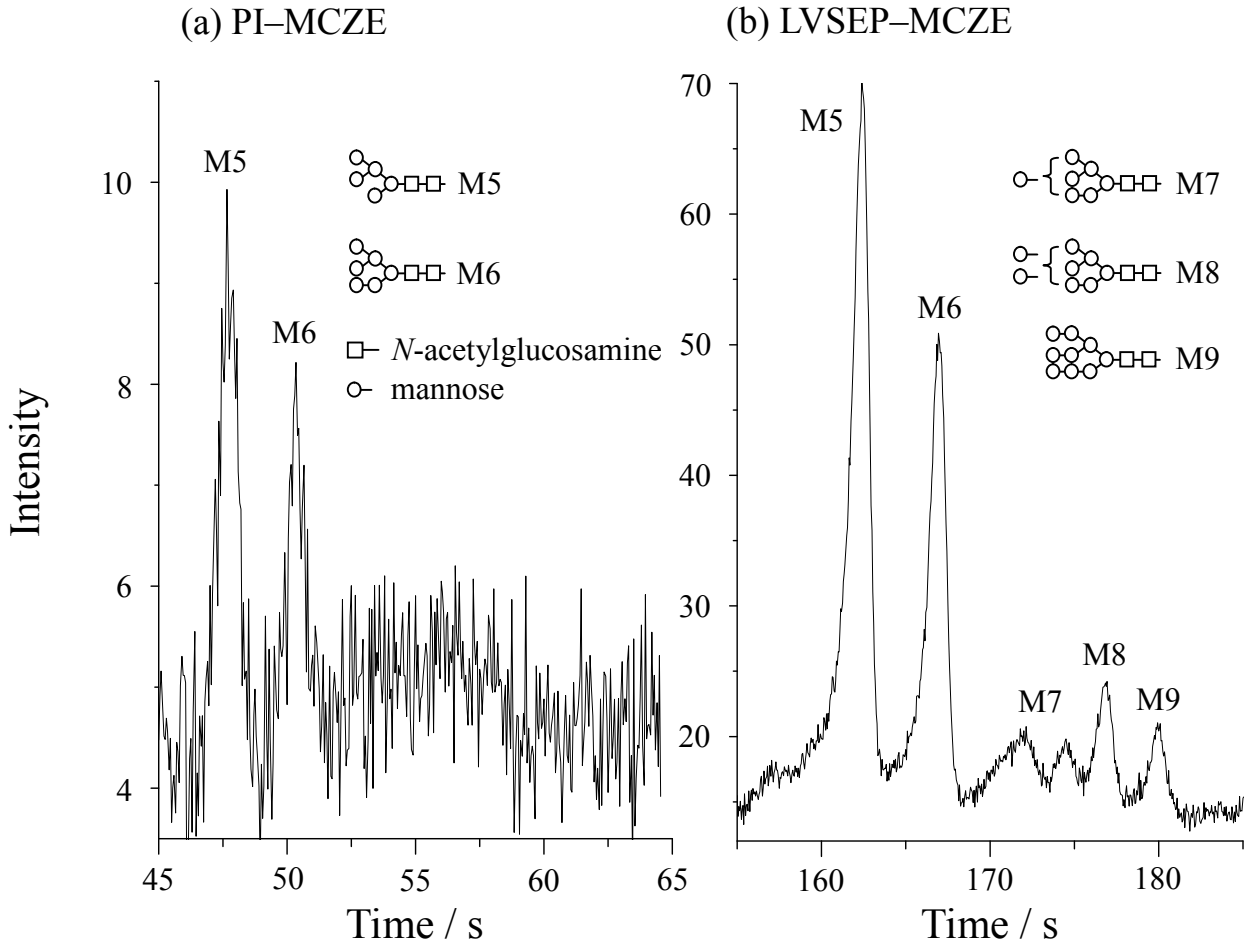

Figure 2-5. (a) Conventional PI-MCZE and (b) LVSEP-MCZE analyses of oligosaccharides released from bovine ribonuclease B. The sample concentration in LVSEP-MCZE was 200-fold lower than that in PI-MCZE.

and separated as well (Figure 2-5). Since oligosaccharides were purified by gel filtration to remove the excess APTS prior to the LVSEP-MCZE analysis, salts in the sample solution were removed, resulting in the reduction of the conductivity in the sample matrix. This demonstrated that the sample dilution with deionized water was not indispensable in LVSEP, and thus, extremely low concentration oligosaccharides in a biological matrix can be detected by combining only APTS labeling and gel filtration with LVSEP.

Table 2-2. Reproducibility and resolution in LVSEP-MCZE and conventional PI-MCZE.

	RSD (%) of t_M[a]	RSD (%) of height[a]	R_s[b]
PI-MCZE	3.9	11	1.8
LVSEP-MCZE	1.1	7.2	2.0

[a] RSDs for the peak of M5 (n = 3).

[b] Resolution between M5 and M6.

In LVSEP-MCZE, the longer the channel length employed, the higher the sensitivity obtained. However, the analysis time should be increased upon increasing the channel length. For further sensitivity improvement, therefore, the application of LVSEP to capillary-based electrophoresis would be better. Actually, the author confirmed that the LVSEP-CZE analysis provided good enrichment and separation of oligosaccharides. In LVSEP-CZE, the analysis time of 20 min was required to detect G20, which was longer than that in LVSEP-MCZE (200 s). Thus, the combination of LVSEP with microchip-based electrophoresis was effective to give both a shorter analysis time and good sensitivity. As summarized in Table 2-2, the reproducibility of LVSEP-MCZE was also investigated. The run-to-run repeatabilities of the migration time (t_M) and peak height (h) were good with relative standard deviations (RSDs) of 1.1% and 7.2%, respectively, which were better than those in PI-MCZE.

To compare the separation performance of LVSEP-MCZE with that of PI-MCZE, plate heights were calculated for the peak of M5. In LVSEP-MCZE, the inversion position and time could be regarded as the starting point and time of the separation, respectively. Hence, the plate height in LVSEP-MCZE was calculated from the effective separation length and migration time determined by the fluorescence imaging of the inversion. As a result, the obtained plate height was 2.7 μm for LVSEP-MCZE, which is

comparable with that of 2.5 μm in PI-MCZE. Although the bandwidth of the concentrated analytes at the inversion position (180 μm) was larger than the injected bandwidth in PI-MCZE (50 μm), comparable plate heights were obtained in LVSEP-MCZE. This means that the contribution of the injection length to the peak variance was negligible compared to that of the diffusion. The comparable efficiency without loss of the effective separation length gave good resolution in LVESP-MCZE.

In LVSEP, however, peak frontings were observed for almost all peaks, which can be explained by the molecular diffusion of the analyte. For the stacked analyte, sample diffusion in the BGS zone freely occurred. In contrast, the concentrated analyte could not penetrate into the SM zone due to faster anodic migration in the enhanced electric field in the SM. Such partial diffusion toward the anode caused partial peak broadening as shown in Figure 2-3f, so the peak fronting was observed in the electropherograms. Thus, the addition of some gel reagents into the BGS may be useful to prevent the peak fronting and to improve the resolution since the sample diffusion is suppressed in the viscous medium [26].

Table 2-3. SEFs of oligosaccharides obtained with the LVSEP-MCZE analysis.

	G1	G5	G10	M5	M6
SEF	930	1700	2900	2200	1900

In the analysis of the glucose ladder, the higher SEFs were obtained for the larger analytes with smaller μ_{ep} as shown in Table 2-3. This result can also be explained by the sample diffusion. In LVSEP-MCZE, the total diffusion time (t_t) is the summation of that in the concentration stage (t_p) and the separation stage (t_s). Meanwhile, the diffusion time in PI-MCZE can be assumed to be almost the same as t_s. Thus, the sample dilution

by diffusion depends on t_t in LVSEP while on t_s in conventional MCZE. Since the t_p value is almost constant for all analytes, the t_p/t_s ratio is smaller for the anionic species with smaller μ_{ep}. Therefore, the contribution of the sample diffusion to the band broadening in LVSEP relative to PI-MCZE should be smaller for the slowly migrating anionic species, which caused the higher SEFs for the analytes with smaller μ_{ep} values. This indicates that the LVSEP technique is appropriate for the analysis of slowly migrating molecules. However, He and Lee reported the insufficient enrichment of weakly dissociated anions in LVSEP-CZE [8], which conflicted with the result obtained in this study. In conventional LVSEP-CZE, the enhanced EOF was too fast at 1×10^{-3} $cm^2V^{-1}s^{-1}$ for the slowly migrating anions to be recovered. In the LVSEP-MCZE proposed by the author, however, the enhanced EOF was not so fast for the removal of the analytes but fast enough for the SM removal to allow the analyses of very slowly migrating G20 with an μ_{ep} of 1.0×10^{-4} $cm^2V^{-1}s^{-1}$. The author also found that anionic warfarin, which has only one dissociative hydroxyl group, could be well enriched by LVSEP without APTS labeling. Successful concentration of the monovalent anion and slowly migrating G20 indicates that LVSEP can be applied to the analysis of a wide variety of anionic molecules including peptides and nucleic acids. Therefore, the newly developed LVSEP-MCZE in the PVA-coated microchannel is suitable for concentrating and separating anionic biopolymers, and work along this line is now in progress.

2-4. Conclusions

The mechanism of LVSEP on the EOF-suppressed straight channel microchip was investigated on the basis of the theoretical model and fluorescence imaging. In the

LVSEP-MCZE analysis of oligosaccharides, both sample concentration and separation were achieved with up to a 2900-fold increase in the sensitivity compared to that of the conventional PI-MCZE analysis. The straight channel geometry and the simplification of the voltage program for fluidic control should be effective for high-throughput analysis. High analytical performance of the LVSEP-MCZE technique will contribute to the more practical analyses not only for oligosaccharides but also for anionic biomolecules, e.g., DNA, peptides, proteins, organic acids, metabolites, and so on.

2-5. Appendix

EOF Enhancement on PVA-coated Surfaces

The main aim of this study is the development of the LVSEP–MCZE technique to analyze biomolecules. It is well-known that adsorption of biomolecules onto the channel surface often causes serious band broadening in MCE. To suppress the sample adsorption, the channel surface is usually coated with appropriate polymers such as poly(vinyl alcohol) (PVA), polyethylene glycol and hydroxypropyl methylcellulose [A1]. By modifying the microchannel with these polymers, the EOF in the microchannel should be suppressed. In conventional LVSEP of anionic analytes, the EOF must be fast enough to remove the unnecessary SM in the concentration stage, while in the separation stage the EOF should be suppressed to allow the electrophoretic migration of the anionic analytes toward the anode. Hence, it is difficult to apply LVSEP to polymer-coated microchannel since the remained SM can not be removed out due to the suppressed EOF both in the sample solution and BGS. Contrary to the author's expectation, he found that LVSEP could be applied to the PVA-coated capillary

and microchannel. Although Chun and Chung reported a preliminary application of LVSEP to dimethylpolysiloxane and linear polyacrylamide coated capillaries, the driving force for removing the SM was not discussed [A2]. Therefore, the mechanism of LVSEP in the polymer-coated capillary/microchannel should be clarified. To elucidate the mechanism of LVSEP in the PVA-coated channel, in this study, the EOF velocity measurements in a low ionic strength solution was carried out. Based on the results of the EOF measurements, the mechanism of the SM removal in the PVA-coated microchannel is discussed in terms of the EOF enhancement in the sample solution.

A fused silica capillary (Polymicro Technologies, Phoenix, AZ) with total/effective lengths of 40/30 cm was activated and washed with 1 M NaOH and methanol, respectively, followed by the injection of 2% PVA into the whole capillary. After the PVA solution was removed, the capillary was heated at 110 °C for 15 min under the nitrogen gas flow. As with the microchip coating, the injection of the PVA solution and the heating of the capillary were repeated three times. All CZE experiments were performed on a P/ACE MDQ system (Beckman Coulter, Fullerton, CA) equipped with a diode-array UV detector. To determine the EOF velocity, the migration time of thiourea was measured in 0.1 ~ 25 mM HEPES buffer (pH 8.0) or deionized water filled in the PVA-coated capillary. The capillaries were conditioned with the BGS for 3 min at 20 psi prior to use. Sample injections were performed with a pressure of 0.5 psi for 3 s (injection volume, 3.9 nL). The applied voltage and the temperature were set at + 20 kV and 25 °C, respectively. UV detection was performed at 200 nm.

To evaluate the EOF velocity in the microchannel, generally, a current monitoring technique has been used [A3]. However, it was difficult to monitor a smaller difference of the current in the microchannel filled with the low ionic strength solution. In this

study, μ_{EOF} was calculated from the apparent mobility of fluorescein. CZE experiments were carried out to determine the electrophoretic mobility of fluorescein in the low concentration BGS. To evaluate the electrophoretic mobility in diluted BGSs, the migration velocity of fluorescein was determined in bare fused silica capillaries. Other conditions were the same as described above.

The electroosmotic mobility (μ_{EOF}) depends on the zeta potential (ζ) of the capillary or microchannel surface:

$$\mu_{EOF} = -\frac{\varepsilon \cdot \zeta}{\eta} \tag{A2-1}$$

According to Debye–Hückel theory, ζ exhibits a positive correlation with the ionic strength (I) of the BGS. It has been reported that ζ can be approximated as a linear function of $I^{-1/2}$ in low ζ region [A4]. Thus, the μ_{EOF} under suppressed EOF condition should be proportional to $I^{-1/2}$:

$$\mu_{EOF} \propto I^{-\frac{1}{2}} \tag{A2-2}$$

To verify the hypothesis that the EOF velocity in the PVA-coated capillary/microchannel is enhanced by filling a low ionic strength solution, the CZE analysis of the EOF marker was carried out. The obtained μ_{EOF} values were proportional to the $I^{-1/2}$ as shown in Figure A2-1a. At the BGS concentration of 25 mM, the EOF was well suppressed less than 2.8×10^{-5} $cm^2V^{-1}s^{-1}$, while the EOF velocity in a low ionic strength solution was enhanced up to 5.0×10^{-4} $cm^2V^{-1}s^{-1}$ (in deionized water). Such behavior in the EOF enhancement was also observed in the capillaries coated with poly(vinyl pyrrolidone) and highly hydrolyzed PVA (data not shown). Hence, the acceleration of the EOF velocity in the low ionic strength solution is not specific to the PVA coated capillary.

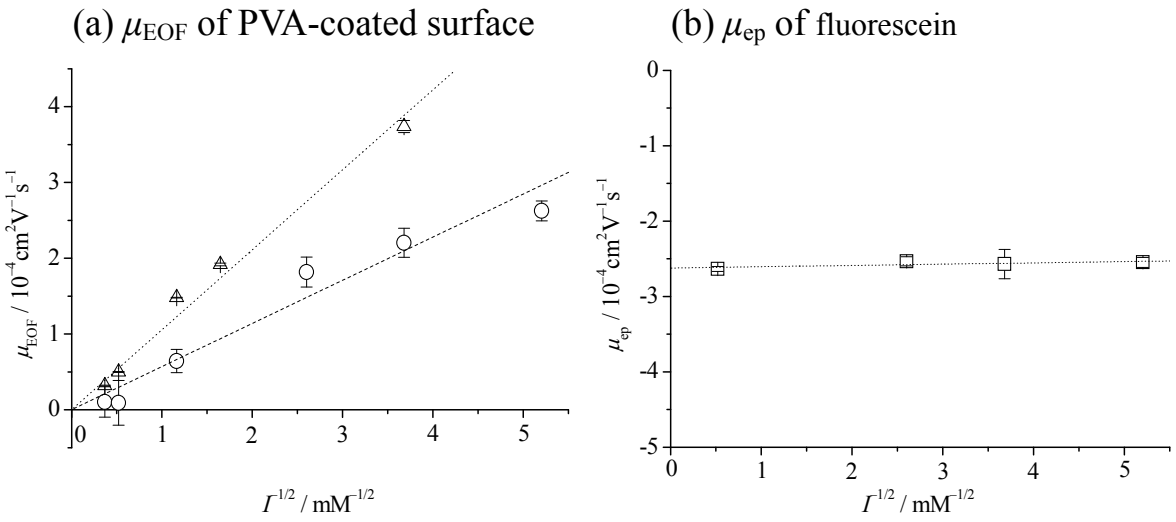

Figure A2-1. Dependence of (a) the electroosmotic mobilities in the PVA-coated capillary/microchannel and (b) the electrophoretic mobility of fluorescein on the BGS concentration ranging from 0.1 to 10 mM. The triangular and circular symbols represent the μ_{EOF} obtained in the capillary and microchannel, respectively.

To estimate μ_{EOF} in the PVA-coated microchannel, MCZE experiments were performed. As shown in Figure A2-1b, the electrophoretic mobility (μ_{ep}) of fluorescein, which was determined by the conventional CZE measurement, remained almost constant ranging from 2.5 to 2.6 × 10^{-4} cm^{2}V^{-1}s^{-1} even in the low ionic strength solution. Such dependence of the μ_{ep} on the ionic strength agreed well with the previous reports by Li *et al.* [A5] and Albert *et al*. [A6]. Thus, μ_{EOF} in the PVA-coated microchannel at the low ionic strength can be estimated from the difference between the apparent mobility and μ_{ep} of fluorescein. The apparent mobility was evaluated by fluorescence imaging of fluorescein migrating from the inlet reservoir. As summarized in Figure A2-1a and Table 2-1, the obtained μ_{EOF} in the PVA coated channel was increased with decreasing the *C*. Hence, in the PVA-coated capillary/microchannel, the EOF velocity was well enhanced by diluting the BGS concentration. Kirby *et al*. reported that zeta potential was increased with decreasing the counter ion concentration on polymeric

substrates [A4], supporting the findings of the enhanced EOF on the PVA-coated surface. This EOF enhancement should work as the driving force for removing the SM in LVSEP.

Changes in $v_{ep,BGS}$ and v_{EOF}

From Eqs. (2-5) and (2-7) in the main text, $v_{ep,BGS}$ and v_{EOF} can be expressed as a functions of x_b. The apparent velocity of the analyte in the BGS zone (v_{app}) is given as follows:

$$\begin{aligned} v_{app} &= v_{ep,BGS} + v_{EOF} \\ &= \frac{\mu_{ep} V}{(\gamma - 1)x_b + L} + \frac{\gamma \mu_{EOF,SM} V x_b}{\{(\gamma - 1)x_b + L\}L} \\ &= \frac{\mu_{ep} VL + \gamma \mu_{EOF,SM} V x_b}{\{(\gamma - 1)x_b + L\}L} \end{aligned} \tag{A2-3}$$

In Figure A2-2, $v_{ep,BGS}$, v_{EOF} and v_{app} are plotted against x_b/L. The term x_b/L represents the fraction of the SM remained in the capillary. Before applying the voltage, x_b/L is unity. After applying voltage, $v_{ep\cdot BGS}$ and v_{EOF} remains almost constant at $\mu_{EOF,SM}\cdot V/L$ and 0, respectively, till x_b/L becomes ca. 0.1. Until most of the SM zone is removed out of the capillary/microchannel, therefore, the apparent velocity of the concentrated analyte is almost the same as the EOF velocity. When the remained SM zone becomes short ($x_b/L < 0.1$), v_{EOF} is drastically decreased to 0, whereas $v_{ep,BGS}$ is increased to $\mu_{ep}\cdot V/L$. Thus, the apparent velocity of the analyte changes suddenly from positive to negative, resulting in the inversion of the moving direction. In the next section, x_b at the apparent velocity of 0 is calculated to estimate the inversion position.

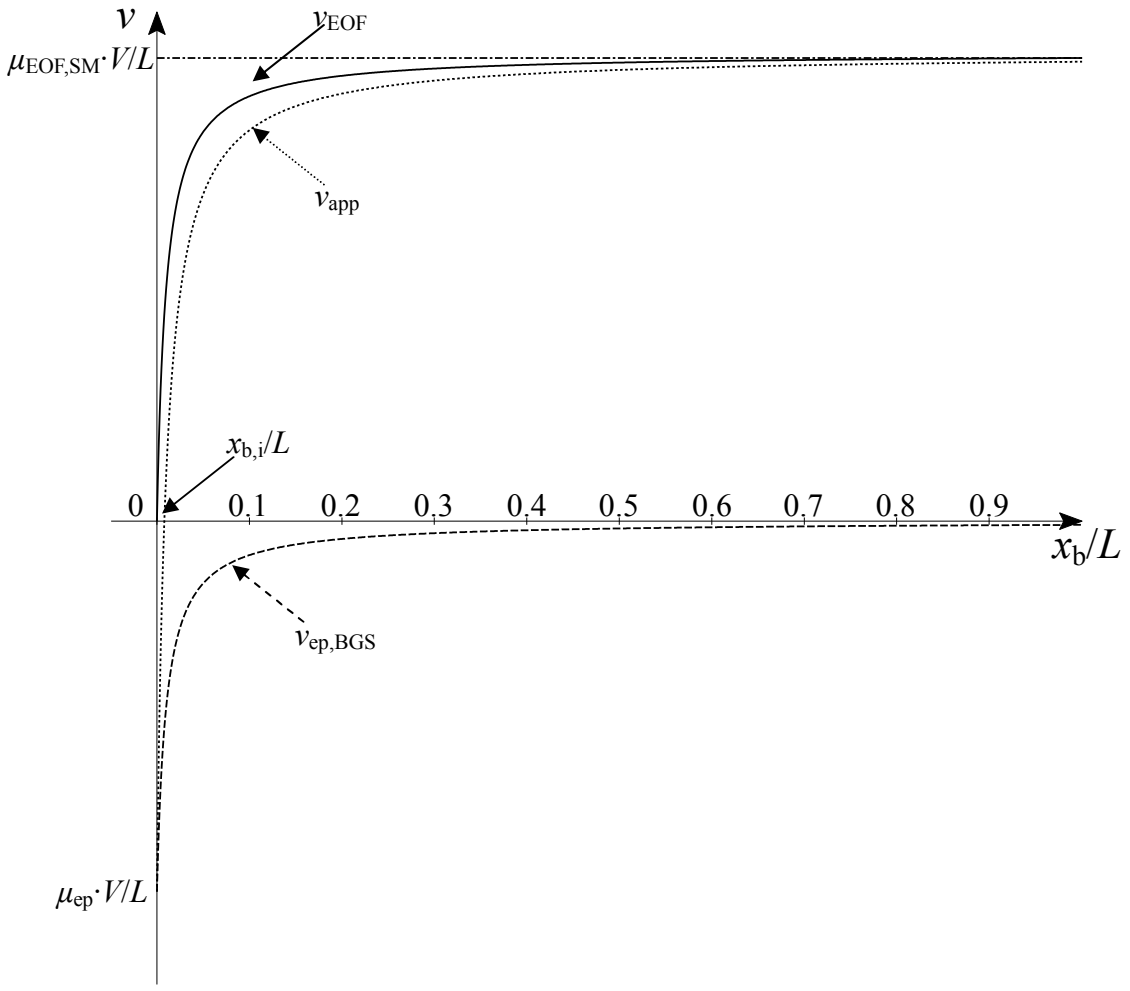

Figure A2-2. v_{EOF}, v_{ep}, and v_{app} represent as a function of x_b/L. The solid line, broken line, and dotted line show v_{EOF}, v_{ep}, and v_{app}, respectively.

Calculation of the inversion position of the concentrated analytes

In the main text, calculation details from Eqs. (2-7) to Eq. (2-9) are skipped to be easily understood. In the Appendix, the calculations are proposed to obtain w and $x_{sc,i}$.

The SM/BGS boundary moves according to the EOF, x_b can be expressed as a function of t:

$$x_b = L - \int_0^t \frac{\mu_{EOF,SM} \gamma V x_b}{\{(\gamma-1)x_b + L\}L} dt$$

$$= L - \int_0^t \frac{\mu_{EOF,SM} \gamma V}{(\gamma-1)L} dt + \int_0^t \frac{\mu_{EOF,SM} \gamma V}{\{(\gamma-1)x_b + L\}(\gamma-1)} dt$$

$$= L - \frac{\mu_{\mathrm{EOF,SM}}\gamma V}{(\gamma-1)L}t + \int_0^t \frac{\mu_{\mathrm{EOF,SM}}\gamma V}{\{(\gamma-1)x_\mathrm{b}+L\}(\gamma-1)}dt$$
$$\int_0^t \frac{V}{\{(\gamma-1)x_\mathrm{b}+L\}}dt = \frac{(\gamma-1)}{\gamma\mu_{\mathrm{EOF,SM}}}\left\{x_\mathrm{b} - L + \frac{\gamma\mu_{\mathrm{EOF,SM}}V}{(\gamma-1)L}t\right\} \quad \text{(A2-4)}$$

If x_{sa} is the position of the anode-side end of the concentrated sample band as shown in Figure 2-2, (x_{sa}–x_b) is the length by which the analytes at the anode-side end migrate electrophoretically from the boundary. Therefore, (x_{sa}–x_b) can also be calculated by integrating $v_{\mathrm{ep,BGS}}$ and expressed as a function of t:

$$x_{\mathrm{sa}} - x_\mathrm{b} = \int_0^t \frac{-\mu_{\mathrm{ep}}V}{(\gamma-1)x_\mathrm{b}+L}dt \quad \text{(A2-5)}$$

Substitution of Eq. (A2-4) into Eq. (A2-5) gives the following equation:

$$x_{\mathrm{sa}} - x_\mathrm{b} = \frac{-\mu_{\mathrm{ep}}(\gamma-1)}{\mu_{\mathrm{EOF,SM}}\gamma}\left\{x_\mathrm{b} - L + \frac{\mu_{\mathrm{EOF,SM}}\gamma V}{(\gamma-1)L}t\right\}$$
$$= -\frac{\mu_{\mathrm{ep}}V}{L}t + \frac{\mu_{\mathrm{ep}}(\gamma-1)}{\mu_{\mathrm{EOF,SM}}\gamma}(L - x_\mathrm{b}) \quad \text{(A2-6)}$$

Here, by solving the differential equation of t and x,

$$x_\mathrm{b} = L - \int_0^t \frac{\mu_{\mathrm{EOF,SM}}\gamma V x_\mathrm{b}}{\{(\gamma-1)x_\mathrm{b}+L\}L}dt$$
$$\frac{dx_\mathrm{b}}{dt} = -\frac{\mu_{\mathrm{EOF,SM}}\gamma V x_\mathrm{b}}{\{(\gamma-1)x_\mathrm{b}+L\}L}$$
$$-\frac{\{(\gamma-1)x_\mathrm{b}+L\}L}{\mu_{\mathrm{EOF,SM}}\gamma V x_\mathrm{b}}dx_\mathrm{b} = dt$$
$$\int -\left\{\frac{(\gamma-1)L}{\gamma\mu_{\mathrm{EOF,SM}}V} + \frac{L^2}{\gamma\mu_{\mathrm{EOF,SM}}V}\frac{1}{x_\mathrm{b}}\right\}dx_\mathrm{b} = \int dt \quad \text{(A2-7)}$$

From initial condition, x_b is equal to L when $t = 0$. Thus, Eq. (A2-7) is solved as

$$t = \frac{(\gamma-1)}{\gamma\mu_{\mathrm{EOF,SM}}V}(L - x_\mathrm{b}) + \frac{L^2}{\gamma\mu_{\mathrm{EOF,SM}}V}\ln\left(\frac{L}{x_\mathrm{b}}\right) \quad \text{(A2-8)}$$

By substituting Eq. (A2-8) into Eq. (A2-6), the term (x_{sa}–x_b) can be expressed as a

function of x_b:

$$x_{sa} - x_b = \frac{-\mu_{ep} L}{\gamma \mu_{EOF,SM}} \ln\left(\frac{L}{x_b}\right) \tag{A2-9}$$

Provided that x_b is $x_{b,B}$ when $v_{ep,SM}$ exceeds v_{EOF}, and that x_b is $x_{b,F}$ when the whole analytes are stacked out, $x_{b,F}$ can be given as follows.

i) If $\mu_{EOF,SM} > \mu_{ep}$, some of the analytes were flashed out from the cathodic end due to the fast EOF. After decreasing the length of the SM zone and increasing the electric field, the analyte can move against the EOF toward the anode. Hence, this balanced condition can be expressed as follows:

$$\begin{aligned} v_{EOF} &= -v_{ep,SM} \\ \frac{\gamma \mu_{EOF,SM} V x_{b,B}}{\{(\gamma-1)x_{b,B} + L\}L} &= \frac{-\gamma \mu_{ep} V}{(\gamma-1)x_{b,B} + L} \\ x_{b,B} &= \frac{-\mu_{ep} L}{\mu_{EOF,SM}} \end{aligned} \tag{A2-10-1}$$

Meanwhile, if $v_{ep,SM} > v_{EOF}$, the analyte at the cathodic end moves by the length of $x_{b,B}$ from $t = t_B$ to $t = t_F$. Therefore, $x_{b,B}$ can be also given by the following equation:

$$\begin{aligned} x_{b,B} &= \int_{t_B}^{t_F} \frac{-\gamma \mu_{ep} V}{(\gamma-1)x + L} dt \\ &= \int_{x_{b,B}}^{x_{b,F}} \frac{-\gamma \mu_{ep} V}{(\gamma-1)x_b + L} \cdot \frac{-\{(\gamma-1)x_b + L\}L}{\gamma \mu_{EOF,SM} V x_b} dx_b \\ &= \frac{\mu_{ep} L}{\mu_{EOF,SM}} \int_{x_B}^{x_F} \frac{dx_b}{x_b} \\ &= -\frac{\mu_{ep} L}{\mu_{EOF,SM}} \ln\left(\frac{x_{b,B}}{x_{b,F}}\right) \end{aligned} \tag{A2-11}$$

By solving Eqs. (A2-10) and (A2-11), $x_{b,F}$ is expressed by the Eq. (A2-12):

$$\ln\left(\frac{x_{b,B}}{x_{b,F}}\right) = 1$$

$$x_{\mathrm{b,F}} = \frac{x_{\mathrm{b,B}}}{e} = \frac{\mu_{\mathrm{ep}} L}{e\mu_{\mathrm{EOF,SM}}} \tag{A2-12-1}$$

ii) If $\mu_{\mathrm{EOF,SM}} \leq \mu_{\mathrm{ep}}$, the analyte can migrate against the fast EOF immediately after the applying the voltage. Thus, $x_{\mathrm{b,B}}$ is equal to L:

$$x_{\mathrm{b,B}} = L \tag{A2-10-2}$$

As with Eq. (A2-11), L can be expressed as follows:

$$\begin{aligned} L &= \int_0^{t_{\mathrm{F}}} \frac{-\gamma\mu_{\mathrm{ep}} V}{(\gamma-1)x_{\mathrm{b}} + L} dt \\ &= \int_L^{x_{\mathrm{b,F}}} \frac{-\gamma\mu_{\mathrm{ep}} V}{(\gamma-1)x_{\mathrm{b}} + L} \cdot \frac{-\{(\gamma-1)x_{\mathrm{b}} + L\}L}{\gamma\mu_{\mathrm{EOF,SM}} V x_{\mathrm{b}}} dx_{\mathrm{b}} \\ &= \frac{\mu_{\mathrm{ep}} L}{\mu_{\mathrm{EOF,SM}}} \int_L^{x_{\mathrm{b,F}}} \frac{dx_{\mathrm{b}}}{x_{\mathrm{b}}} \\ &= \frac{-\mu_{\mathrm{ep}} L}{\mu_{\mathrm{EOF,SM}}} \ln\left(\frac{L}{x_{\mathrm{b,F}}}\right) \\ \ln\left(\frac{L}{x_{\mathrm{b,F}}}\right) &= -\frac{\mu_{\mathrm{EOF,SM}}}{\mu_{\mathrm{ep}}} \\ x_{\mathrm{b,F}} &= Le^{\frac{\mu_{\mathrm{EOF,SM}}}{\mu_{\mathrm{ep}}}} \end{aligned} \tag{A2-12-2}$$

Provided that ($x_{\mathrm{sa,F}}$–$x_{\mathrm{b,F}}$) is w, substitution of Eqs. (A2-10) and (A2-12) into (A2-9) gives w by the following equation:

(when $\mu_{\mathrm{EOF,SM}} > -\mu_{\mathrm{ep}}$) $$w = \frac{-\mu_{\mathrm{ep}} L}{\gamma\mu_{\mathrm{EOF,SM}}} \ln\left(-\frac{e\mu_{\mathrm{EOF,SM}}}{\mu_{\mathrm{ep}}}\right) \tag{A2-13-1}$$

(when $\mu_{\mathrm{EOF,SM}} \leq -\mu_{\mathrm{ep}}$) $$w = \frac{L}{\gamma} \tag{A2-13-2}$$

When the whole analytes are stacked out, the cathodic side of the concentrated band is just on the boundary. Therefore, w can be identified as the width of the concentrated band.

If x_{b} is $x_{\mathrm{b,i}}$ at the inversion point, $x_{\mathrm{b,i}}$ can be expressed as follows:

$$\frac{-\mu_{ep}V}{(\gamma-1)x_{b,i}+L}=\frac{\mu_{EOF,SM}\gamma V x_{b,i}}{\{(\gamma-1)x_{b,i}+L\}L}$$
$$x_{b,i}=\frac{-\mu_{ep}L}{\gamma\mu_{EOF,SM}} \tag{A2-14}$$

The distance between the cathodic end of the stacked analytes and the cathodic end of the channel/capillary (x_{sc}) is equal to ($x_{sa} - w$). From Eqs. (A2-9), (A2-13) and (A2-14), x_{sc} at the inversion time ($x_{sc,i}$) is given as follows:

(when $\mu_{EOF,SM} > -\mu_{ep}$)

$$\begin{aligned} x_{sc,i} &= -\frac{\mu_{ep}L}{\gamma\mu_{EOF,SM}}-\frac{\mu_{ep}L}{\gamma\mu_{EOF,SM}}\ln\left(\frac{\gamma\mu_{EOF,SM}}{\mu_{ep}}\right)+\frac{\mu_{ep}L}{\gamma\mu_{EOF,SM}}\ln\left(\frac{e\mu_{EOF,SM}}{\mu_{ep}}\right) \\ &= -\frac{\mu_{ep}L}{\gamma\mu_{EOF,SM}}\ln\gamma \end{aligned} \tag{A2-15-1}$$

(when $\mu_{EOF,SM} \leq -\mu_{ep}$)

$$x_{sc,i}=-\frac{\mu_{ep}L}{\gamma\mu_{EOF,SM}}-\frac{\mu_{ep}L}{\gamma\mu_{EOF,SM}}\ln\left(\frac{\gamma\mu_{EOF,SM}}{\mu_{ep}}\right)-\frac{L}{\gamma} \tag{A2-15-2}$$

2-6. References

[1] Manz, A.; Graber, N.; Widmer, H. M. *Sens. Actuators B* **1990**, *1*, 244–248.

[2] Jacobson, S. C.; Hergenroder, R.; Koutny, L. B.; Warmack, R. J.; Ramsey, J. M. *Anal. Chem.* **1994**, *66*, 1107–1113.

[3] Sueyoshi, K.; Kitagawa, F.; Otsuka, K.. *J. Sep. Sci.* **2008**, *31*, 2650–2666.

[4] Sueyoshi, K.; Kitagawa, F.; Otsuka, K. *Anal. Chem.* **2008**, *80*, 1255–1262.

[5] Sera, Y.; Matsubara, N.; Otsuka, K.; Terabe, S. *Electrophoresis* **2001**, *22*, 3509–3513.

[6] Wainright, A.; Williams, S. J.; Ciambrone, G.; Xue, Q.; Wei, J.; Harris, D. *J. Chromatogr. A* **2002**, *979*, 69–80.

[7] Myers, P.; Bartle, K. D.; *J. Chromatogr. A* **2004**, *1044*, 253–258.

[8] He, Y.; Lee, H. K. *Anal. Chem.* **1999**, *71*, 995–1001.

[9] Chun, M.-S.; Chung, D. S. *Anal. Chim. Acta* **2003**, *491*, 173–179.

[10] Mikkers, F. E. P.; Everaerts, F. M.; Verheggen, T. *J. Chromatogr.* **1979**, *169*, 11–20.

[11] Burns, M. A.; Johnson, B. N.; Brahmasondra, S. N.; Handique, K.; Webster, J. R.; Krishnan, M.; Sammarco, T. S.; Man, P. M.; Jones, D.; Heldsinger, D.; Mastrangelo, C. H.; Burke, D. T. *Science* **1998**, *282*, 484–487.

[12] Jacobson, S. C.; Hergenruder, R.; Moore, A. W. Jr.; Ramsey J. M. *Anal. Chem.* **1994**, *66*, 4127–4132.

[13] Gottschlich, N.; Jacobson, S. C.; Culbertson, C. T.; Ramsey J. M. *Anal. Chem.* **2001,** *73*, 2669–2674.

[14] Makrilia, N.; Kollias, A.; Manolopoulos, L.; Syrigos, K. *Cancer Invest.* **2009**, *27*, 1023–1037.

[15] Kamoda, S.; Nakanishi, Y.; Kinoshita, M.; Ishikawa, R.; Kakehi, K. *J. Chromatogr. A* **2006**, *1106*, 67–74.

[16] Quirino, J. P.; Terabe, S. *Chromatographia* **2001**, *53*, 285–289.

[17] Kazarian, A. A.; Hilder, E. F.; Breadmore, M. C. *J. Chromatogr. A* **2008**, *1200*, 84–91.

[18] Auriola, S.; Thibault, P.; Sadovskaya, I.; Altman, E. *Electrophoresis* **1998**, *19*, 2665–2676.

[19] Sueyoshi, K.; Nagai, H.; Wakida, S.; Nishii, J.; Kitagawa, F.; Otsuka, K. *Meas. Sci. Technol.* **2006**, *17*, 3154–3161.

[20] Effenhauser, C. S.; Bruin, G. J. M.; Paulus, A.; Ehrat, M. *Anal. Chem.* **1997**, *69*, 3451–3457.

[21] Wu. D.; Luo, Y.; Zhou, X.; Dai, Z.; Lin, B. *Electrophoresis* **2005**, *26*, 211–218.

[22] Dang, F.; Kakehi, K.; Cheng, J.; Tabata, O.; Kurokawa, M.; Nakajima, K.; Ishikawa, M.; Baba, Y. *Anal. Chem.* **2006**, *78*, 1452–1458.

[23] Hruska V.; Gas, B. *Electrophoresis* **2007**, *28*, 3–14.

[24] Albert, M.; Debusschere, L.; Demesmay, C.; Rocca, J. L. *J. Chromatogr. A* **1997**, *757*, 281–289.

[25] Chien, R.-L.; Helmer, J. C. *Anal. Chem.* **1991**, *63*, 1354–1361.

[26] Wu, D.; Regnier, F. E. *Anal. Chem.* **1993**, *65*, 2029–2035.

[A1] Dolník, V. *Electrophoresis* **2004**, *25*, 3589–3601.

[A2] Chun, M.-S.; Chung, D. S. *Anal. Chim. Acta* **2003**, *491*, 173–179.

[A3] Huang, X.; Gordon, M. J.; Zare, R. N. *Anal. Chem* **1988**, *60*, 1837–183.

[A4] Kirby, B. J.; Hasselbrink Jr, E. F. *Electrophoresis* **2004**, *25*, 187–202.

[A5] Li, D.; Fu, S.; Lucy, C. A. *Anal. Chem.* **1999**, *71*, 687–699.

[A6] Albert, M.; Debusschere, L.; Demesmay, C.; Rocca, J. L. *J. Chromatogr. A* **1997**, *757*, 281–289.

Chapter 3.

Highly Sensitive Oligosaccharide Analysis in Capillary Electrophoresis Using Large-volume Sample Stacking with an Electroosmotic Flow Pump

3-1. Introduction

Of many post-translation modifications of proteins, glycosylation plays important roles in living body, such as cell recognition, cell communication, cell proliferation, immune response, and differentiation [1–3]. The glycosylation has been examined by analyzing carbohydrates after releasing them chemically or enzymatically from glycoproteins. Some of the major analytical methods are based on chromatographic separation such as high performance liquid chromatography (HPLC) and anion-exchange chromatography [4–6]. Although they exhibit high resolution and high sensitivity, it is often difficult to separate closely related carbohydrates. Capillary electrophoresis (CE) is also a powerful separation tool which provides rapid and high resolution analysis of oligosaccharide isomers with complicated molecular structures [4,7,8]. However, the concentration sensitivity is quite poor in CE due to the short optical path length and small injection volume, which has been preventing the real oligosaccharide analysis.

To overcome the drawback in CE, various online sample concentration techniques have been developed such as field-amplified sample stacking (FASS) [9], sweeping [10], isotachophoresis [11], and dynamic pH junction [12]. As for the carbohydrate analysis,

several groups have reported the sensitivity enhancement by using these online concentration techniques. Quirino and Terabe reported sweeping of galactose and xylose with up to 40-fold sensitivity increase by using borate-diol interaction [13]. Kamoda *et al*. employed field-amplified sample injection (FASI) for analyzing *N*-linked glycan, succeeding in up to 360-fold sample concentration [14]. Auriola *et al*. reported up to 50-fold enhancement in sample loading by using transient isotachophoresis for the analysis of *O*-linked oligosaccharides [15]. Kazarian *et al*. combined FASS with dynamic pH junction for the analysis of mono-, di-, and trisaccharides, where tens-fold sensitivity improvement was achieved [16]. Although these techniques showed a good analytical performance, further improvements of the sensitivity, separation performance, complicated experimental procedure, and low repeatability are desired. Hence, the author focused on the online sample concentration by large-volume sample stacking with an electroosmotic flow (EOF) pump (LVSEP) [17], which allows an efficient sample concentration without loss of the effective separation length in a simple experimental procedure, *i.e.*, the whole capillary is filled with the sample solution followed by only the application of a constant voltage. The author have already reported the simple and sensitive analysis by microchip electrophoresis (MCE) using LVSEP in a single straight channel, resulting in up to a 2900-fold sensitivity increase in the oligosaccharide analysis [18]. To obtain further enhanced sensitivity and resolution, LVSEP was combined with capillary zone electrophoresis (CZE) in a long separation capillary, where increased amount of sample can be injected and longer effective separation length will be available. Although longer analysis time such as a few tens minutes will be required in the case of the long capillary, it will not increase the total analysis time for the oligosaccharide analysis, most of which is occupied for sample

derivatization and pretreatment processes.

The aim of this study is to establish a simple, sensitive, and high resolution method for the LVSEP-CZE analysis of oligosaccharides, as well as to study LVSEP-CE as a versatile analytical method. To suppress the EOF and sample adsorption onto the capillary surface, a capillary coated with poly(vinyl alcohol) (PVA) was employed. As reported in the previous work [18], the EOF enhancement is important in LVSEP using an EOF-suppressed capillary, so the author estimated the electroosmotic mobility to confirm the proper EOF change in a PVA-coated capillary for the LVSEP process. Although many excellent applications of LVSEP-CZE have been reported [19–26], no one has reported the limitation of sample conductivity, sample inversion position, and correction of detection time. Hence, effect of the sample conductivity was also evaluated by changing the electrolyte concentration in the sample matrix (SM) in the LVSEP-CZE analysis of two fluorescent dyes. Glucose oligomer was then analyzed as model carbohydrates both by conventional CZE and by LVSEP-CZE, where sample inversion position, separation performance, and correction of detection time were discussed. Finally, the author performed the analysis of *N*-linked glycans by LVSEP-CZE.

3-2. Experimental Section

Materials and Chemicals

A fused silica capillary of 50 μm i.d. was purchased from Polymicro Technologies (Phoenix, AZ, USA). Acetic acid, 2-[4-(2-hydroxyethyl)-1-pyperazinyl]ethylsulfonic acid (HEPES), and maltoheptaose (G7), were purchased from Nacalai Tesque (Kyoto,

Japan), sodium cyanoborohydride, 8-aminopyrene-1,3,6-trisulfonic acid (APTS), tetrahydrofuran (THF), bovine ribonuclease (RNase) B, fetuin from fetal calf serum, and human α_1-acid glycoprotein (AGP) from Sigma-Aldrich (St. Louis, MO, USA), thiourea from Wako (Osaka, Japan), glucose oligomer from J-Oil mills (Tokyo, Japan), peptide-*N*-glycosidase F (PNGase F) from Prozyme (San Leandro, CA, USA), fluorescein sodium salt from Tokyo Chemical Industry (Tokyo, Japan), Alexa Fluor-488 carboxylic acid succinimidyl ester (Alexa) from Invitrogen (Carlsbad, CA, USA), and PVA (M_w = 88 000, 99% hydrolyzed) from Japan VAM and POVAL (Tokyo, Japan). All solutions were prepared with deionized water purified with a Direct-Q System (Nihon Millipore, Japan), and filtered through a 0.45 μm pore membrane filter prior to use.

Capillary Coating

A fused silica capillary was coated with PVA in the same way as the previous papers [27,28]. Briefly, the capillary was activated and washed with 1 M NaOH and water, followed by the injection of a 5% PVA solution into the whole capillary. Both the capillary ends were immersed in the same PVA solution and left at room temperature for 15 min. The PVA solution was then removed out of the capillary and the capillary was heated at 140 °C for 18 h under a nitrogen gas flow. The capillary was filled with deionized water and stored at room temperature. Prior to use, the capillary was flushed with a back ground solution (BGS) for 15 min.

Apparatus

All CE experiments were performed on a P/ACE MDQ system (Beckman Coulter, Fullerton, CA, USA) equipped with a diode-array UV detector or a laser-induced

fluorescence (LIF) detector. The LIF detector consisted of a 488 nm argon ion laser module and photomultiplier detector with a 520 nm band pass filter. UV detection was performed at 200 nm.

Sample Preparation

Oligosaccharides were released from glycoproteins with PNGase F enzyme using the methods reported previously [18]. For fluorescence labeling, oligosaccharides released from 200 μg glycoprotein or 80 μg glucose oligomer were mixed with 5 μL of 0.1 M APTS in 15% acetic acid and 10 μL of 0.5 M $NaCNBH_3$ in THF. The mixture was kept at 55 °C for 2 h, followed by dilution with water to 50 μL. In the analysis of oligosaccharides from glycoproteins, the sample solution was desalted with a Centri-Spin-10 column (Princeton separations, NJ, USA) to remove an excess APTS and reagents used in the enzymatic reaction. These samples were diluted to the desired concentration with deionized water and BGS in the LVSEP-CZE and the conventional CZE analysis, respectively.

Procedure

The conductivity of the solution was measured by a conductivity meter B173 (Horiba, Kyoto, Japan). Prior to each run, the capillary with the total/effective lengths of 60/50 cm was conditioned with deionized water in LVSEP-CZE or with a 25 mM HEPES buffer (pH 8.0) in conventional CZE for 3 min at 20 psi. Sample injection was performed with a pressure of 20 psi for 90 s (whole capillary injection, 1.2 μL) in LVSEP or of 0.3 psi for 3 s (injection volume, 1.7 nL) in conventional CZE. The applied voltage and temperature were set at –30 kV and 25 °C, respectively.

3-3. Results and Discussion

Fundamental Study of LVSEP-CZE

The concept of LVSEP using an EOF-suppressed microchannel has been discussed in the previous paper [18]. The mechanism of the capillary-based LVSEP is the same as that in the microchannel. Briefly, the EOF-suppressed capillary is filled with a low ionic strength solution containing anionic analytes. After applying the voltage, anionic analytes are concentrated at the sample matrix (SM)/BGS boundary by the difference in the electric field strength between the two zones. The focused analytes move toward the cathode and the BGS is introduced into the capillary by the enhanced EOF in the low ionic strength SM. As the analytes migrate to the cathode, the EOF velocity becomes slower and the electric field strength in the BGS becomes higher. When almost all the SM in the capillary is removed out from the cathodic end, the electrophoretic velocity of the analytes exceeds the EOF rate, resulting in the inversion of the sample migration direction. After the complete removal of the SM, the analytes are separated by CZE during the anodic migration (see the Appendix).

In LVSEP-CZE, therefore, the EOF in the capillary must be suppressed in the high ionic strength BGS and be enhanced in the low ionic strength SM. Hence the author investigated the effect of the ionic strength of the BGS on the electroosmotic mobility (μ_{EOF}) (see the Appendix). As a typical result, μ_{EOF} in deionized water was enhanced to be 5.0×10^{-4} $cm^2V^{-1}s^{-1}$ and that in 25 mM HEPES buffer was suppressed to be 3.0×10^{-5} $cm^2V^{-1}s^{-1}$, which gave a sufficient EOF change for the LVSEP process.

In employing FASS-based online concentration methods including LVSEP, the conductivities (σ) of the sample solution and the BGS are important. To estimate the

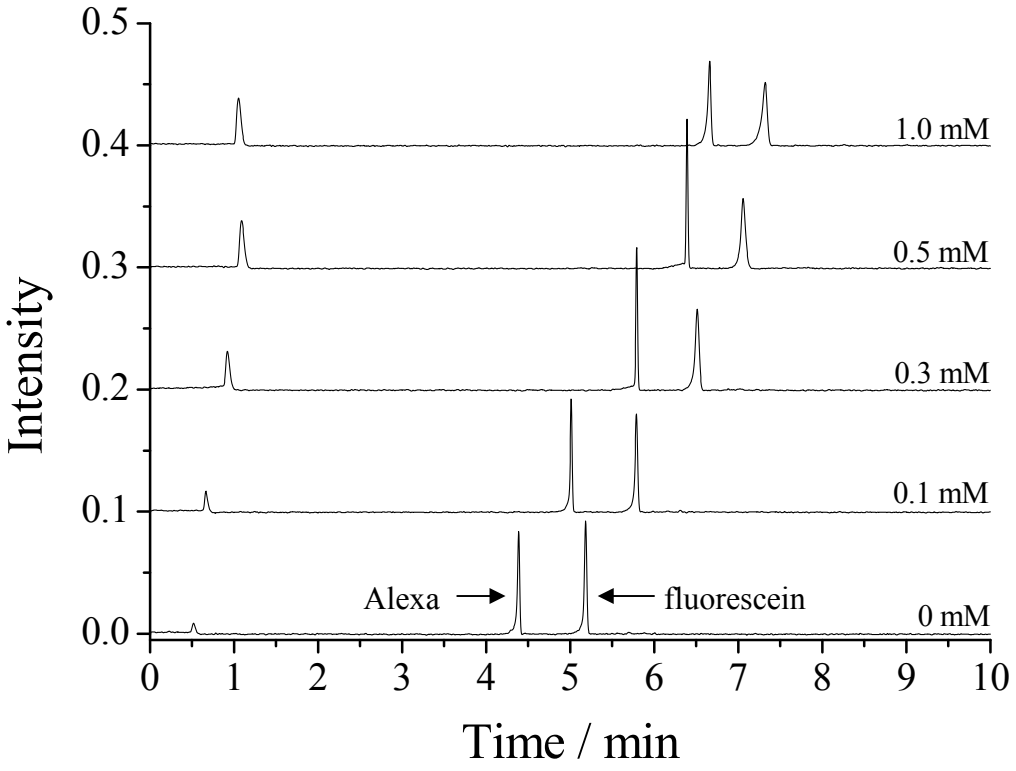

Figure 3-1. Electropherograms obtained with the LVSEP-CZE analyses of 100 pM Alexa and 100 pM fluorescein. BGS: 25 mM HEPES buffer (pH 8.0), SM: 0–1.0 mM HEPES buffer (pH 8.0).

conductivity limit of the sample solution in LVSEP-CZE, a HEPES buffer was used as the SM, of which concentration ranged from 0 mM (deionized water, σ = 0.055 μS/cm) to 1 mM (σ = 53 μS/cm). When 25 mM HEPES (σ = 1090 μS/cm) and a mixture of 100 pM fluorescein and 100 pM Alexa were employed as the BGS and analytes, respectively, the LVSEP-CZE analyses were successfully performed under the SM concentration less than 1 mM as shown in Figure 3-1. The first peak detected before 2 min was assigned to the concentration boundary moving toward the cathode from anodic capillary end by the enhanced EOF. Since the analytes are focused on the anodic-side SM/BGS boundary by field-amplified sample stacking in LVSEP, the boundary can be detected as the sharp peak even in LIF detection. The detection time of this peak was gradually delayed as the

SM concentration was increased, which supports that the EOF was increased with the decrease in the ionic strength as discussed previously. The gradual delay in the detection time of both Alexa and fluorescein was observed, which was also caused by the decrease in the EOF velocity. On the contrary, the peak-to-peak distance for the two analytes was not changed, indicating that the effective separation length in LVSEP was independent of the ionic strength of the SM. The peak width of Alexa was kept constant until the SM concentration reached 0.5 mM, whereas that in 1.0 mM SM became slightly broadened, probably because the insufficient conductivity difference between the 1.0 mM SM and 25 mM BGS reduced the stacking efficiency. The gradual broadening of the fluorescein peak could be explained in the same way. Theoretically, the slowly migrating fluorescein requires a long time to be completely concentrated, which might result in slightly broadened peak. The author also observed that up to 2.0 mM HEPES buffer (100 μS/cm) could be applied to the SM in LVSEP, but the detection times were further delayed and peaks were more broadened. These results showed that a sample containing a small amount of salt can be analyzed by LVSEP-CZE. For example, the glucose ladder sample after the APTS labeling as described in the Experimental Section could be used in LVSEP without desalting since the conductivity in the sample was estimated to be around 100 μS/cm.

In the early work on the conductivity in FASS [29,30], the conductivity ratio γ of 10 is the best to obtain the highest peak, which conflicts with the obtained data. In FASS, too large γ generates an EOF mismatch between the SM/BGS zones and/or decreases the electric field in the BGS (E_{BGS}), resulting in the band broadening. In LVSEP, of course, the EOF mismatch occurs between the SM/BGS zones, resulting in the band distortion and broadening in the concentration stage. In the LVSEP-MCE analysis

shown in the previous report [18], however, the author had found that the concentrated band was further focused around the sample inversion timing, resulting in the sharp peak in spite of the whole capillary injection. Hence the effect of the boundary distortion is relatively small in LVSEP. The second effect by the decrease in E_{BGS} can also be neglected because E_{BGS} is recovered after the concentration in LVSEP. In LVSEP, the salt in the SM decrease the sample focusing efficiency, which directly broadens the focused band. The salts also decrease the EOF velocity in the SM zone. The slow SM removal causes the band broadening due to the longitudinal diffusion.

Performance of LVSEP-CZE in Oligosaccharide Analysis

To evaluate the performance of LVSEP-CZE for oligosaccharide analysis, a glucose oligomer was analyzed as a model sample. The PVA-modified capillary was employed as the separation column to suppress the sample adsorption onto the inner surface. Among several buffer systems (phosphate, acetate, Tris–HCl, HEPES, HEPPS, PIPES, MES, TES, BES and MOPS), the author found that the 25 mM HEPES buffer was the optimal BGS in the LVSEP-CZE analysis of oligosaccharides. When the conductivity ratio between the sample solution and the BGS was high enough (*e.g.* >100), further improvement of the concentration efficiency was not attained by increasing the BGS concentration more than 25 mM. This result indicated that the obtained peak height was not determined by the concentrated bandwidth immediately after the stacking process, but mainly by the peak broadening caused by the molecular diffusion during the anodic migration.

The APTS-labeled glucose oligomer was analyzed both by conventional CZE and LVSEP-CZE. As shown in Figure 3-2, 32 ppt glucose oligomer was well concentrated

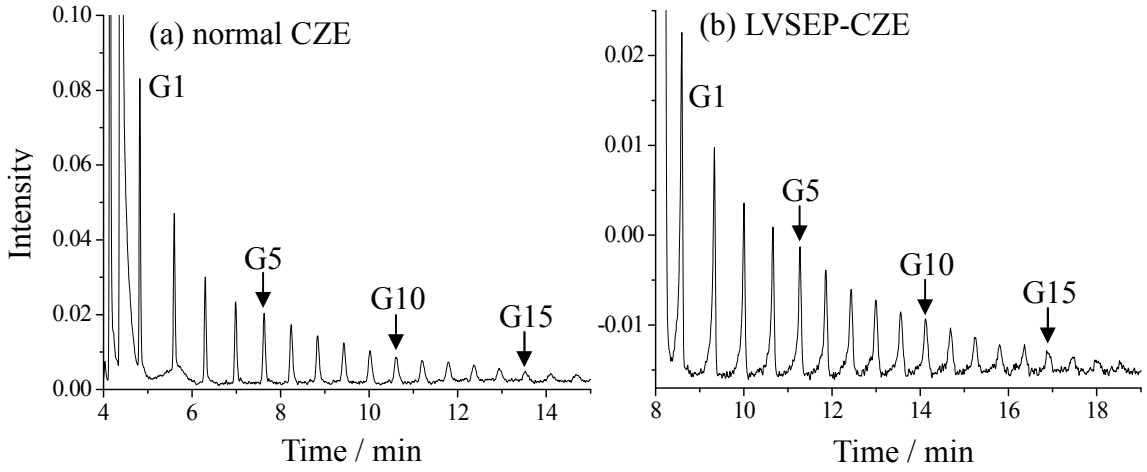

Figure 3-2. Electropherograms of glucose oligomer obtained with (a) conventional CZE and (b) LVSEP-CZE. The sample concentration: (a) 16 ppb, (b) 32 ppt.

and separated without significant loss of resolution in the LVSEP-CZE analysis compared with the result in conventional CZE. Since the separation of concentrated analytes in LVSEP-CZE starts near the cathodic capillary end as in conventional CZE, the electropherogram obtained in LVSEP-CZE were quite similar to that in conventional CZE. All the peak-to-peak distances (d) in LVSEP-CZE (d_{LVSEP}) were 5% smaller than those in conventional CZE (d_{CZE}). As shown in the following equation, d depends on the effective separation length in the uniform electric field,

$$\begin{aligned} d_{\mathrm{CZE}} &= t_{\mathrm{M2,CZE}} - t_{\mathrm{M1,CZE}} \\ &= \frac{Ll_{\mathrm{CZE}}}{V\mu_{\mathrm{ep2}}} - \frac{Ll_{\mathrm{CZE}}}{V\mu_{\mathrm{ep1}}} \\ &= \left(\frac{1}{\mu_{\mathrm{ep2}}} - \frac{1}{\mu_{\mathrm{ep1}}}\right)\frac{L}{V} l_{\mathrm{CZE}} \end{aligned} \tag{3-1}$$

$$\begin{aligned} d_{\mathrm{LVSEP}} &= t_{\mathrm{M2,LVSEP}} - t_{\mathrm{M1,LVSEP}} \\ &= (t_{\mathrm{M2,LVSEP}} - t_{\mathrm{i}}) - (t_{\mathrm{M1,LVSEP}} - t_{\mathrm{i}}) \\ &= \frac{Ll_{\mathrm{LVSEP}}}{V\mu_{\mathrm{ep2}}} - \frac{Ll_{\mathrm{LVSEP}}}{V\mu_{\mathrm{ep1}}} \end{aligned}$$

$$= \left(\frac{1}{\mu_{ep2}} - \frac{1}{\mu_{ep1}}\right)\frac{L}{V} l_{LVSEP} \tag{3-2}$$

where t_M, t_i, V, L, and l are the detection time, starting time of the separation in LVSEP-CZE, applied voltage, whole capillary length, and effective separation length, respectively. Hence, the d_{LVSEP}/d_{CZE} of 0.95 can be assumed as the ratio of the effective separation lengths. Since 5% of the effective separation length of 30 cm or 1.5 cm can be assumed as the position of the sample inversion in LVSEP-CZE, it was revealed that at most 96% of the whole capillary length (38.5 cm) could be used for the effective separation in the LVSEP-CZE analysis. This result shows the good agreement with the inversion position of 94% which was determined by the fluorescence imaging in LVSEP-MCE in the previous paper [18]. It also matched with the value of ($t_{M,LVSEP} - t_{cur}$)/$t_{M,CZE}$ (*e.g.*, for G7 peak, 97%), where t_{cur} is the time when current reaches the half of the stable current in the separation stage of LVSEP-CZE (see the Appendix). Since the current is expected to be drastically increased around the complete removal of SM with the low conductivity, t_{cur} can be approximated as the time of SM removal, or the starting point of separation (t_i). Hence, it is reasonable that ($t_{M,LVSEP} - t_{cur}$)/$t_{M,CZE}$ is identical to the ratio of the effective separation lengths as shown in the following equations.

$$t_{M,CZE} = \frac{Ll_{CZE}}{V\mu_{ep}} \tag{3-3}$$

$$t_{M,LVSEP} - t_{cur} = t_{M,LVSEP} - t_i = \frac{Ll_{LVSEP}}{V\mu_{ep}} \tag{3-4}$$

$$\frac{t_{M,LVSEP} - t_{cur}}{t_{M,CZE}} = \frac{l_{LVSEP}}{l_{CZE}} \tag{3-5}$$

The ratio of the peak areas for oligosaccharides was also examined. Although the

sample solution was injected by pressure in LVSEP, there was a possibility that some slowly migrating analytes might be lost out of the cathodic capillary end by the fast EOF [17]. Hence, the author calculated the peak area ratio of G1, G3, G5, and G10, of which electrophoretic mobility ranged from 1.6×10^{-4} $cm^2V^{-1}s^{-1}$ to 3.4×10^{-4} $cm^2V^{-1}s^{-1}$, whereas the enhanced μ_{EOF} in the LVSEP condition was estimated as 7.0×10^{-4} $cm^2V^{-1}s^{-1}$ (see the Appendix). As a result, the peak area ratio in the LVSEP analysis was estimated to be 1.00:0.52:0.42:0.22, which agreed with the ratio of 1.00:0.51:0.41:0.23 obtained with conventional CZE. This result implied that even slowly migrating analytes were not lost in LVSEP-CZE, which will be helpful for quantitative analysis.

The limit of detection (LOD) of G7 in LVSEP-CZE was evaluated. Since many *N*-linked glycans obtained from glycoproteins consist of more than six monosaccharides, it is reasonable to select G7 as a model analyte. In the LVSEP-CZE analysis, an obtained peak height was plotted against the molar concentration of the analyte to depict the calibration line. In the LVSEP-CZE analysis, the regression slope, intercept, and correlation coefficient (*R*) were calculated to be 3.37×10^{13} M^{-1}, 23.48, and 0.999, respectively, whereas those in conventional CZE were estimated as 6.36×10^{10} M^{-1}, 1.26, and 0.993, respectively (see the Appendix). The LODs (S/N = 3) were estimated to be 1 nM and 2 pM in conventional CZE and LVSEP-CZE, respectively, indicating that a 500-fold sensitivity increase was achieved by LVSEP-CZE.

Analysis of N-linked Glycans Otained from Glycoproteins

Three glycoproteins, bovine RNase B, bovine fetuin, and human AGP were treated with peptide-*N*-glycosidase and acetic acid to obtain asialo *N*-linked glycans. Since

peak assignments and characterizations of the molecular structure were difficult in the analysis of sialo glycans without MS detection, only asialo glycans were analyzed in this study, where the peak assignment was performed by comparing the results with those in the previous reports [14,31,32]. The obtained glycans were derivatized with APTS, followed by the purification with a gel filtration column [30]. This purification could reduce the concentration of unnecessary small ions in a few minutes without significant loss of glycans, resulting in the reduction in both the ionic strength and conductivity (*e.g.* less than ~100 μS/cm) of the sample solution. Although the concentration by LVSEP without sample dilution using deionized water could be carried out, several-fold sample dilution was recommended to obtain good resolution.

The prepared glycan samples were analyzed by LVSEP-CZE. As shown in Figures 3-3–3-5, all glycan samples were successfully concentrated and separated in the LVSEP-CZE analyses without loss of the separation efficiency. Compared with the conventional CZE analyses, the sensitivity enhancement factors (SEFs) were estimated

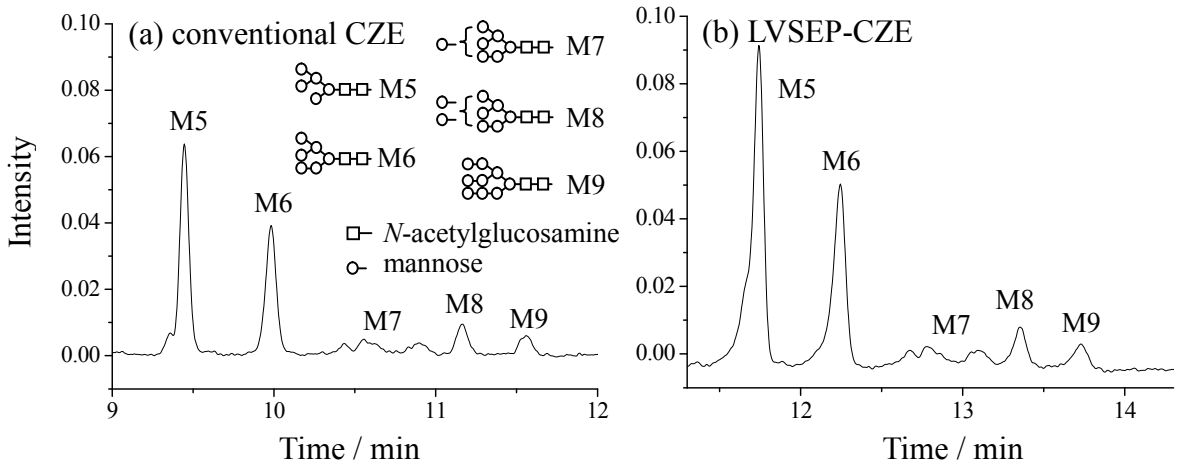

Figure 3-3. (a) Conventional CZE and (b) LVSEP-CZE analyses of oligosaccharides released from ribonuclease B. Sample concentration in LVSEP-CZE was 500-fold lower than that in normal CZE.

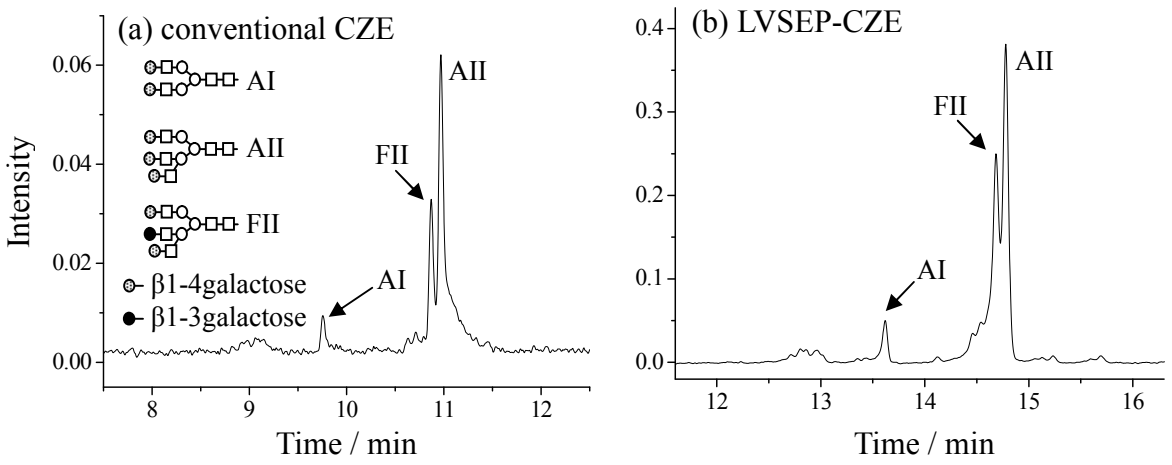

Figure 3-4. Electropherograms of fetuin glycans obtained in (a) conventional CZE and (b) LVSEP-CZE. Sample concentration in LVSEP-CZE was 100-fold lower than that in conventional CZE.

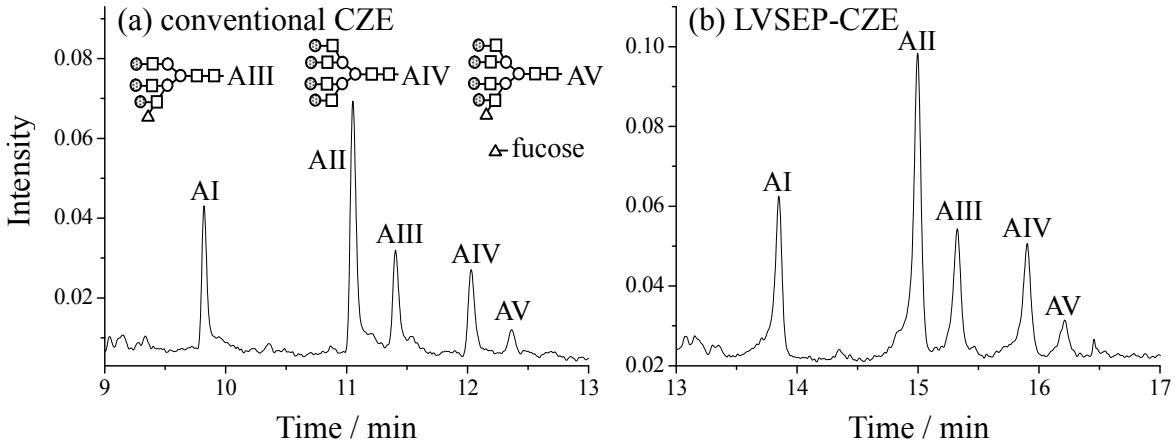

Figure 3-5. (a) Conventional CZE and (b) LVSEP-CZE analyses of glycans obtained from AGP. Sample concentration in LVSEP-CZE was 400-fold lower than that in conventional CZE.

to be ranging from 400 to 770 as summarized in Table 3-1. As far as the author knows, these SEF values were the best compared to previous papers on the online concentration of oligosaccharides in CE. This is because LVSEP can stack the theoretically maximum amount, *i.e.*, whole capillary volume, of analytes in the case of

the pressure injection. These results showed the high concentration performance of LVSEP-CZE and its compatibility with the oligosaccharide analysis. For the further concentration by LVSEP, the longer capillary should be used although the longer analysis time will be taken.

Table 3-1. SEFs of oligosaccharides obtained with the LVSEP-CZE analysis.

	M5	M9	AI	AV	FII
SEF	770	750	400	520	–

In the research on the glycoprotein activity, quantification of each structure of glycans including minor ones is very important [33]. In the conventional CZE analysis of glycans from human AGP, the peak intensity was so low that the author could not detect more than 10 minor glycan peaks. To detect more minor glycan peaks, LVSEP

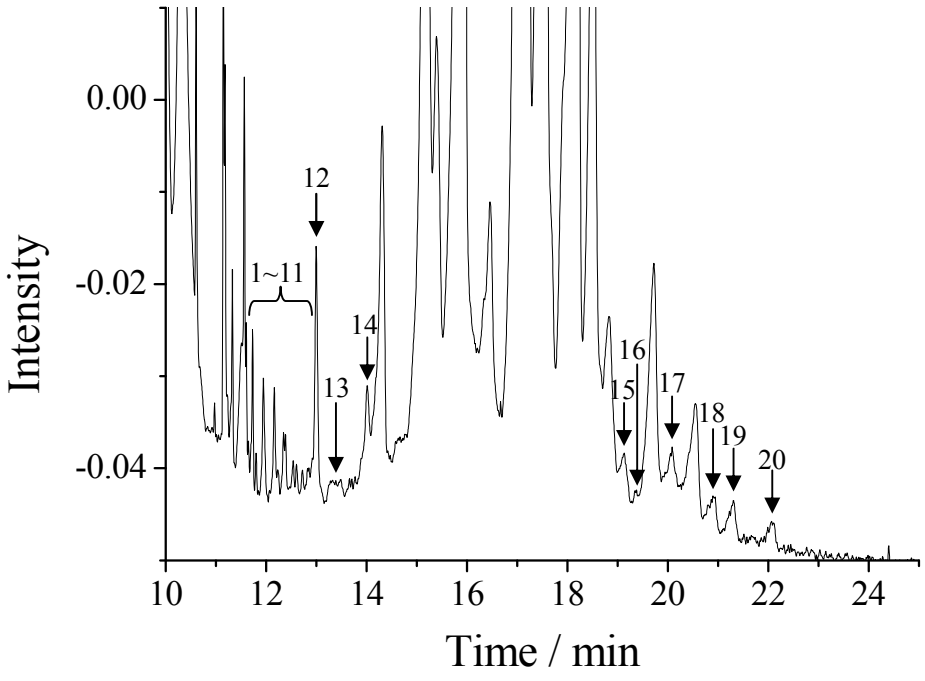

Figure 3-6. Detection of minor glycans obtained from AGP by LVSEP-CZE. 20 peaks indicated with arrows could not be detected in conventional CZE.

was applied. As a typical result, at least 20 more peaks could be detected in the LVSEP-CZE analysis as shown in Figure 3-6 despite the sample concentration was 10-fold lower than that in conventional CZE. When the original sample solution was analyzed by LVSEP-CZE, the main glycan peaks became broader, which impaired the separation of minor peaks. For further better detectability of minor peaks, higher performance desalting column would be necessary. Although the author could not confirm the glycan structure of minor peaks without MS detection system in this study, LVSEP-CZE showed good potential for studying minor glycans.

Table 3-2. Separation parameters in LVSEP-CZE and conventional CZE.

sample	analytical mode	Rs^a	d^a / min	$W_{1/2}{}^b$ /min
RNase B	CZE	4.7	0.53	0.059
	LVSEP-CZE	4.0	0.50 (94%)	0.069 (117%)
Fetuin	CZE	–	1.11	0.058
	LVSEP-CZE	–	1.06 (95%)	0.066 (114%)
AGP	CZE	14.5	1.23	0.048
	LVSEP-CZE	10.7	1.14 (93%)	0.060 (125%)

[a] Resolution or peak distance between the first two peaks, M5–M6, AI–FII, or AI−AII.

[b] Width at half of the highest peak intensity for M5 or AI.

Resolution for the first- and second-migrating peaks was also examined (Table 3-2). Although the author could not estimate the correct resolution of oligosaccharides from fetuin due to the peak overlap, the resolution values obtained with LVSEP analyses of oligosaccharides released from other glycoproteins were as low as 74%–85% of those in conventional CZE. Since d_{LVSEP}/d_{CZE} ranged from 93% to 95% as shown in Table 3-2, the decrease in resolution was not caused only by the difference in the separation length, but mainly by the increase in the peak width. The peak width at the half height ($W_{1/2}$)

was also shown in Table 3-2, where $W_{1/2}$ in the LVSEP-CZE analysis was as wide as 114%–125% of $W_{1/2}$ in the conventional CZE. This band broadening or the peak fronting is caused by the sample diffusion in the concentration step in LVSEP. Hence, the suppression of the molecular diffusion by an addition of some gel reagents and/or additional application of another concentration process to reduce the band broadening effect will be necessary to obtain the better resolution.

Table 3-3. Repeatability in LVSEP-CZE and conventional CZE.

sample	analytical mode	%RSD of t_M[a]	%RSD of peak height[a]	%RSD of peak area[a]
RNase B	CZE	0.1	9.0	10.9
	LVSEP-CZE	1.3	1.2	2.8
Fetuin	CZE	0.1	19.6	4.1
	LVSEP-CZE	0.1	1.7	4.9
AGP	CZE	0.2	13.0	13.4
	LVSEP-CZE	0.4	1.4	4.1

[a] RSDs for the first peak, M5 or AI (n = 3).

To evaluate the analytical reproducibility, relative standard deviations (RSDs) of t_M, the peak height, and peak area were calculated. As summarized in Table 3-3, the RSDs of t_M in the LVSEP-CZE analysis of M5 or AI from glycoproteins were higher than those in conventional CZE. It should be noted that the unstable EOF rate in LVSEP caused poor repeatability of the starting time of the separation or t_{cur}. As shown in the previous section, the author can predict the starting time of the separation from the current change. Hence, when t_M of the analyte was corrected with subtraction by t_{cur} or by t_M of free APTS which was used as an internal standard, the RSD was improved to less than 0.1%. If the SM contains many salts which make the SM removal very slow,

the approximation of t_{cur} as t_i may be incorrect. This would make the correction of the detection time less efficient. On the other hand, the RSDs of the peak height in LVSEP-CZE were as good as 1.2%–1.7%, which were better than those in conventional CZE, 9.0%–19.6%. In conventional CZE, the sample solution was injected by a weak pressure of 0.3 psi for just 3.0 s to avoid the band broadening, resulting in less repeatable sample injection with poor RSD values. In contrast, the injected sample volume in LVSEP-CZE was constantly equal to the column volume, so that the repeatable injection with good RSD values could be performed. The RSD values of the peak area in LVSEP-CZE (2.8%–4.9%) were smaller than those in conventional CZE (4.1%–13.4%), which showed the good agreement with the discussion mentioned above.

The analytical performance of LVSEP-CZE in the oligosaccharide analysis was compared with that of the other online concentration methods [13–16]. The sensitivity enhancement factors (SEFs) more than 400 in LVSEP-CZE were higher than those ever reported. This is because the largest-volume sample could be stacked to a narrow band. Although Kamoda *et al*. reported the field-amplified sample injection method with up to a 360-fold sensitivity increase, the obtained repeatability was poor because the repetitive electrokinetic sample injection changes the balance of the ion components in the sample solution [24,25]. On the other hand, the repeatability in LVSEP-CZE was sufficient for the peak assignment. The separation performance of LVSEP-CZE was also comparable to or better than the other online sample concentration methods. This was because a long effective separation length can be utilized in LVSEP-CZE. The experimental procedure of LVSEP-CZE was quite simple: only the application of a constant voltage to the capillary entirely filled with the sample solution. Hence, no

optimization of the sample injection was required unlike in the other online concentration techniques. Therefore, LVSEP-CZE realized the quite high sensitivity improvement with good repeatability in a simple experimental procedure for the oligosaccharide analysis.

3-4. Conclusions

The effects of the EOF velocity and the conductivity of the sample matrix on the concentration and separation performance of LVSEP-CZE using the PVA-coated capillary were investigated. The author found that the γ larger than 20 and the ionic strength of the sample less than 740 μM were needed to obtain the LVSEP effect. In the LVSEP-CZE analysis of oligosaccharides, up to a 2500-fold sensitivity improvement, good resolution utilizing long effective separation length with 95% of the total length, and good repeatability were achieved with a simple experimental procedure. Since LVSEP-CZE can be performed without diluting the sample solution, LVSEP should be widely applied to the CE analysis of various oligosaccharides. The high analytical performance will also contribute to the more practical analyses not only for oligosaccharides but also anionic biomolecules, *e.g.*, DNA, peptides, proteins, organic acids, metabolites, and so on.

3-5. Appendix

Estimation of the EOF Rate in the EOF-suppressed Capillary

In LVSEP-CZE, the EOF in the capillary should be suppressed in the high ionic

strength BGS zone and enhanced in the low ionic strength SM zone. In the previous paper [18], it was shown that μ_{EOF} in the PVA-coated PDMS microchannel was proportional to $I^{-1/2}$ of the BGS, where μ_{EOF} and I are the electroosmotic mobility and ionic strength, respectively. To confirm the enhanced EOF effect in CE, μ_{EOF} in the PVA-coated fused silica capillary was investigated. Thiourea was employed as an EOF marker and was analyzed in the conventional CZE mode using the HEPES buffer of which concentration was ranging from 0.1 to 25 mM. As a result, a linear relationship between μ_{EOF} and $I^{-1/2}$ was observed as shown in Figure S2, where μ_{EOF} in deionized water was enhanced to be 5.0×10^{-4} $cm^2V^{-1}s^{-1}$ and that in the 25 mM HEPES buffer was suppressed to be 3.0×10^{-5} $cm^2V^{-1}s^{-1}$. Such drastic changes in the EOF rate agreed with the μ_{EOF} values determined in the PVA-coated PDMS microchannel [18]. The author also estimated μ_{EOF} of the poly(vinyl pyrrolidone) (PVP)-coated capillary, where

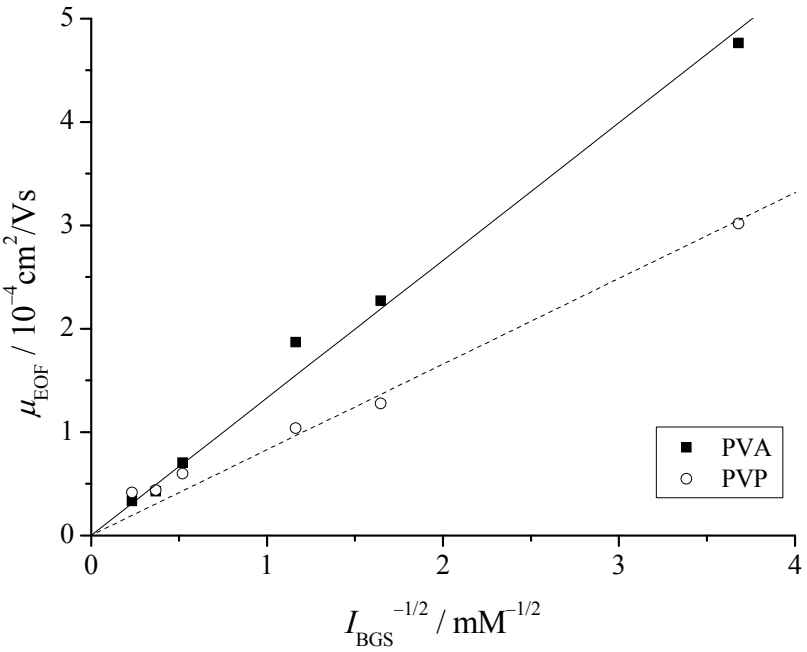

Figure A3-1. Dependence of the electroosmotic mobilities in the EOF-suppressed capillary on the HEPES concentration in the SM ranging from 0.1 to 10 mM. Closed squares and open circles represent μ_{EOF} obtained in the PVA-coated and PVP-coated capillary, respectively.

similar relationship between μ_{EOF} and $I^{-1/2}$ was observed. Since LVSEP could be conducted in the PVP-coated capillary, the estimation of the EOF by the ionic strength will be useful to check whether the capillary is suitable for LVSEP or not.

Estimation of the EOF Rate in the LVSEP process

It has been proved that the EOF is enhanced in a low *I* solution both in the capillary and the microchannel. However, there has not been the direct evidence of the EOF occurrence in the LVSEP process. Hence, the EOF marker (thiourea) was analyzed by LVSEP-CZE. Since neutral thiourea migrates only by the EOF, its detection shows the detection of the EOF. In this analysis, the HEPES buffer containing thiourea and deionized water were employed as the BGS and the sample solution, respectively (Figure A3-2), where no analyte was concentrated but the EOF introduced the BGS into the capillary until completely filled, resulting in the baseline increase in the UV absorbance signal by thiourea in the BGS. As a result, a baseline shift was observed at 1.4 min (Figure A3-3) at the detection point of 30 cm from the anodic capillary end, indicating the generation of quite fast EOF with μ_{EOF} of 7.0×10^{-4} $cm^2V^{-1}s^{-1}$ in average. This value was 1.4-times larger than μ_{EOF} of 5.0×10^{-4} $cm^2V^{-1}s^{-1}$ in deionized water shown above, which contradicts the theoretical model shown in the previous paper: the EOF is gradually decreased as the BGS is introduced into the capillary, so that μ_{EOF} should have been less than 5.0×10^{-4} $cm^2V^{-1}s^{-1}$ in average. Therefore, the faster EOF indicates the gradual increase in the EOF velocity due to the change in pH, the ionic strength and/or electric field in the SM zone. The ion balance in the SM zone containing little electrolyte could easily be changed near the boundary with the BGS, through where several ions such as H^+, OH^-, $HEPES^-$, Na^+ migrated. In the simulation using the

SIMUL software (http://web.natur.cuni.cz/~gas/), actually, a little change was observed in pH with up to 0.5 and in the ionic strength and conductivity with up to a two-fold increase. More detailed study is now in progress in Otsuka laboratory.

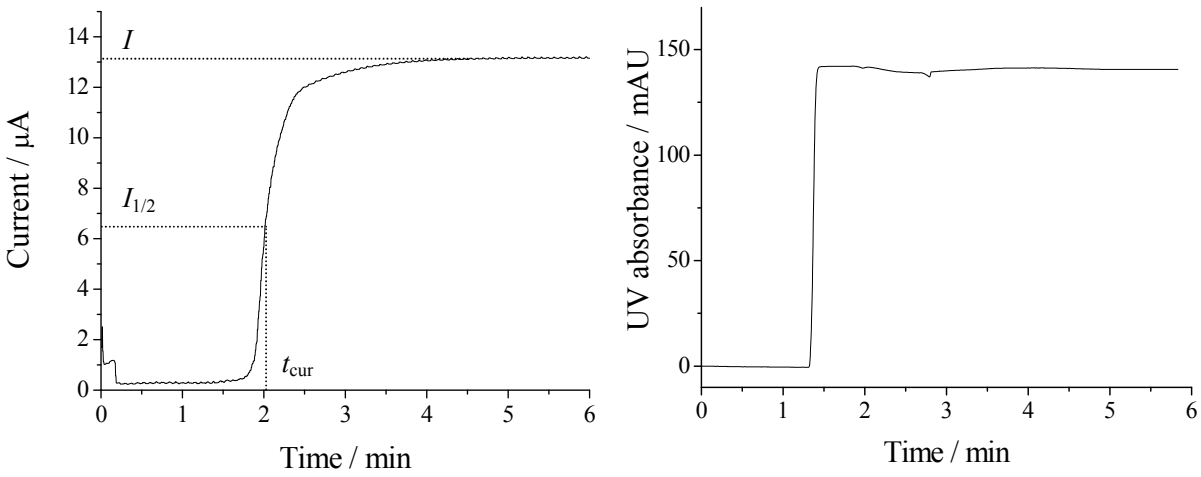

Figure A3-2. Changes of the baseline signal and the electric current in LVSEP-CZE. The PVA-coated capillary was filled with deionized water as a blank sample solution, and the HEPES buffer containing 100 ppm thiourea was employed as the BGS. Applied voltage was 20 kV.

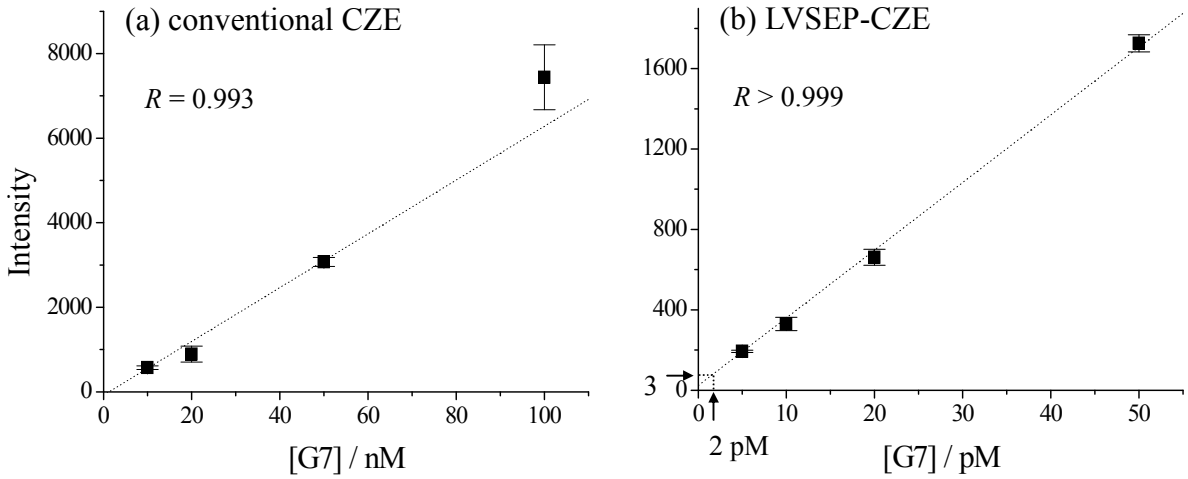

Figure A3-3. Calibration curve of G7 obtained with (a) conventional CZE and (b) LVSEP-CZE.

3-6. References

[1] Ghazarian, H.; Idoni, B.; Oppenheimer, S.B. *Acta Histochem.* **2011**, *113*, 236–247.

[2] Smets, L. A.; van Beek, W. P. *Biochim. Biophys. Acta* **1984**, *738*, 237–249.

[3] Makrilia, N.; Kollias, A.; Manolopoulos, L.; Syrigos, K. *Cancer Invest.* **2009**, *27*, 1023–1037.

[4] Geyer, H.; Geyer, R. *Biochim. Biophys. Acta* **2006**, *1764*, 1853–1869.

[5] Alpert, A. J.; Shukla, M.; Shuklab, A. K.; Zieske, L. R.; Yuenc, S. W.; Fergusond, M. A. J.; Mehlertd, A.; Pauly, M.; Orlando, R. *J. Chromatogr. A* **1994**, *676*, 191–202.

[6] Hardy, M. R.; Townsend, R. R.; Lee, Y. C. *Anal. Biochem.* **1988**, *170*, 54–62.

[7] Rassi, Z. E. *Electrophoresis* **1999**, *20*, 3134–3144.

[8] Amon, S.; Zamfir, A. D.; Rizzi, A. *Electrophoresis* **2008,** *29*, 2485–2507.

[9] Burgi, D. S.; Chien, R.-L. *Anal. Biochem.* **1992**, *202*, 306–309.

[10] Quirino, J. P.; Terabe, S. *Anal. Chem.* **1999**, *71*, 1638–1644.

[11] Timerbaev, A. R.; Hirokawa, T. *Electrophoresis* **2006**, *27*, 323–340.

[12] Britz-McKibbin, P.; Chen, D. D. Y. *Anal. Chem.* **2000**, *72*, 1242–1252.

[13] Quirino, J. P.; Terabe, S. *Chromatographia* **2001**, *53*, 285–289.

[14] Kamoda, S.; Nakanishi, Y.; Kinoshita, R.; Ishikawa, M.; Kakehi, K. *J. Chromatogr. A* **2006**, *1106*, 67–74.

[15] Auriola, S.; Thibault, P.; Sadovskaya, I.; Altman, E. *Electrophoresis* **1998**, *19*, 2665–2676.

[16] Kazarian, A. A.; Hilder, E. F.; Breadmore, M. C. *J. Chromatogr. A* **2008**, *1200*, 84–91.

[17] He, Y.; Lee, H. K. *Anal. Chem.* **1999**, *71*, 995–1001.

[18] Kawai, T.; Sueyoshi, K.; Kitagawa, F.; Otsuka, K. *Anal. Chem.* **2010,** *82*, 6504–6511.

[19] Han, J. H.; Chun, M.-S.; Riaz, A.; Chung, D. S. *Electrophoresis* **2005,** *26*, 480–486.

[20] Chun, M.-S.; Chung, D. S. *Anal. Chim. Acta* **2003**, *491*, 173–179.

[21] Zhu, Z.; Zhang, L.; Marimuthu, A.; Yang, Z. *Electrophoresis* **2002,** *23*, 2880–2887.

[22] Macià, A.; Borrull, F.; Aguilar, C.; Calull, M. *Electrophoresis* **2003**, *24*, 2779–2787.

[23] Kim, J.; Chun, M.-S.; Choi, K.; Chung, D. S. *Electrophoresis* **2009**, *30*, 1046–1051.

[24] Chun, M.S.; Kang, D.; Kim, Y.; Chung, D. S. *Microchem. J.* **2001**, *70*, 247–253.

[25] Kim, B.; Chung, D. S. *Electrophoresis* **2002**, *23*, 49–55.

[26] Lee, J. H.; Choi, O.-K.; Jung, H. S.; Kim, K.-R.; Chung, D.S. *Electrophoresis* **2000**, *21*, 930–934.

[27] Gllges, M.; Kleemlss, M. H.; Schomburg, G. *Anal. Chem.* **1994**, *66*, 2038–2046.

[28] Okamoto, Y.; Kitagawa, F.; Otsuka, K. *Anal. Chem.* **2007**, *79*, 3041–3047.

[29] Chien, R.-L.; Helmer, J. C. *Anal. Chem.* **1991**, *63*, 1354–1361.

[30] Huhn, C.; Pyell, U. *J. Chromatogr. A* **2010**, *1217*, 4476–4486.

[31] Dang, F.; Kakehi, K.; Cheng, J.; Tabata, O.; Kurokawa, M.; Nakajima, K.; Ishikawa, M.; Baba, Y. *Anal. Chem.* **2006**, *78*, 1452–1458.

[32] Suzuki, H.; Müller, O.; Guttman, A.; Karger, B. L. *Anal. Chem.* **1997**, *69*, 4554–4559.

[33] Gennaro, L. A.; Salas-Solano, O. *Anal. Chem.* **2008**, *80*, 3838–3845.

Chapter 4.

Highly Sensitive Chiral Analysis in Capillary Electrophoresis with Large-volume Sample Stacking with an Electroosmotic Flow Pump

4-1. Introduction

Chiral compounds are recognized to play important roles in chemistry, biology, medicine, and pharmacology [1–3], so that the analytical methods for the chiral compounds require the high sensitivity, high optical resolution, and short analysis time. Among several chiral separation methods, such as high-performance liquid chromatography (HPLC), gas chromatography, and capillary electrophoresis (CE), CE exhibits high resolution with little sample consumption in a short analysis time. Several separation modes have been developed for chiral separation in CE, including micellar electrokinetic chromatography (MEKC), cyclodextrin (CD)-modified capillary zone electrophoresis (CDCZE), CD electrokinetic chromatography (CDEKC), CD-modified MEKC (CDMEKC), affinity capillary electrophoresis (ACE), and nonaqueous CE (NACE) [4–6]. However, the concentration sensitivity is quite poor because of the short optical path length and the small injection volume of sample solution.

To overcome such the drawback of CE, several online sample preconcentration techniques have been developed [7–21]. Although up to 1,000-fold sensitivity increases have been achieved in chiral analysis [7–16], optimization of the preconcentration conditions is usually required because the resolution was reduced due to the decrease in the effective separation length accompanying the increase in the sample injection

volume [17–19]. Since the enantioseparation is not so easy without the optimal electrolyte composition, additional optimization of the preconcentration condition is one of the most serious disadvantages. Moreover, highly efficient preconcentration techniques often require multi-step procedures [16,20], which are quite bothersome and often cause the reduction in the analytical reproducibility. Hence, the author focused on an online sample preconcentration technique using field amplified sample stacking, large-volume sample stacking with an electroosmotic flow (EOF) pump (LVSEP) [21–23], which provides the high sensitivity with almost no loss of resolution in a simple experimental procedure. In the author's previous work [22], up to 780-fold sensitivity increases were achieved with good separation performance in the CE analysis of oligosaccharides. Moreover, we did not need to optimize the sample injection volume, because the sample filled in the whole capillary could be concentrated. Thus, the application of LVSEP to the chiral analysis in CE is expected to improve the sensitivity with high enantioseparation efficiency and to minimize the optimization procedure of the experimental conditions and the multi-step preconcentration procedure.

In spite of the high preconcentration and separation ability of LVSEP, there has been no report on the separation performance in combining LVSEP with any separation modes except for the most basic separation mode, capillary zone electrophoresis (CZE). In LVSEP, the separation performance is determined by the inversion position of the sample migration where the EOF velocity and electrophoretic velocity of the analyte in a background solution (BGS) is balanced [23]. Hence, the change in the effective electrophoretic mobility in the different separation mode can cause the increase or decrease in the resolution. It is important to consider the effect of the separation mode on the resolution both theoretically and experimentally.

The author's aims in this study are to clarify the effects of the separation mode on the resolution in LVSEP and to achieve the efficient improvement of the concentration sensitivity without loss of optical resolution and without complicated experimental procedures including the optimization steps. Theoretical investigation on the resolution in the LVSEP-applied chiral analysis using CDs as chiral selectors was performed by estimating the inversion position, which is expected to directly affect the effective separation length. Three enantioseparation modes, CDCZE, CDEKC, and CDMEKC, were carried out to evaluate the performance of the sensitivity improvement and the enantioseparation. An enantio-excess (EE) assay was also carried out in LVSEP-CDCZE. Finally, the author performed the analysis of a drug component dissolved in a urine matrix to show how to analyze real samples containing a large amount of unnecessary background salts. The purification using a C18 solid-phase extraction (SPE) column was applied for the LVSEP analysis of the urine sample.

4-2. Experimental Section

Materials and Chemicals

A fused silica capillary was purchased from Polymicro Technologies (Phoenix, AZ, USA), poly(vinyl alcohol) (PVA, M_w = 88,000, 99% hydrolyzed) was obtained from Japan Vam and Poval (Osaka, Japan), warfarin was purchased from Dr. Ehrenstorfer GmbH (Augsburg, Germany), thiourea, (±)-abscisic acid, racemic ibuprofen, (S)-(+)-2-(4-isobutylphenyl)propionic acid ((S)-ibuprofen), 2,6-di-*O*-methyl-β-cyclodextrin (DM-β-CD), and 2,3,6-tri-*O*-methyl-β-cyclodextrin (TM-β-CD) were purchased from Wako (Osaka, Japan), quaternary β-cyclodextrin

(QA-β-CD) and DL-leucine were purchased from Sigma-Aldrich (St. Louis, MO, USA), and all other reagents were purchased from Nacalai Tesque (Kyoto, Japan). All solutions were prepared with deionized water purified by using a Direct-Q System (Nihon Millipore, Japan), and filtered through a 0.45 μm pore membrane filter (Nacalai Tesque) prior to use.

Derivatization of Amino Acids

Amino acids were derivatized with fluorescein isothiocyanate (FITC) for laser-induced fluorescence (LIF) detection as in the previous report [24]. Briefly, 5 μL of 50 mM amino acids and 5 μL of 50 mM FITC dissolved in 50 mM borate buffer (pH 9.5) were mixed and left for 24 h at room temperature. The solution was diluted with deionized water or a BGS for the appropriate concentrations.

SPE Purification of Urine Sample

Urine samples spiked with ibuprofen were purified with a C18 SPE column (Inert Sep C18, GL science, Kyoto, Japan). Urine was sampled from a healthy male volunteer and filtered with a 0.45 μm pore membrane filter. Ibuprofen dissolved in methanol (1%, w/v) was spiked in the urine for certain concentration, followed by adjusting pH to around 3 by adding 6 M hydrochloric acid. After conditioning the SPE column with 1 mL methanol and 1 mL water, 500 μL of the urine sample was passed through the cartridge with a gentle gravity pressure at a flow rate of about 0.3 mL/min. The column was washed with 1.5 mL of water, 0.5 mL of 25 mM formic acid in ACN/water (20/80, v/v), and 1.5 mL of water again. Ibuprofen was then eluted with 0.5 mL of ACN. The eluent was lyophilized and the residue was diluted with 500 μL of water for the LVSEP

analysis.

Capillary Coating

A fused silica capillary was coated with PVA in the same way as the previous papers [22,25,26]. Briefly, the capillary was activated and washed with 1 M NaOH and water, followed by the injection of a 5% PVA solution into the whole capillary. Both the capillary ends were immersed in the same PVA solution and left at room temperature for 15 min. The PVA solution was then removed out of the capillary and the capillary was heated at 140 °C for 18 h under a nitrogen gas flow. The capillary was filled with deionized water and stored at room temperature. Prior to use, the capillary was flushed with a BGS for 15 min.

Apparatus

All CE experiments were performed on a P/ACE MDQ system (Beckman Coulter, Fullerton, CA, USA) equipped with a diode-array UV detector or a LIF detector. The LIF detector used in the LVSEP-CDMEKC analysis consisted of a 488 nm argon ion laser module and photomultiplier detector with a 520 nm band pass filter. UV detection was performed at 200 nm in LVSEP-CDCZE or 250 nm in LVSEP-CDEKC.

Analytical Procedure

The capillary with total/effective lengths of 40/30 cm was employed in the CDCZE analysis and that of 60/50 cm in the CDEKC and CDMEKC analyses. They were conditioned with deionized water in applying LVSEP or with the BGS in the conventional CDCZE/CDEKC/CDMEKC analyses at 20 psi for 3 min prior to each run.

Sample injections were performed with a pressure of 20 psi for 90 s (whole capillary injection) in the LVSEP-applied analyses or 0.3 psi for 3 s in the other conventional analyses. The applied voltage and the temperature were set at –30 kV and 25 °C, respectively, except in the CDCZE analysis of ibuprofen with voltage application of − 25 kV.

4-3. Results and Discussion

Theoretical Consideration

In LVSEP-CDCZE/CDEKC/CDMEKC, the EOF-suppressed capillary is filled with a low ionic strength solution containing anionic analytes, whereas the inlet and outlet vials are filled with the high ionic strength BGS containing CD (Figure 4-1a). After applying the voltage, anionic analytes are concentrated at the sample matrix (SM)/BGS boundary by the difference in the electric field strength between the two zones. The focused analytes move toward the cathode and the BGS is introduced into the capillary by the enhanced EOF in the low ionic strength SM (Figure 4-1b). As the analytes migrate toward the cathode, the EOF velocity becomes slower and the electric field strength in the BGS becomes higher (Figure 4-1c). When almost all the SM in the capillary is removed out from the cathodic capillary end, the electrophoretic velocity of the analytes exceeds the EOF rate, resulting in the inversion of the sample migration direction (Figure 4-1d). After the complete removal of the SM, the analytes are separated by CDCZE/CDECK/CDMEKC during the anodic migration (Figure 4-1e).

In the LVSEP analysis, the inversion position of the concentrated analytes is significant for the separation performance [23]. To estimate the effects of the difference

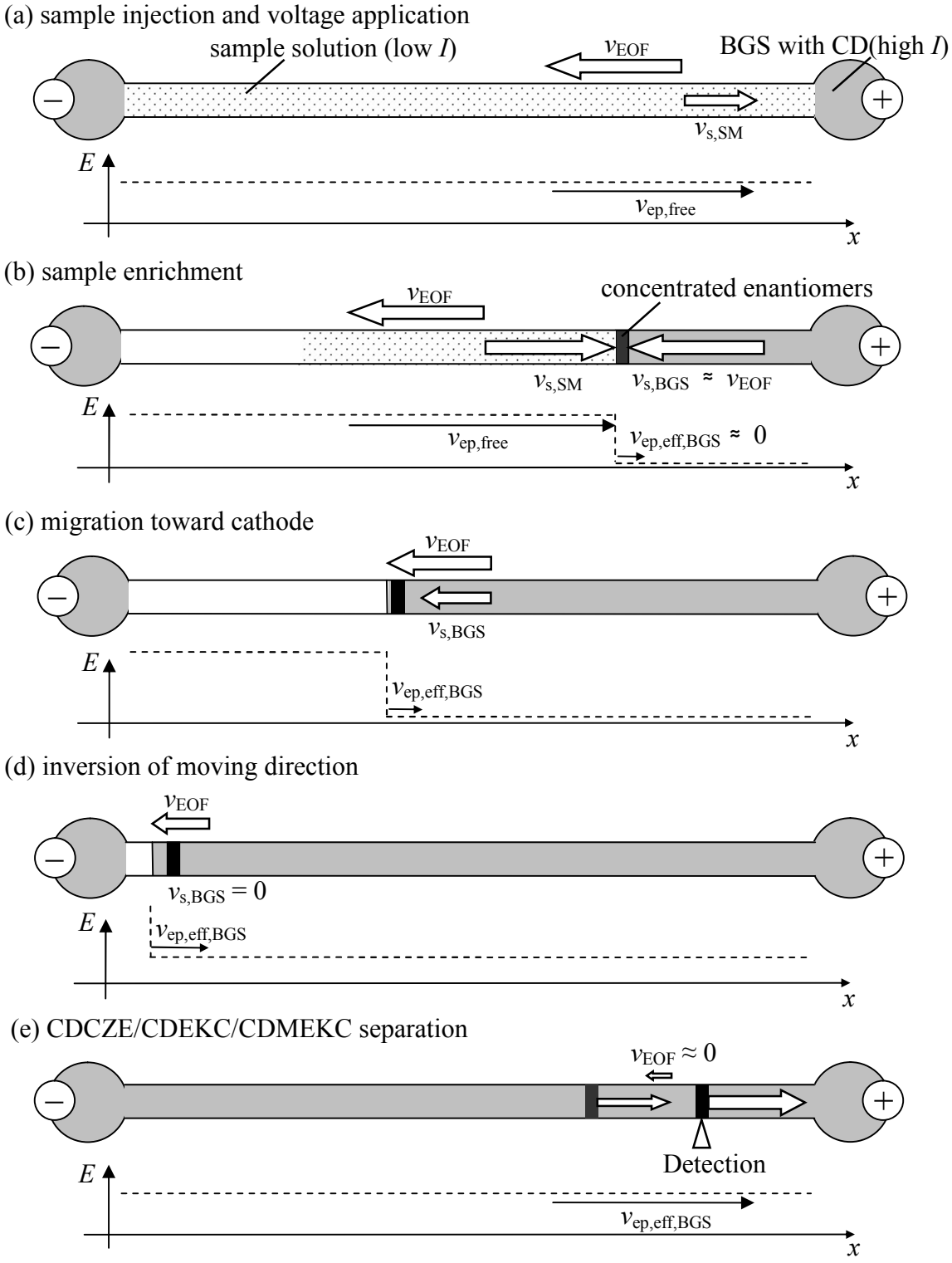

Figure 4-1. Concept of LVSEP-CDCZE/CDEKC/CDMEKC in the PVA-coated capillary. v_{ep}, v_{EOF} and v_s mean the electrophoretic velocity of the analyte, the EOF velocity, and apparent velocity of the analyte, respectively.

in the separation mode from normal CZE employed in the previous studies, the inversion position is theoretically considered. In the CDCZE/CDEKC analysis, the effective electrophoretic velocity in the BGS ($v_{ep,eff,BGS}$) is expressed as follows [27]:

$$\begin{aligned} v_{ep,eff,BGS} &= \left(\frac{1}{(K_b[CD]+1)} \mu_{ep,free} + \frac{K_b}{(K_b[CD]+1)} \mu_{ep,complex} \right) \frac{V}{L} \\ &= \mu_{ep,eff,BGS} \frac{V}{L} \end{aligned} \quad (4\text{-}1)$$

where $\mu_{ep,free}$, $\mu_{ep,complex}$, $\mu_{ep,eff,BGS}$, K_b, [CD], L, V are the electrophoretic mobilities of the free analyte and the analyte-CD complex, effective electrophoretic mobility of the analyte in the BGS, binding constant of the analyte with CD, the concentration of CD, whole capillary length, and applied voltage, respectively. From Eq. (1), the author theoretically calculated the band width (w) and inversion position of the concentrated analyte from the inlet capillary end ($x_{sc,i}$) in the same way discussed in the previous paper [23]. The detailed calculation process is shown in the Supporting Information. The estimated results are expressed as follows.

$$w = -\frac{\mu_{ep,eff,BGS} L}{\gamma \mu_{EOF,SM}} \ln\left(-\frac{e\mu_{EOF,SM}}{\mu_{ep,free}} \right) \quad (\text{when } \mu_{EOF,SM} > -\mu_{ep,free}) \ (4\text{-}2\text{-}1)$$

$$w = -\frac{\mu_{ep,eff,BGS}}{\mu_{ep,free}} \frac{L}{\gamma} \quad (\text{when } \mu_{EOF,SM} \le -\mu_{ep,free}) \ (4\text{-}2\text{-}2)$$

$$x_{sc,i} = -\frac{\mu_{ep,eff,BGS} L}{\gamma \mu_{EOF,SM}} \ln \gamma \quad (\text{when } \mu_{EOF,SM} > -\mu_{ep,free}) \ (4\text{-}3\text{-}1)$$

$$x_{sc,i} = -\frac{\mu_{ep,eff,BGS} L}{\gamma \mu_{EOF,SM}} \ln\left(-\frac{e\gamma\mu_{EOF,SM}}{\mu_{ep,free}} \right) - \frac{\mu_{ep,eff,BGS}}{\mu_{ep,free}} \frac{L}{\gamma} \quad (\text{when } \mu_{EOF,SM} \le -\mu_{ep,free}) \ (4\text{-}3\text{-}2)$$

where $\mu_{EOF,SM}$, γ, and e are the electroosmotic mobility in the SM, conductivity ratio between the SM and the BGS, and base of the natural logarithm, respectively. It should

be noted that all the estimated values are changed from those previously reported by the factor of $\mu_{ep,eff,BGS}/\mu_{ep,free}$. In the case of CDMEKC with more complicated interactions between the micelle, CD, and analytes, the same consideration can also be carried out because not the complicated interactions but only the obtained value of $\mu_{ep,eff,BGS}$ is important in this calculation.

In terms of w, it becomes narrower if the ratio $\mu_{ep,eff,BGS}/\mu_{ep,free}$ is smaller than unity, which means that the analytes are more sharply focused. To the author's knowledge, however, w mainly depends on the molecular diffusion in the separation step [23], so that the effect of $\mu_{ep,eff,BGS}/\mu_{ep,free}$ will be limited.

In terms of $x_{sc,i}$, the theoretical calculation was carried out on the basis of Eq. (4-3-1). In LVSEP using a PVA-coated capillary, typical $\mu_{EOF,SM}$ of 5.0×10^{-4} $cm^2V^{-1}s^{-1}$ is usually larger than $\mu_{ep,free}$ of most anionic analytes so that Eq. (4-3-1) should be applied. The calculation was performed in the case of the typical LVSEP conditions, $\mu_{ep,free} = -1.0 \times 10^{-4}$ $cm^2V^{-1}s^{-1}$ and $\mu_{EOF,SM} = 5.0 \times 10^{-4}$ $cm^2V^{-1}s^{-1}$. The estimated inversion positions of the concentrated analytes from the anodic capillary end are summarized in Table 4-1. The inversion position shifts toward the cathode if the ratio $\mu_{ep,eff,BGS}/\mu_{ep,free}$ is smaller than unity, which means that longer part of the capillary can be used for the effective separation. In the chiral analysis of anionic analytes, CDCZE with neutral chiral selectors or CDEKC with cationic chiral selectors are often employed, because the reduction in the electrophoretic mobility extends the separation window. Hence, $\mu_{ep,eff,BGS}/\mu_{ep,free}$ is often smaller than unity, where more efficient sample concentration and separation with more than 99% effective separation length are expected as shown in Table 4-1. In CDMEKC, on the other hand, the analytes interact with the fast migrating surfactant so that $\mu_{ep,eff,BGS}/\mu_{ep,free}$ tends to be more than unity. In

this case, the inversion position moves toward the anode especially with small γ, causing less effective separation. As shown in Table 4-1, however, the effective separation length was estimated to be more than 93.74% indicating the loss of separation length will not be so significant. In general, loss of effective separation length would be more minimized by reducing the salt concentration of the SM and by making the conductivity of the BGS high to provide enough large γ.

Table 4-1. Theoretical estimation of the inversion position of the concentrated analytes from the anodic capillary end.

$\mu_{ep,eff,BGS}/\mu_{ep,free}$	γ				
	50	100	200	500	1,000
0.25	99.61	99.77	99.87	99.94	99.97
0.5	99.22	99.54	99.74	99.88	99.93
1	98.44	99.08	99.47	99.75	99.86
2	96.87	98.16	98.94	99.50	99.72
4	93.74	96.32	97.88	99.01	99.45

Calculation condition, $\mu_{ep,free} = -1.0 \times 10^{-4}$ $cm^2V^{-1}s^{-1}$ and $\mu_{EOF,SM} = 5.0 \times 10^{-4}$ $cm^2V^{-1}s^{-1}$.
Expressed as %ratio of the whole capillary length.

LVSEP-CDCZE of Warfarin

The most fundamental enantioseparation mode, CDCZE using neutral CD was coupled with LVSEP. To compare the separation performance with that of the conventional analysis, the same experimental conditions were employed such as the capillary length, applied voltage, and BGS composition, except for the sample concentration and sample matrix. The same strategy was also applied to the CDEKC and CDMEKC analyses in this study.

In the CDCZE analysis, warfarin was analyzed as a model analyte employing 10 mM DM-β-CD as a neutral chiral selector in 25 mM MES buffer (pH 6.0), in

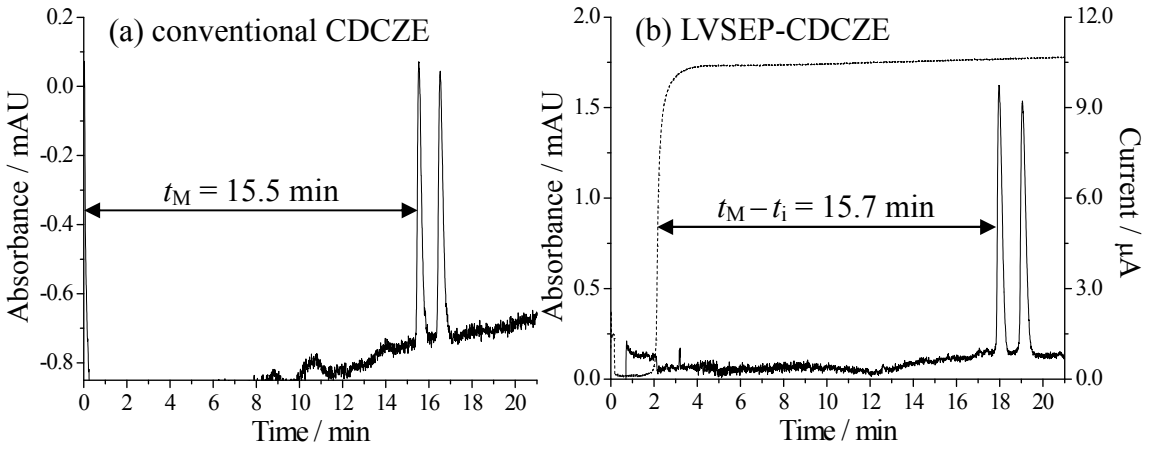

Figure 4-2. Electropherograms of warfarin obtained in (a) conventional CDCZE and (b) LVSEP-CDCZE. Sample concentration, (a) 50 ppm and (b) 100 ppb; UV detection, 200 nm. The broken line represents the current change in LVSEP-CDCZE.

accordance with the previous paper [28,29]. In the conventional CDCZE analysis, 50 ppm warfarin was well optically separated (Figure 4-2a) with the resolution of 2.5 (Table 4-2). In the LVSEP-CDCZE analysis, on the other hand, even 100 ppb racemic warfarin could be detected with the resolution of 2.6 (Figure 4-2b), where the sensitivity enhancement factor (SEF) was estimated to be 1,000. Since the noise level in LVSEP-CDCZE was similar to that in conventional CDCZE, the SEF was simply calculated from the following equation:

$$\mathrm{SEF} = \frac{h_{\mathrm{LVSEP}}}{h_{\mathrm{Conventional}}} \times \frac{C_{\mathrm{Conventional}}}{C_{\mathrm{LVSEP}}} \tag{4-4}$$

where, h and C are the peak height and sample concentration, respectively. The relative standard deviations (RSDs, n = 3) of the detection time, peak height, and peak area in LVSEP-CDCZE were estimated as 2.0%, 2.1%, and 5.8%, respectively, whereas those in the conventional CDCZE were 1.6%, 12%, and 17%, respectively.

In the CDCZE analyses, the anionic analytes form complexes with the neutral CD. Since the number of total negative charges is not changed in the complex formation but

the size is increased compared with the free analytes, the charge to size ratio of the complex is decreased, causing the reduction in the electrophoretic mobility. In the LVSEP-CDCZE analysis of warfarin, $\mu_{ep,eff,BGS}/\mu_{ep,free}$ was theoretically evaluated as 0.76 and 0.81 for first- and second migrating enantiomer, respectively, at $\gamma = 500$. The maintained effective separation length was theoretically calculated to be more than 99.8% (see Supporting Information). As with the previous report [22], the effective separation length in LVSEP-CDCZE was experimentally estimated by subtracting the migration time (t_M) with the time of the drastic current change (t_i). As shown in Figure 4-2, t_M in conventional CDCZE was 15.5 min, whereas ($t_M - t_i$) in LVSEP-CDCZE was 15.7 min. These almost identical separation times gave the comparable resolutions, 2.5 and 2.6 obtained with Figures 4-2a and 4-2b, respectively. The effective separation length of 101% of the inlet-to-detector length estimated from $(t_{M,LVSEP} - t_i)/t_{M,CDCZE}$ agreed well with the theoretically calculated length of 99.8%.

Table 4-2. Summary of the separation mode, employed BGS composition, obtained resolution, and SEF for each analyte.

analyte	separation mode	BGS composition	σ_{BGS} / mS/cm	R_s (normal / LVSEP)	SEF
warfarin	CDCZE	10 mM DM-β-CD, 25 mM MES buffer (pH 6.0)	0.54	2.5 / 2.6	1,000
ibuprofen	CDCZE	40 mM TM-β-CD, 25 mM MES buffer (pH 6.0)	0.54	6.7 / 6.9	500
abscisic acid	CDEKC	1.5 mM quaternary-β-CD, 20 mM MES buffer (pH 6.0)	1.43	5.0 / 4.5	800
FITC-Arg	CDMEKC	30 mM SDS, 10 mM γ-CD, 40 mM borate buffer (pH 9.5)	2.70	5.1 / 4.2	1,000
FITC-Met				5.7 / 5.5	1,100
FITC-Leu				6.0 / 6.0	1,300

LVSEP-CDEKC of Abscisic Acid

CDEKC using a charged CD was combined with LVSEP for analyzing a plant hormone, abscisic acid, as a model analyte. The author employed 1.5 mM quaternary-β-CD as a charged chiral selector dissolved in 20 mM MES buffer (pH 6.0), as shown in the previous paper [29]. In the conventional CDEKC analysis, 250 ppm racemic abscisic acid was well separated (Figure 4-3a) with the resolution of 5.0 (Table 4-2). In the LVSEP-CDEKC analysis, even 100 ppb racemic abscisic acid could be detected with the resolution of 4.5 (Figure 4-3b), where the SEF was estimated as 800. The RSDs (n = 3) of the detection time, peak height, and peak area in LVSEP-CDEKC were estimated as 1.3%, 4.4%, and 4.6%, respectively, whereas those in the conventional CDCZE were 0.1%, 4.0%, and 3.5%, respectively.

The difference in the detection times of conventional CDEKC and LVSEP-CDEKC was found to be larger than that in CDCZE, which was mainly caused by the slow matrix removal. In CDEKC, the author employed the longer capillary with the total/effective lengths of 60/50 cm than that of CDCZE with the lengths of 40/30 cm,

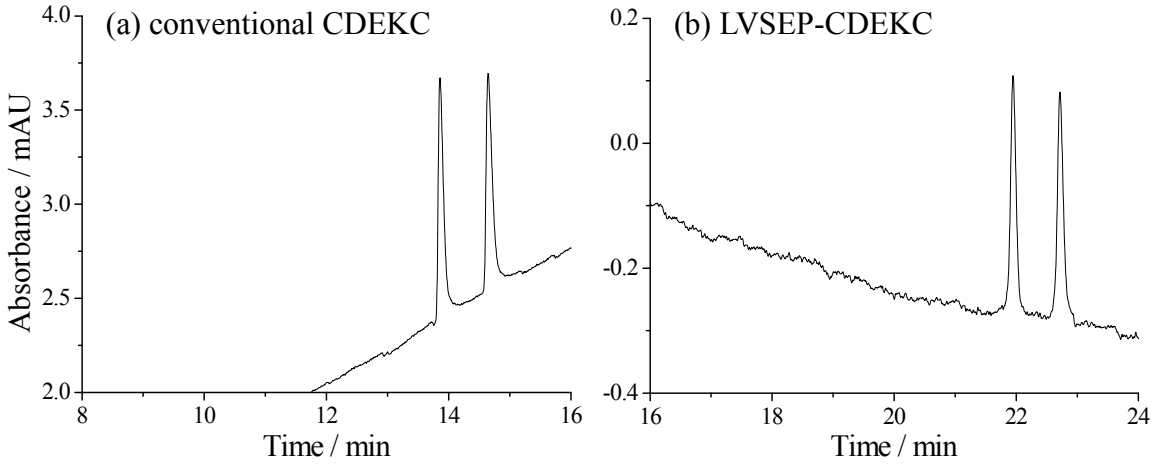

Figure 4-3. Enantioseparation of racemic abscisic acid by (a) conventional CDEKC and (b) LVSEP-CDEKC. Sample concentration, (a) 250 ppm and (b) 100 ppb; UV detection, 250 nm.

but the applied voltage of –30 kV was the same in both cases. From the EOF rate in LVSEP-CDCZE, the time required for the matrix removal in LVSEP-CDEKC was calculated to be 5.5 min. However, the actual time (t_i) of 7.5 min was longer than that expected, indicating the reduction in the negative zeta potential of the inner capillary surface, where QA-β-CD might be adsorbed. Since the zeta potential of the PVA-coated capillary is fundamentally quite small, even a slight change in the surface condition tends to cause the drastic change in the enhanced EOF rate.

In the CDEKC analyses, the anionic analytes form complexes with the cationic CD, where the number of total negative charges is reduced in the complex formation and the size is increased compared with the free analytes. Hence the decrease in the charge to size ratio of the complex causes the reduction in the electrophoretic mobility as in CDCZE. The ratios of $\mu_{ep,eff,BGS}/\mu_{ep,free}$ (0.56 and 0.59) are smaller than unity, supporting that the separation ability was maintained in the LVSEP-CDEKC analysis.

LVSEP-CDMEKC of FITC-labeled Amino Acids

Amino acids are very important analytical targets in biological analysis, because they are related with many biological functions such as the protein metabolism, glucose metabolism, and neural transmission. Recently, the importance of D-amino acids has been recognized since they are found to be increased or decreased in a human body suffering from several diseases in brain, kidney, and liver [2]. Hence, the chiral analysis of small amount of amino acids with high sensitivity and high resolution is required. Here, the combination of the LVSEP concentration, high resolution of the CDMEKC separation, and the high sensitive LIF detection was investigated to achieve the high performance chiral analyses.

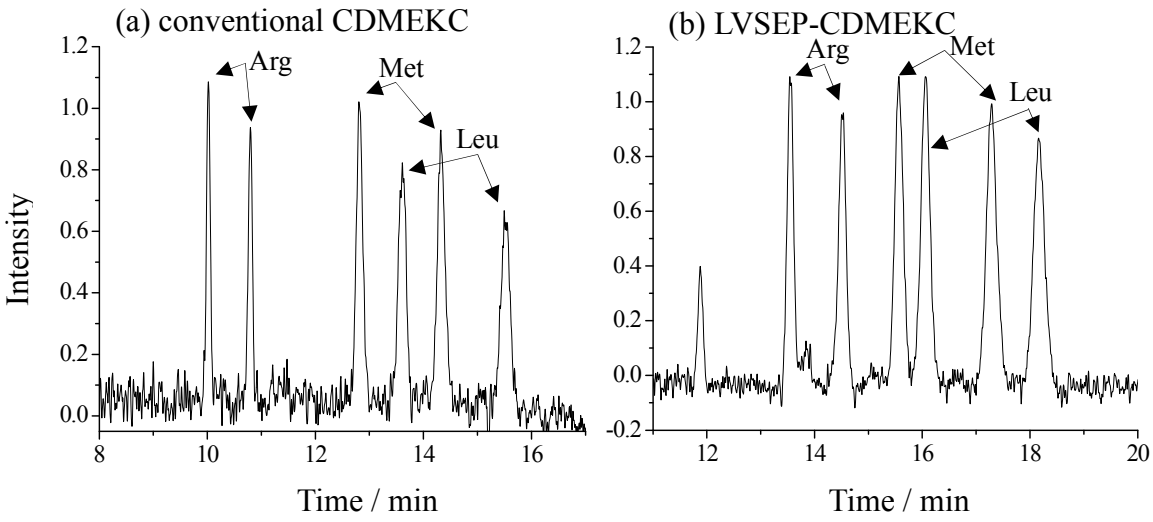

Figure 4-4. Enantioseparation of FITC-labeled amino acids in (a) conventional CDMEKC and (b) LVSEP-CDMEKC. Sample concentration, (a) 100 nM and (b) 100 pM; LIF detection, $\lambda_{ex}/\lambda_{em}$ of 488/520 nm.

CDMEKC employing SDS and neutral CD were combined with LVSEP. In the CDMEKC analysis, arginine (Arg), methionine (Met), and leucine (Leu) derivatized with FITC were analyzed as model analytes by employing 30 mM SDS and 10 mM γ-CD as the chiral selector in 40 mM borate buffer (pH 9.5), in accordance with the previous paper [24]. In the conventional CDMEKC analysis, 100 nM amino acids were optically resolved (Figure 4-4a). The resolutions were estimated as 5.1, 5.7, and 6.0 for Arg, Met, and Leu, respectively (Table 4-2). In the LVSEP-CDMEKC analysis, even 100 pM amino acids could be detected with the resolution of 4.2, 5.5, and 6.0 for Arg, Met, and Leu, respectively (Figure 4-4b). The SEFs were estimated as 1000, 1100, and 1300 for Arg, Met, and Leu, respectively. Opposite to LVSEP-CDEKC, t_i of 2.9 min was much smaller than that expected from LVSEP-CDCZE, probably because the slight adsorption of anionic SDS increased the negative zeta potential of the inner surface of the capillary.

Since the electrophoretic mobility of the FITC-labeled amino acids are increased by the interaction with the SDS micelle, the ratio $\mu_{ep,eff,BGS}/\mu_{ep,free}$ is larger than unity especially for earlier detected analytes, which might cause the slight band broadening and the reduction in the peak-to-peak distance. Typical reduction in resolution for the first detected Arg with the largest $\mu_{ep,eff,BGS}$ supported the author's theoretical consideration. Anyway, the optical resolutions were almost kept up as that in LVSEP-CDCZE/CDEKC, indicating the effect of $\mu_{ep,eff,BGS}$ on the preconcentration is often limited. These good results demonstrated the versatile applicability of LVSEP to many separation modes.

It should be emphasized again in LVSEP-CDCZE/CDEKC/CDMEKC that the sample filled in the whole capillary, which is theoretically the maximum injection volume by pressure, could be well concentrated and separated without much loss of the effective separation length. Thus, it is not necessary to optimize the sample injection volume in the LVSEP analysis. This is one of the most invaluable advantages of LVSEP coupled with any separation modes in CE.

EE Assay of Ibuprofen

Quantification of a minor enantiomer from the excessive amount of the major enantiomer is one of the most important issues in the chiral analysis. However, the large peak of the excess amount of the enantiomer often overlaps the other peak, making the quantitative EE assay difficult. If the conventional online concentration techniques were applied to the EE assay, the reduction in optical resolution would make the chiral separation more difficult, resulting in poor EE quantification. On the other hand, one of the most significant advantages of LVSEP is the capability of maintaining the separation

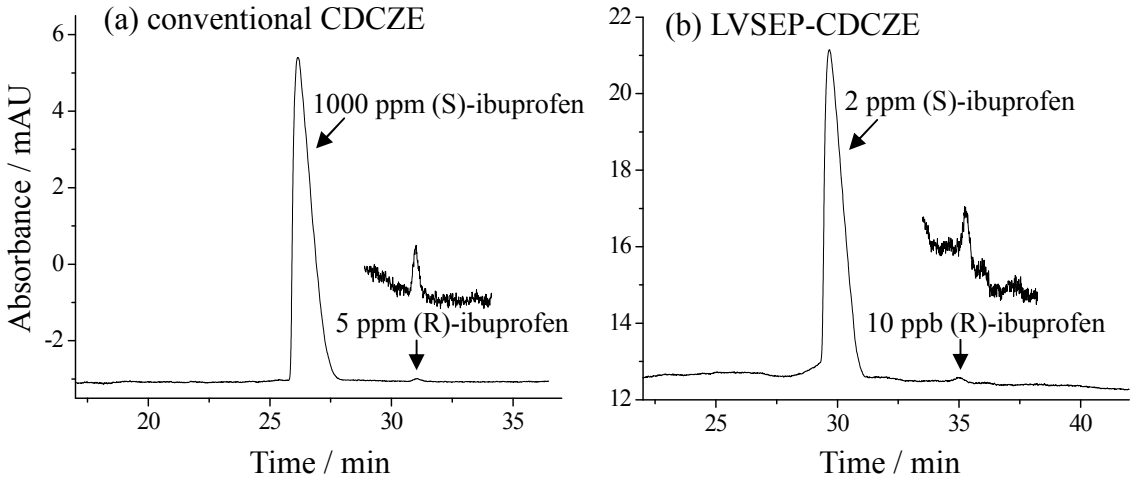

Figure 4-5. EE assay of ibuprofen in (a) conventional CDCZE and (b) LVSEP-CDCZE. Sample concentration, (a) 1000 ppm (S)-ibuprofen and 5 ppm (R)-ibuprofen; (b) 2 ppm (S)-ibuprofen and 10 ppb (R)-ibuprofen. UV detection, 200 nm.

performance, so that the comparable enantioseparation and quantification with a conventional mode is expected to be provided. Hence, the EE assay was performed to verify the compatibility of LVSEP with the chiral analysis.

As a typical assay of 99% EE, the mixture of 99.5% (S)-ibuprofen with 0.5% (R)-ibuprofen was analyzed both by conventional CDCZE and by LVSEP-CDCZE using TM-β-CD as a chiral selector [30]. In LVSEP-CDCZE, 2 ppm (S)-ibuprofen and 10 ppb (R)-ibuprofen were well separated with the resolution of 4.7 (Figure 4-5b), whereas 1000 ppm (S)-ibuprofen and 5 ppb (R)-ibuprofen were resolved with the resolution of 4.8 (Figure 4-5a). The SEF was evaluated as 500 for both enantiomers, and the limits of detection (LODs) (S/N = 3) in LVSEP-CDCZE were estimated to be 3.7 ppb and 4.7 ppb for (R)- and (S) ibuprofen, respectively. For quantitative analysis of enantiomers, the peak areas must be corrected with the factor of v_s [31], which is the sample velocity at the detection point. In the conventional CDCZE analysis, the electrophoretic mobility is proportional to $1/t_M$, where t_M is the detection time of the

analyte, so that the area can easily be corrected with the factor of $1/t_M$. In LVSEP-CDCZE, on the other hand, $1/t_M$ is not proportional to v_s because t_M includes the time of the LVSEP concentration process. Since the time of the LVSEP concentration can be estimated from t_i [22], t_M was corrected by subtracting with t_i in this study for the EE quantification. As a result, EE was estimated as 99.05% ± 0.048% (n = 4) in LVSEP-CDCZE and 99.11% ± 0.082% (n = 4) in conventional CDCZE, indicating that good chiral quantification performance of CDCZE was maintained even after applying LVSEP. Moreover, the author also succeeded in the assays of the EE ratio up to 99.60%, where 5 ppm (S)-ibuprofen and 10 ppb (R)-ibuprofen were analyzed by LVSEP-CDCZE. In conventional CDCZE, on the other hand, such higher EE ratio could not be determined because the required concentration of (S)-ibuprofen, 2,500 ppm, was too high to be dissolved in the BGS. Hence, LVSEP-CDCZE is also suitable for the assay of the high EE ratio.

Analysis of Ibuprofen in Urine Sample

Some of the most important targets of the chiral analysis are drug components in biological fluids such as blood, saliva, and urine. Since these fluids contain many salts which directly interfere with the LVSEP preconcentration process, purification such as gel filtration [22], liquid phase microextraction (LPME) [32], and SPE [33] are required in the LVSEP-CDCZE analysis. Taking into account of the molecular size of the analytes, LPME and SPE are suitable in this study. In LPME-LVSEP, however, the EOF velocity would become too slow in the preconcentration stage due to the combination of the PVA-coated capillary and a hydrophobic solvent. Thus, SPE-LVSEP with a C_{18} column was employed in this study. The conductivity of the reconstituted sample

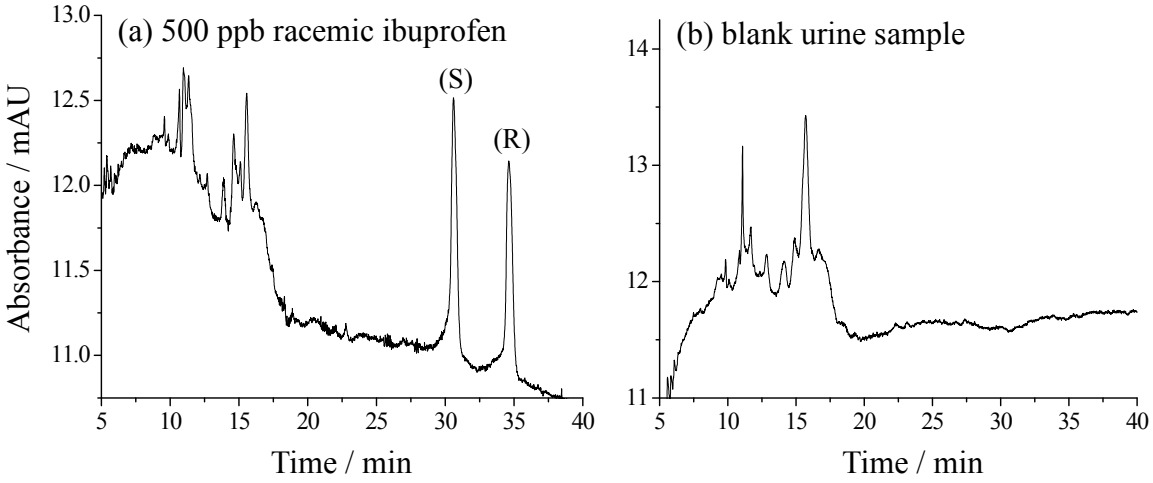

Figure 4-6. LVSEP-CDCZE of purified ibuprofen from the urine sample. The original concentrations of ibuprofen in the urine, (a) 500 ppb and (b) 0 ppb (blank); UV detection, 200 nm.

solution was reduced to 10 μS/cm from 20 mS/cm in the original urine sample. As shown in the previous report [22], the LVSEP analysis could be performed without dilution when the conductivity of the sample solution is less than 100 μS/cm. Hence, the desalting performance of the SPE is sufficient for the LVSEP concentration.

Urine sample containing 500 ppb racemic ibuprofen after the SPE purification was analyzed in the same LVSEP conditions as discussed in the previous section on the EE assay. As a typical result, racemic ibuprofen was well detected and optically separated with the resolution of 5.1 as shown in Figure 4-6a. By the calibration curve determined from the analysis of ibuprofen spiked in the blank urine sample with the SPE purification, the recovery rate was estimated as 84.0% for (S)-ibuprofen and 86.6% for (R)-ibuprofen. The similar results were obtained in the sample concentration ranging from 25 ppb to 4.0 ppm, where the limits of quantification (LOQs) (S/N = 10) were estimated as 14 ppb and 17 ppb for (R)- and (S)-ibuprofen, respectively. Compared with the LOQs of 500 ppb and 250 ppb in previous reports using SPE-CDCZE [34] and

SPE-HPLC [35], respectively, the better sensitivity in this study indicated the practical utility of SPE-LVSEP-CDCZE. Thus, sufficient desalting was achieved for the successful analysis of urine sample by LVSEP-CDCZE. Further improvement of the analytical performance for several important analytes with more optimized recovery is expected to be realized soon by the combination of LVSEP with the SPE preconcentration.

4-4. Conclusions

The effects of the chiral selectors on the LVSEP performance were investigated both theoretically and experimentally. The author demonstrated that the excellent preconcentration efficiency up to 1,300-fold sensitivity increases was achieved with maintaining similar optical resolutions. The EE assay of up to 99.6% was also carried out without loss of analytical performance by LVSEP-CDCZE. Finally, the combination of the sample purification by using the C_{18} SPE column with LVSEP-CDCZE was shown to be useful for the analyses of the real sample containing many unnecessary salts. Therefore, the application of the easy operating and high performance LVSEP to the chiral analysis will contribute in many areas such as biology, chemistry, medicine, and pharmaceutics.

4-5. Appendix

Calculation of the inversion position of the concentrated analytes

In the main text, detailed calculations from Eq. (4-1) to Eqs. (4-2) and (4-3) are

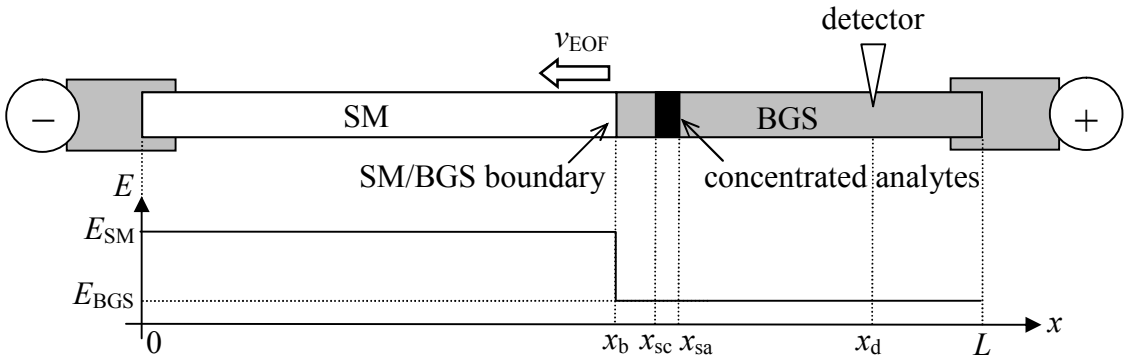

Figure A4-1. Schematic representation for the parameters used in the theoretical model. E and x mean electric field and the position from the cathodic capillary end. All positions are expressed as the distance from the cathodic channel end. Subscripts b, sc, sa, and d mean anodic side of the SM/BGS boundary, cathodic side of the concentrated analyte zone, anodic side of the concentrated analyte zone, and detector, respectively.

skipped to be easily understandable. In this supporting section, the complicated calculations are proposed to obtain w and $x_{sc,i}$. Although the main stream of the calculation process is almost the same as that in the previous report, the effect of adding CD into the electrolyte was discussed in detail.

At first, the author defined many parameters, x_b, x_{sa}, x_{sc}, E_{BGS}, E_{SM}, and so on as shown in Figure A4-1. The electroosmotic mobility in the PVA-coated capillary filled with the BGS ($\mu_{EOF,BGS}$) was less than 0.3×10^{-4} $cm^2V^{-1}s^{-1}$, so that $\mu_{EOF,BGS}$ was neglected in this study. As discussed in the previous report [18], fundamental parameters are calculated as Eqs. (A4-1) ~ (A4-4):

$$E_{SM} = \frac{\gamma V}{(\gamma - 1)x_b + L} \tag{A4-1}$$

$$E_{BGS} = \frac{V}{(\gamma - 1)x_b + L} \tag{A4-2}$$

$$v_{ep,BGS} = \frac{\mu_{ep} V}{(\gamma - 1)x_b + L} \tag{A4-3}$$

$$v_{EOF} \approx \frac{\gamma \mu_{EOF,SM} V x_b}{\{(\gamma - 1)x_b + L\}L} \tag{A4-4}$$

The SM/BGS boundary moves according to the EOF, x_b can be expressed as a function of t:

$$\begin{aligned} x_b &= L - \int_0^t \frac{\mu_{EOF,SM}\gamma V x_b}{\{(\gamma-1)x_b + L\}L} dt \\ &= L - \int_0^t \frac{\mu_{EOF,SM}\gamma V}{(\gamma-1)L} dt + \int_0^t \frac{\mu_{EOF,SM}\gamma V}{\{(\gamma-1)x_b + L\}(\gamma-1)} dt \\ &= L - \frac{\mu_{EOF,SM}\gamma V}{(\gamma-1)L} t + \int_0^t \frac{\mu_{EOF,SM}\gamma V}{\{(\gamma-1)x_b + L\}(\gamma-1)} dt \end{aligned} \quad \text{(A4-4)}$$

$$\int_0^t \frac{V}{\{(\gamma-1)x_b + L\}} dt = \frac{(\gamma-1)}{\gamma\mu_{EOF,SM}} \left\{ x_b - L + \frac{\gamma\mu_{EOF,SM}V}{(\gamma-1)L} t \right\} \quad \text{(A4-5)}$$

If x_{sa} is the position of the anode-side end of the concentrated sample band as shown in Figure A4-1, (x_{sa}–x_b) is the length by which the analytes at the anode-side end migrate electrophoretically from the boundary. Therefore, (x_{sa}–x_b) can also be calculated by integrating $v_{ep,BGS}$ and expressed as a function of t:

$$x_{sa} - x_b = \int_0^t \frac{-\mu_{ep,eff,BGS}V}{(\gamma-1)x_b + L} dt \quad \text{(A4-6)}$$

Substitution of Eq. (A4-5) into Eq. (A4-6) gives the following equation:

$$\begin{aligned} x_{sa} - x_b &= \frac{-\mu_{ep,eff,BGS}(\gamma-1)}{\mu_{EOF,SM}\gamma} \left\{ x_b - L + \frac{\mu_{EOF,SM}\gamma V}{(\gamma-1)L} t \right\} \\ &= -\frac{\mu_{ep,eff,BGS}V}{L} t + \frac{\mu_{ep,eff,BGS}(\gamma-1)}{\mu_{EOF,SM}\gamma}(L - x_b) \end{aligned} \quad \text{(A4-7)}$$

Here, by solving the differential equation of t and x,

$$x_b = L - \int_0^t \frac{\mu_{EOF,SM}\gamma V x_b}{\{(\gamma-1)x_b + L\}L} dt \quad \text{(A4-8)}$$

$$\frac{dx_b}{dt} = -\frac{\mu_{EOF,SM}\gamma V x_b}{\{(\gamma-1)x_b + L\}L} \quad \text{(A4-9)}$$

$$-\frac{\{(\gamma-1)x_b + L\}L}{\mu_{EOF,SM}\gamma V x_b} dx_b = dt \quad \text{(A4-10)}$$

$$\int -\left\{ \frac{(\gamma-1)L}{\gamma\mu_{EOF,SM}V} + \frac{L^2}{\gamma\mu_{EOF,SM}V} \frac{1}{x_b} \right\} dx_b = \int dt \quad \text{(A4-11)}$$

From initial condition, x_b is equal to L when $t = 0$. Thus, Eq. (A4-11) is solved as

$$t = \frac{(\gamma - 1)}{\gamma \mu_{EOF,SM} V}(L - x_b) + \frac{L^2}{\gamma \mu_{EOF,SM} V} \ln\left(\frac{L}{x_b}\right) \quad \text{(A4-12)}$$

By substituting Eq. (A4-12) into Eq. (A4-7), the term (x_{sa}–x_b) can be expressed as a function of x_b:

$$x_{sa} - x_b = \frac{-\mu_{ep,eff,BGS} L}{\gamma \mu_{EOF,SM}} \ln\left(\frac{L}{x_b}\right) \quad \text{(A4-13)}$$

Provided that x_b is $x_{b,B}$ when $v_{ep,free,SM}$ exceeds v_{EOF}, and that x_b is $x_{b,F}$ when the whole analytes are stacked out, $x_{b,F}$ can be given as follows.

i) If $\mu_{EOF,SM} > \mu_{ep,free}$, some of the analytes were flashed out from the cathodic end due to the fast EOF. After decreasing the length of the SM zone and increasing the electric field, the analyte can move against the EOF toward the anode. Hence, this balanced condition can be expressed as follows:

$$v_{EOF} = -v_{ep,free,SM} \quad \text{(A4-14-1)}$$

$$\frac{\gamma \mu_{EOF,SM} V x_{b,B}}{\{(\gamma - 1)x_{b,B} + L\}L} = \frac{-\gamma \mu_{ep,free} V}{(\gamma - 1)x_{b,B} + L} \quad \text{(A4-15-1)}$$

$$x_{b,B} = \frac{-\mu_{ep,free} L}{\mu_{EOF,SM}} \quad \text{(A4-16-1)}$$

Meanwhile, if $v_{ep,free,SM} > v_{EOF}$, the analyte at the cathodic end moves by the length of $x_{b,B}$ from $t = t_B$ to $t = t_F$. Therefore, $x_{b,B}$ can be also given by the following equation:

$$\begin{aligned} x_{b,B} &= \int_{t_B}^{t_F} \frac{-\gamma \mu_{ep,free} V}{(\gamma - 1)x + L} dt \\ &= \int_{x_{b,B}}^{x_{b,F}} \frac{-\gamma \mu_{ep,free} V}{(\gamma - 1)x_b + L} \cdot \frac{-\{(\gamma - 1)x_b + L\}L}{\gamma \mu_{EOF,SM} V x_b} dx_b \end{aligned}$$

$$= \frac{\mu_{\mathrm{ep,free}} L}{\mu_{\mathrm{EOF,SM}}} \int_{x_{\mathrm{B}}}^{x_{\mathrm{F}}} \frac{dx_{\mathrm{b}}}{x_{\mathrm{b}}}$$
$$= -\frac{\mu_{\mathrm{ep,free}} L}{\mu_{\mathrm{EOF,SM}}} \ln\left(\frac{x_{\mathrm{b,B}}}{x_{\mathrm{b,F}}}\right) \quad \text{(A4-17)}$$

By solving Eqs. (A4-16-1) and (A4-17), $x_{\mathrm{b,F}}$ is expressed by the Eq. (A4-19-1):

$$\ln\left(\frac{x_{\mathrm{b,B}}}{x_{\mathrm{b,F}}}\right) = 1 \quad \text{(A4-18-1)}$$

$$x_{\mathrm{b,F}} = \frac{x_{\mathrm{b,B}}}{e} = -\frac{\mu_{\mathrm{ep,free}} L}{e\mu_{\mathrm{EOF,SM}}} \quad \text{(A4-19-1)}$$

ii) If $\mu_{\mathrm{EOF,SM}} \leq \mu_{\mathrm{ep,free}}$, the analyte can migrate against the fast EOF immediately after the applying the voltage. Thus, $x_{\mathrm{b,B}}$ is equal to L:

$$x_{\mathrm{b,B}} = L \quad \text{(A4-16-2)}$$

As with Eq. (A4-15), L can be expressed as follows:

$$L = \int_0^{t_{\mathrm{F}}} \frac{-\gamma\mu_{\mathrm{ep,free}} V}{(\gamma-1)x_{\mathrm{b}} + L} dt$$
$$= \int_L^{x_{\mathrm{b,F}}} \frac{-\gamma\mu_{\mathrm{ep,free}} V}{(\gamma-1)x_{\mathrm{b}} + L} \cdot \frac{-\{(\gamma-1)x_{\mathrm{b}} + L\}L}{\gamma\mu_{\mathrm{EOF,SM}} V x_{\mathrm{b}}} dx_{\mathrm{b}}$$
$$= \frac{\mu_{\mathrm{ep,free}} L}{\mu_{\mathrm{EOF,SM}}} \int_L^{x_{\mathrm{b,F}}} \frac{dx_{\mathrm{b}}}{x_{\mathrm{b}}} \quad \text{(A4-17-2)}$$
$$= \frac{-\mu_{\mathrm{ep,free}} L}{\mu_{\mathrm{EOF,SM}}} \ln\left(\frac{L}{x_{\mathrm{b,F}}}\right)$$

$$\ln\left(\frac{L}{x_{\mathrm{b,F}}}\right) = -\frac{\mu_{\mathrm{EOF,SM}}}{\mu_{\mathrm{ep,free}}} \quad \text{(A4-18-2)}$$

$$x_{\mathrm{b,F}} = L e^{\frac{\mu_{\mathrm{EOF,SM}}}{\mu_{\mathrm{ep,free}}}} \quad \text{(A4-19-2)}$$

Provided that ($x_{\mathrm{sa,F}}$–$x_{\mathrm{b,F}}$) is w, substitution of Eq. (A4-19) into (A4-13) gives w by the following equation:

(when $\mu_{\mathrm{EOF,SM}} > -\mu_{\mathrm{ep,free}}$) $$w = -\frac{\mu_{\mathrm{ep,eff,BGS}} L}{\gamma \mu_{\mathrm{EOF,SM}}} \ln\left(-\frac{e\mu_{\mathrm{EOF,SM}}}{\mu_{\mathrm{ep,free}}}\right) \quad \text{(A4-20-1)}$$

(when $\mu_{\mathrm{EOF,SM}} \leq -\mu_{\mathrm{ep,free}}$) $$w = -\frac{\mu_{\mathrm{ep,eff,BGS}}}{\mu_{\mathrm{ep,free}}} \frac{L}{\gamma} \quad \text{(A4-20-2)}$$

When the whole analytes are stacked out, the cathodic side of the concentrated band is just on the boundary. Therefore, w can be identified as the width of the concentrated band.

When the concentrated analytes start to move against the EOF, the SM plug length remaining in the channel/capillary ($x_{\mathrm{b,i}}$) is expressed by the following Eq. (A4-22):

$$\frac{-\mu_{\mathrm{ep,eff,BGS}} V}{(\gamma - 1)x_{\mathrm{b,i}} + L} = \frac{\mu_{\mathrm{EOF,SM}} \gamma V x_{\mathrm{b,i}}}{\{(\gamma - 1)x_{\mathrm{b,i}} + L\} L} \quad \text{(A4-21)}$$

$$x_{\mathrm{b,i}} = \frac{-\mu_{\mathrm{ep,eff,BGS}} L}{\gamma \mu_{\mathrm{EOF,SM}}} \quad \text{(A4-22)}$$

The distance between the cathodic end of the stacked analytes and the cathodic end of the channel/capillary (x_{sc}) is equal to ($x_{\mathrm{sa}} - w$). From Eqs. (A4-13), (A4-20) and (A4-22), x_{sc} at the inversion time ($x_{\mathrm{sc,i}}$) is given as follows:

(when $\mu_{\mathrm{EOF,SM}} > -\mu_{\mathrm{ep,free}}$)

$$\begin{aligned} x_{\mathrm{sc,i}} &= -\frac{\mu_{\mathrm{ep,eff,BGS}} L}{\gamma \mu_{\mathrm{EOF,SM}}} - \frac{\mu_{\mathrm{ep,eff,BGS}} L}{\gamma \mu_{\mathrm{EOF,SM}}} \ln\left(-\frac{\gamma \mu_{\mathrm{EOF,SM}}}{\mu_{\mathrm{ep,free}}}\right) + \frac{\mu_{\mathrm{ep,eff,BGS}} L}{\gamma \mu_{\mathrm{EOF,SM}}} \ln\left(-\frac{e\mu_{\mathrm{EOF,SM}}}{\mu_{\mathrm{ep,free}}}\right) \\ &= -\frac{\mu_{\mathrm{ep,eff,BGS}} L}{\gamma \mu_{\mathrm{EOF,SM}}} \ln \gamma \end{aligned} \quad \text{(A4-23-1)}$$

(when $\mu_{\mathrm{EOF,SM}} \leq -\mu_{\mathrm{ep,free}}$)

$$x_{\mathrm{sc,i}} = -\frac{\mu_{\mathrm{ep,eff,BGS}} L}{\gamma \mu_{\mathrm{EOF,SM}}} - \frac{\mu_{\mathrm{ep,eff,BGS}} L}{\gamma \mu_{\mathrm{EOF,SM}}} \ln\left(-\frac{\gamma \mu_{\mathrm{EOF,SM}}}{\mu_{\mathrm{ep,free}}}\right) - \frac{\mu_{\mathrm{ep,eff,BGS}}}{\mu_{\mathrm{ep,free}}} \frac{L}{\gamma}$$

$$= -\frac{\mu_{\mathrm{ep,eff,BGS}} L}{\gamma \mu_{\mathrm{EOF,SM}}} \ln\left(-\frac{e\gamma \mu_{\mathrm{EOF,SM}}}{\mu_{\mathrm{ep,free}}} \right) - \frac{\mu_{\mathrm{ep,eff,BGS}}}{\mu_{\mathrm{ep,free}}} \frac{L}{\gamma} \qquad \text{(A4-23-2)}$$

Therefore, the effective separation length ($x_d - x_{sc,i}$) is estimated as follows:

(when $\mu_{EOF,SM} > -\mu_{ep,free}$)

$$x_d - x_{sc,i} = x_d + \frac{\mu_{\mathrm{ep,eff,BGS}} L}{\gamma \mu_{\mathrm{EOF,SM}}} \ln \gamma \qquad \text{(A4-24-1)}$$

(when $\mu_{EOF,SM} \leq -\mu_{ep,free}$)

$$x_d - x_{sc,i} = x_d + \frac{\mu_{\mathrm{ep,eff,BGS}} L}{\gamma \mu_{\mathrm{EOF,SM}}} \ln\left(-\frac{e\gamma \mu_{\mathrm{EOF,SM}}}{\mu_{\mathrm{ep,free}}} \right) + \frac{\mu_{\mathrm{ep,eff,BGS}}}{\mu_{\mathrm{ep,free}}} \frac{L}{\gamma} \qquad \text{(A4-24-2)}$$

4-6. References

[1] Hutt, A. J.; O'Grady, J. *J. Antimicrob. Chemother.* **1996**, *37*, 7–32.

[2] Hamase, K.; Morikawa, A.; Zaitsu, K. *J. Chromatogr. B* **2002**, *781*, 73–91.

[3] Mori, K. *Bioorg. Med. Chem.* **2007**, *15*, 7505–7523.

[4] Kitagawa, F.; Otsuka, K. *J. Chromatogr. B* in press.

[5] Fanali, S. *J. Chromatogr. A* **2000**, *875*, 89–122.

[6] Blaschke, G..; Chankvetadz, B. *J. Chromatogr. A* **2001**, *906*, 309–363.

[7] García-Ruiz, C.; Marina, M. L. *Electrophoresis* **2006**, *27*, 195–212.

[8] Sánchez-Hernández, L.; Crego, A. L.; Marina, M. L.; García-Ruiz, C. *Electrophoresis* **2008**, *29*, 237–251.

[9] Sánchez-Hernández, L.; García-Ruiz, C.; Marina, M. L.; Crego, A. L. *Electrophoresis* **2010**, *31*, 28–43.

[10] Burgi, D. S.; Chien, R.-L. *Anal. Biochem.* **1992**, *202*, 306–309.

[11] Quirino, J. P.; Terabe, S. *Anal. Chem.* **1999**, *71*, 1638–1644.

[12] Quirino, J. P.; Terabe, S.; Otsuka, K.; Vincent, J. B.; Vigh, G. *J. Chromatogr. A* **1999**, *838*, 3–10.

[13] Kodama, S.; Yamamoto, A.; Matsunaga, A.; Soga, T.; Minoura, K. *J. Chromatogr. A* **2000**, *875*, 371–377.

[14] Wang, F.; Khaledi, M. G. *J. Chromatogr. B Biomed. Sci. Appl.* **1999**, *731*, 187–197.

[15] Song, J.-Z.; Chen, J.; Tian, S.-J.; Sun, Z.-P. *J. Pharm. Biomed. Anal.* **1999**, *21*, 569–576.

[16] Wang, Z.; Liu, C.; Kang, J. *J. Chromatogr. A* **2011**, *1218*, 1775–1779.

[17] Quirino, J. P.; Terabe, S. *Science* **1998**, *282*, 465–468.

[18] Timerbaev, A. R.; Hirokawa, T. *Electrophoresis* **2006**, *27*, 323–340.

[19] Britz-McKibbin, P.; Chen, D. D. Y. *Anal. Chem.* **2000**, *72*, 1242–1252.

[20] Sueyoshi, K.; Hashiba, K.; Kawai, T.; Kitagawa, F.; Otsuka, K. *Electrophoresis* **2011**, *32*, 1233–1240.

[21] He, Y.; Lee, H. K. *Anal. Chem.* **1999**, *71*, 995–1001.

[22] Kawai, T.; Watanabe, M.; Sueyoshi, K.; Kitagawa, F.; Otsuka, K. *J. Chromatogr. A* in press.

[23] Kawai, T.; Sueyoshi, K.; Kitagawa, F.; Otsuka, K. *Anal. Chem.* **2010**, *82*, 6504–6511.

[24] Jin, L. J.; Rodriguez, I.; Li, S. F. Y. *Electrophoresis* **1999**, *20*, 1538–1545.

[25] Gllges, M.; Kleemlss, M. H.; Schomburg, G.. *Anal. Chem.* **1994**, *66*, 2038–2046.

[26] Okamoto, Y.; Kitagawa, F.; Otsuka, K. *Anal. Chem.* **2007**, *79*, 3041–3047.

[27] Tanaka, Y.; Yanagawa, M.; Terabe, S. *J. High Resol. Chromatogr.* **1996**, *19*, 421–433.

[28] Ufer, M.; Kammerer, B.; Kirchheiner, J.; Rane, A.; Svensson, J.-O. *J. Chromatogr. B* **2004**, *809*, 217–226.

[29] Tanaka, Y.; Terabe, S. *J. Chromatogr. A* **1997**, *781*, 151–190.

[30] Blance, M.; Coello, J.; Iturriaga, H.; Maspoch, S.; Perez-Maseda, C. *J. Chromatogr. A* **1998**, *793*, 165–175.

[31] Blomberg, L. G.; Wan, H. *Electrophoresis* **2000**, *21*, 1940–1952.

[32] Choi, K.; Jin, Y. G.; Chung, D. S. *J. Chromatogr. A* **2009**, *1216*, 6466–6470.

[33] Macià, A.; Borrull, F.; Aguilar, C.; Calull, M. *Electrophoresis* **2003**, *24*, 2779–2787.

[34] Główka, F. K.; Karaźniewicz, M. *Anal. Chim. Acta* **2005**, *540*, 95–102.

[35] Oliveira, A. R. M.; Cesarino, E. J.; Bonato, P. S. *J. Chromatogr. B* **2005**, *818*, 285–291.

Chapter 5.

Capillary Electrophoresis of Cationic Compounds Using Large-volume Sample Stacking with an Electroosmotic Flow Pump

5-1. Introduction

Capillary/microchip electrophoresis (CE/MCE) exhibits the high resolution, high speed, and little sample consumption so that much attention has been attracted from many analytical fields such as biology, pharmacy, medicine, and so on. However, the concentration sensitivity is quite low because of the short optical path length and small injection volume of sample, which has been one of the most serious disadvantages of CE/MCE. To overcome the drawback, several online sample concentration techniques have been developed [1–6]. However, application of online concentration techniques often causes the complication of experimental procedure and the reduction in resolution [3–6], causing the hesitation of many researchers to apply these techniques.

Recently, the author has found that both the sensitivity improvement and simplification of experimental procedure could be simultaneously realized in MCE by employing large-volume sample stacking with an electroosmotic flow pump (LVSEP) [7] in a poly(vinyl alcohol) (PVA)-coated microchannel. Up to 2,900-fold sensitivity increases were achieved in an oligosaccharide analysis with the following advantages: simplification of the voltage control from four channels for two steps to two channels for one step; simplification of channel geometry from cross to single; and almost no loss of resolution. Up to 1,300-fold sensitivity improvements were also achieved in the

analysis of oligosaccharides and chiral compounds without almost any loss of resolution in LVSEP-CE employing a PVA-modified capillary [8,9]. Hence, the high-performance and simple LVSEP-CE/MCE is expected to be a next-generation analytical technique. In the normal LVSEP-CE/MCE analysis, however, the applicable analytes have been limited to anionic compounds because cationic analytes are flushed out from the cathodic capillary/microchannel end by the EOF toward the cathode generated during the concentration. For the analysis of cations in LVSEP-CE/MCE, therefore, it is important to reverse the EOF toward the anode. So far, such strategies using the reversed EOF have been employed for CE analyses of cations coupled with large-volume sample stacking (LVSS) [10–13]. In the case employing cationic surfactant to reverse the EOF [10–12], the EOF was not suppressed in the wide pH range, so that the polarity switching had to be employed to detect slowly migrating cations. In the LVSS analysis using a zwitterion surfactant [13], on the other hand, the EOF rate was well regulated by changing the anionic components in the electrolyte. However, a serious band broadening occurred in the LVSEP-CE analysis even with the smaller-volume sample injection (*e.g.*, 0.5 psi for 60 s, around 50 nL). To minimize the band broadening, moreover, a delicate and complicated voltage regulation was required (*e.g.*, 10 kV for 3 min and then switched to 20 kV). Since the similar results were obtained in the LVSEP-CE analyses of hydrophobic anions by employing a poly(vinylpyrrolidone)-modified capillary with quite slow EOF rate and insufficient resistance to the sample adsorption (not published), these less efficient focusing performance seemed to be caused by the sample adsorption onto the capillary wall and by the sample diffusion during the slow and long-term removal of sample matrix. Therefore, both EOF-suppressed and adsorption-resistant modifier like PVA should be

employed to realize more efficient concentration in the LVSEP-CE/MCE analyses of cations.

The aim of this study is to establish the method to analyze cationic compounds by LVSEP-CE/MCE with high sensitivity and efficient separation. In this study, the strategy to achieve the LVSEP-CE/MCE of cationic compounds was based on the investigations of surface modification techniques. In conventional LVSEP-CE/MCE for anion analysis, a PVA coating has been mainly employed, where the EOF is fundamentally well suppressed but drastically enhanced only in the sample matrix (SM) with the a low ionic strength (*I*). Such a characteristic probably derives from the quite weekly negative-charged PVA surface [14]. Hence, weakly positive-charged surface should be employed for the LVSEP-CE/MCE analysis of cationic compounds. To achieve an appropriate EOF rate and suppression of the sample adsorption, in this study, the combination of cationic and neutral coatings was investigated mainly in the CE system. Three kinds of surface modification methods were employed: thermo-assisted physical coating with polymer mixture of PVA and poly(allylamine) (PAA); covalent modification with a copolymer synthesized from acrylamide (AA) and 3-(methacryloylamino)propyltrimethylammonium chloride (MPC) [15]; weak physical coating with dimethyldioctadecylammonium bromide (DODAB) and polyoxyethylene stearate (POES) [16]. To evaluate the EOF property for the LVSEP concentration and the following separation, electroosmotic mobility against pH and ionic strength was evaluated for each coated capillary. The LVSEP-CE analysis of aromatic amines was then carried out to estimate its concentration and separation performance.

5-2. Experimental Section

Materials and Chemicals

A fused silica capillary was purchased from Polymicro Technologies (Phoenix, AZ, USA), PVA (M_w = 88,000, 99% hydrolyzed) was obtained from Japan Vam and Poval (Osaka, Japan), DODAB, POE (40) stearate, 3-(trimethoxysilyl)propylmethacrylate (TPM), *N*,*N*,*N'*,*N'*-tetramethylethylenediamine (TEMED), and 1-naphthylethylamine (NEA) were purchased from Sigma-Aldrich (St. Louis, MO, USA), PAA (M_w = 60,000) was purchased from Nittobo (Fukushima, Japan), thiourea and MPC was purchased from Wako (Osaka, Japan), and all other reagents were purchased from Nacalai Tesque (Kyoto, Japan). All solutions were prepared with deionized water purified with a Direct-Q System (Nihon Millipore, Japan), and filtered through a 0.45 μm pore membrane filter (Nacalai Tesque) prior to use.

Polymer Synthesis

For the covalent surface modification, random copolymer of AA and MPC (PAA-ran-PMPC) was synthesized according to the previous report [15]. Briefly, mixture of 360 mM AA and 6 mM MPC dissolved in water was polymerized with 0.2% TEMED (v/v) and 0.4% APS (w/v) in a nitrogen atmosphere for 48 h at 10 ˚C. About 10-times larger amount of acetone was then added into the reactant to precipitate the synthesized polymer. After washing with acetone twice, the precipitate was lyophilized to dryness.

Capillary Coating

As a common experimental condition, the fused silica capillary was activated with 1 M NaOH for 1 h and rinsed with water for 5 min prior to the following modifications

For the PVA+PAA-coating, polymers were physically stabilized on the capillary surface with thermal treatment according to the conventional PVA-modification method [17]. A fused silica capillary was filled with the polymer mixture of 4.75% PVA and 0.25% PAA (w/v) and left for 15 min with both capillary ends immersed in the same polymer solution. The polymer solution inside the capillary was removed out and the capillary was heated at 140 ˚C for 18 h under a gentle nitrogen gas flow. The capillary was filled with water and stored at room temperature. Prior to use, the capillary was flushed with the BGS for 15 min.

For the modification with PAA-ran-PMPC, the capillary surface was covalently modified according to the previous report [16]. Briefly, a fused silica capillary was rinsed with 1 % acetic acid for 2 h, treated with 1.5% TPM dissolved in 1% acetic acid for 24 h, and finally rinsed with 5% PAA-ran-PMPC solution with 0.05% TEMED and 0.05% ammonium persulfate for 30 min. The capillary was then heated at 80 ˚C for 18 h with the both capillary ends immersed in the same polymer solution. The capillary was filled with water and stored at room temperature. Prior to use, the capillary was flushed with the BGS for 15 min.

For the DODAB+POES coating, the polymers were adsorbed onto the surface according to the previous report [17]. Briefly, a fused silica capillary was rinsed with 0.1 mM DODAB for 5 min, with 0.01% POE stearate for 5 min, and with the BGS for 3 min, respectively, prior to each run.

Procedure

All CE experiments were performed on a P/ACE MDQ system (Beckman Coulter, Fullerton, CA, USA) equipped with a diode-array UV detector. The modified capillary with total/effective lengths of 60/50 cm was employed in all experiments. To determine the EOF rate, the migration time of thiourea was measured in 20 mM phosphate buffer (pH 3.0–7.0), 0.5–100 mM acetate buffer (pH 4.0), or 100 μM TFA (~pH 4.0). In LVSEP-CZE, analytes dissolved in 100 μM TFA were injected into the whole capillary with a pressure of 20 psi for 90 s, whereas in conventional CZE, analytes dissolved in the BGS were injected into the capillary with a pressure of 0.3 psi for 3 s (injection volume, 1.7 nL). The applied voltage and the temperature were always set at 30 kV and 25 °C, respectively. UV detection was performed at 235 nm for thiourea detection and at 200 nm for all other analytes.

5-3. Results and Discussion

Evaluation of the EOF Rate in the Coated Capillaries

To obtain the weakly positive-charged surface, we investigated the following three coating methods: the PVA+PAA coating as a physical coating with thermal stabilization process; the PAA-ran-PMPC modification as a robust covalent coating; and the DODAB+POES coating as a weak physical coating using surfactants. In terms of the suppression and reversal of the EOF, the polymer mixing ratio of PVA:PAA = 95:5 was found to be the best for the PVA+PAA coating, and the PAA-ran-PMPC modification was found to be the optimal with the monomer mixing ratio of AA:MPC = 60:1. The author also found that the EOF in the DODAB+POES-coated capillary became quite

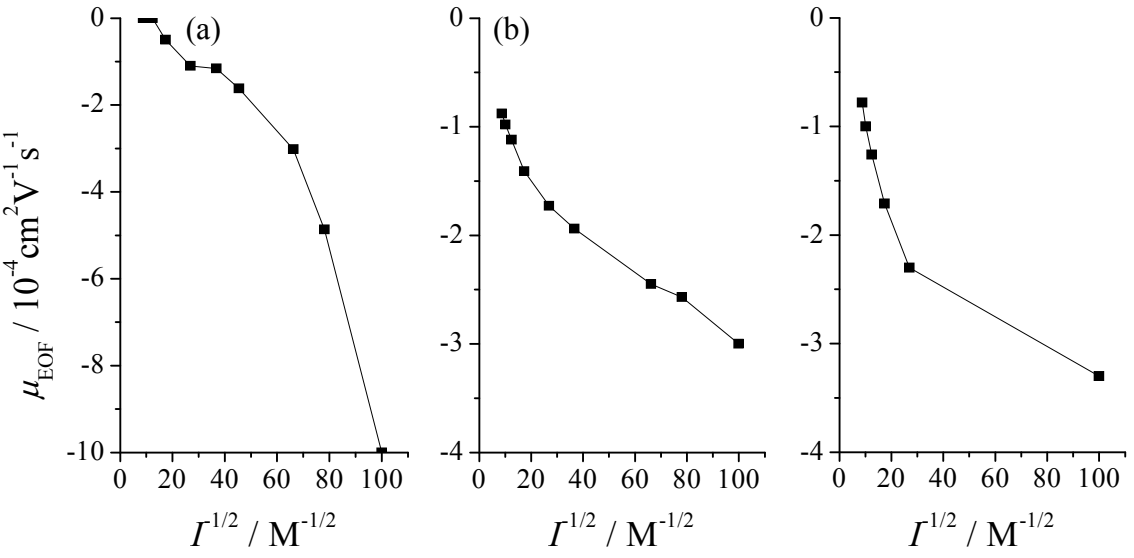

Figure 5-1. Electroosmotic mobility obtained in the electrolytes with different ionic strength. The employed capillary modification, (a) PVA+PAA, (b) PAA-ran-PMPC, and (c) DODAB+POES.

stable by increasing the concentration of POES to 0.1% (originally 0.01%) in the coating process.

In LVSEP using the EOF-suppressed capillary, the EOF must be suppressed in a high *I* BGS but must be enhanced in a low *I* SM. Hence, it is important to check the EOF velocity against *I*. The electroosmotic mobility (μ_{EOF}) in each coated capillary was estimated in the 0.5–100 mM acetate buffers (pH 4.0) or 100 μM TFA (pH ~ 4.0). The obtained μ_{EOF} was plotted against the $I^{-1/2}$ as shown in the Figure 5-1. In the PVA+PAA-coated capillary, μ_{EOF} was well suppressed as less than 2.8×10^{-5} $cm^2V^{-1}s^{-1}$ in the high concentration BGS but was increased up to 1.0×10^{-3} $cm^2V^{-1}s^{-1}$ as *I* is decreased. Similarly, μ_{EOF} in the PAA-ran-PMPC-modified capillary and μ_{EOF} in the DODAB+POES-coated capillary were suppressed as 8.8×10^{-5} $cm^2V^{-1}s^{-1}$ and 7.8×10^{-5} $cm^2V^{-1}s^{-1}$ in a 100 mM BGS but was increased up to 3.0×10^{-4} $cm^2V^{-1}s^{-1}$ and 3.3×10^{-4} $cm^2V^{-1}s^{-1}$ in the 10 μM TFA solution, respectively.

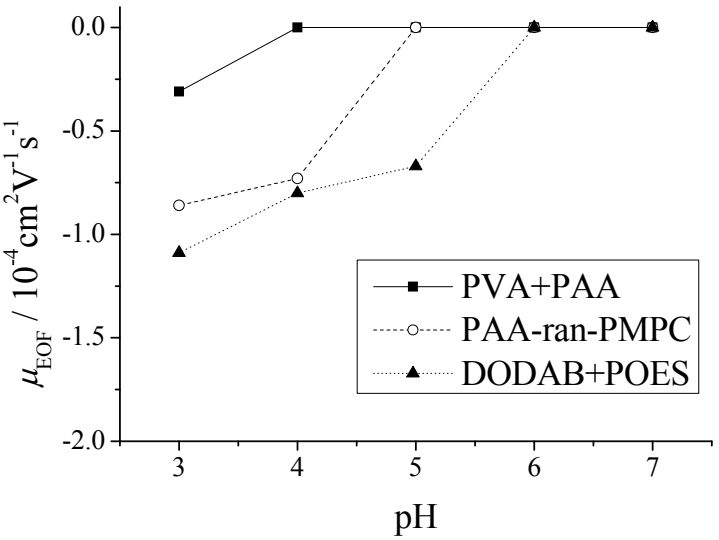

Figure 5-2. Electoosmotic mobilities of the three coated capillaries in a 20 mM phosphate buffer with pH 3.0–7.0. The square, circular, and triangular symbols represent the μ_{EOF} obtained in capillaries coated with PVA+PAA, PAA-ran-PMPC, DODAB+POES, respectively.

To employ many electrolytes, the EOF should also be suppressed in the wide pH range. Hence, μ_{EOF} was also estimated in 20 mM phosphate buffer with the pH ranged from 3.0 to 7.0. The obtained results are shown in Figure 5-2. The PVA+PAA-coating capillary exhibited the efficient suppression of the EOF in the pH range 4.0–7.0, and μ_{EOF} in pH 3.0 (3.1×10^{-5} cm^{2}V^{-1}s^{-1}) was still small enough not to prevent the migration of the cationic analytes. The PAA-ran-PMPC-modified capillary, the EOF was suppressed in the pH range 5.0−7.0, but slightly increased up to 8.6×10^{-5} cm^{2}V^{-1}s^{-1} in the more acidic condition. In the DODAB+POES-coated capillary, the EOF was well suppressed in pH 6.0 and 7.0, but increased up to 1.1×10^{-4} cm^{2}V^{-1}s^{-1} in pH 3.0. The slightly generated EOF in the acidic electrolytes in the PAA-ran-PMPC-modified and DODAB+POEScoated capillaries were expected to be sometimes unsuitable for the analysis of weakly cationic species. In this case, the

PVA+PAA-coated capillary with a good EOF suppression should be employed.

As for the durability of the surface coating, all the capillaries exhibited the good EOF suppression for more than 20-times repetitive analyses. However, few of the PVA+PAA-coated capillaries were likely to be spoiled after several analyses, indicating the slightly poor capillary-to-capillary reproducibility of the PVA-PAA coating. On the other hand, the PAA-ran-PMPC modification and DODAB+POES coating exhibited the better durability and capillary-to-capillary repeatability.

LVSEP–CZE of Aromatic Amines

Since the characteristic of the EOF in the three capillaries were shown to be suitable for the LVSEP-CE analysis of the cationic compounds, the LVSEP-CZE analyses of aromatic amines, BA and NEA, were carried out as model analytes. As shown in Figure 5-3, the LVSEP-CZE analyses of 100 ppb BA and NEA were successfully carried out all in the three capillaries. The separated peak patterns in LVSEP-CZE were almost the same as those in conventional CZE. The resolution and relative standard deviations (RSDs) of the migration time (t_M) and peak height were summarized in Table 5-1. The RSDs of t_M were worsened in LVSEP-CZE compared with those in conventional CZE. Hence, the correction of t_M with subtraction by current change time was carried out as in the previous report [8]. As a result, the RSDs were dramatically improved as 0.1% and 0.3% in the PAA-ran-PMPC-modified capillary and the DODAB+POES-coated capillary, respectively. However, the RSD in the PVA+PAA-coated capillary was not improved probably because the EOF was unstable not only in the concentration stage, but also in the separation stage. The RSDs of the peak height in LVSEP-CZE were better than those in conventional CZE probably due to

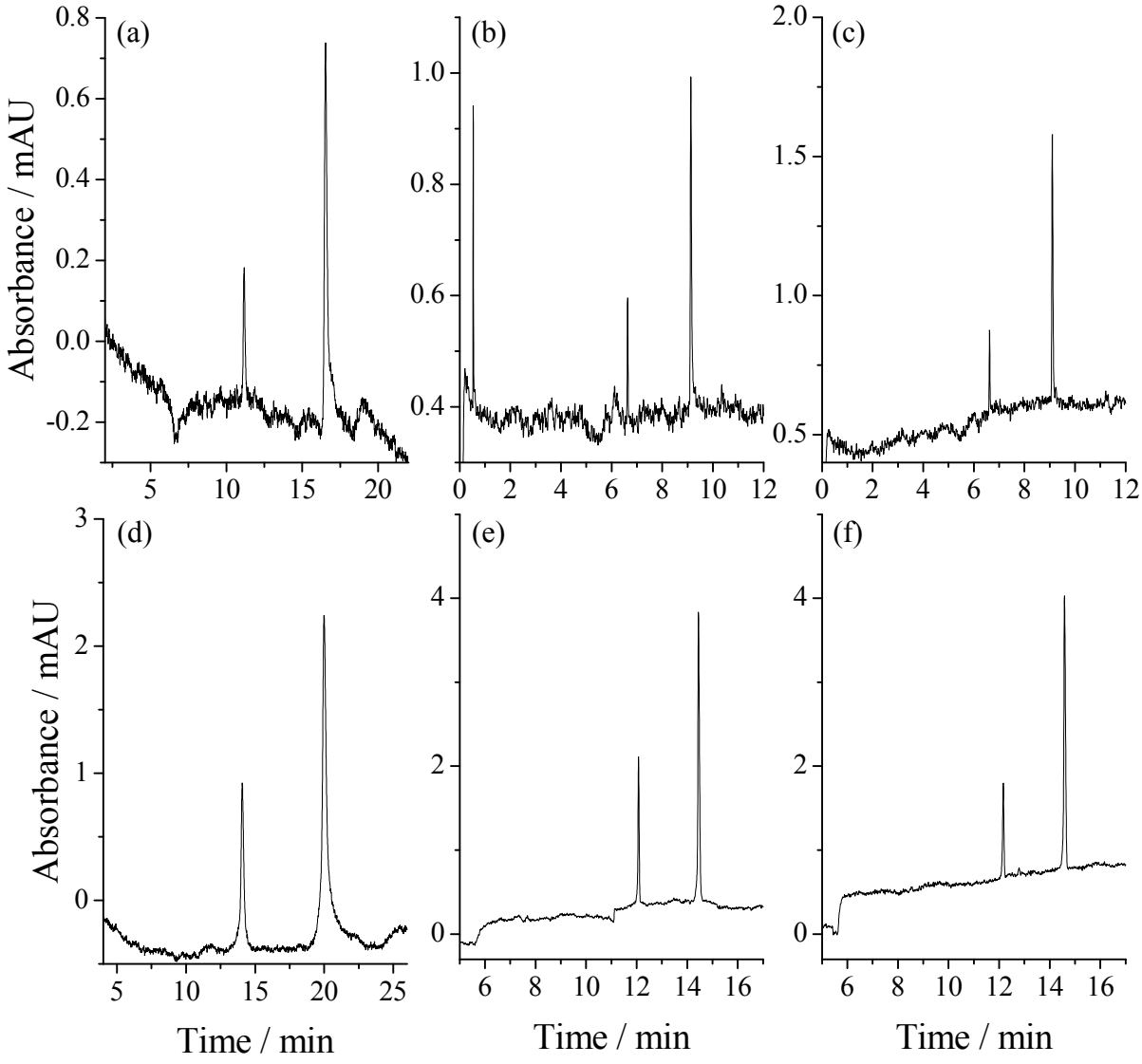

Figure 5-3. Electropherograms obtained (a,b,c) in the conventional CZE analyses of 10 ppm BA and NEA and (d,e,f) in the LVSEP-CZE analyses of 100 ppb BA and NEA. The employed capillary modification, (a,d) PVA+PAA, (b,e) PAA-ran-PMPC, and (c,f) DODAB+POES. BGS, 40 mM phosphate buffer (pH 3.0).

the stable sample injection volume (the whole capillary) in LVSEP-CZE. Resolutions (R_ss) in LVSEP-CZE were slightly worsened compared to those in conventional CZE. Since the peak-to-peak distance in the LVSEP-CZE analysis indicated that 95% of the whole capillary length was maintained for effective separation in this study, the

reduction in the resolution was mainly due to the band broadenings.

Table 5-1. Reproducibility and resolution in LVSEP-CZE and conventional CZE.

capillary coating	analysis mode	RSD (%) of t_M[a]	RSD (%) of height[a]	R_s[b]
PVA+PAA	CZE	1.9	9.1	20
	LVSEP-CZE	8.0 (16.7[c])	9.0	16
PAA-ran-PMPC	CZE	0.1	9.5	35
	LVSEP-CZE	5.7 (0.1[c])	2.3	24
DODAB+POES	CZE	0.4	23	36
	LVSEP-CZE	0.5 (0.3[c])	6.7	22

[a] RSDs for the BA peak (n = 3).

[b] Resolution between BA and NEA.

[c] RSD (%) of the corrected t_M with subtraction by current change time.

The sensitivity enhancement factors were summarized in Table 5-2. Up to 750-fold sensitivity increases were achieved in LVSEP-CZE, that is more than the 10-fold sensitivity improvement from the previous LVSS-CZE analysis [13]. In the case using the PVA+PAA-coated capillary, the least SEFs 290–380 were obtained. This was probably because the sample adsorption onto the capillary surface caused the band broadening and reduction in the peak height. The highest SEFs 590–750 obtained in the PAA-ran-PMPC-modified capillary with the sharpest peak shape also supported this hypothesis.

Similarly, the LVSEP-CZE analyses of four basic proteins, such as cytochrome *c*, lysozyme, ribonuclease A, and α-chymotrypsinogen A, were carried out to demonstrate the high performance LVSEP-CZE analysis of biomolecules. As a typical result obtained in the DODAB+POES-coated capillary, 1 ppm of the four basic proteins were well concentrated and baseline-separated with up to the 100-fold sensitivity improvement (data not shown). LVSEP-cyclodextrin (CD)-modified CZE (CDCZE)

was also performed in the PVA+PAA-coated capillary to confirm the capability of the developed LVSEP methods to be connected with other separation modes than CZE. In the LVSEP-CDCZE analysis of chlorpheniramine employing 16 mM β–CD as a chiral selector, 1 ppm chlorpheniramine was well optically resolved with the 80-fold sensitivity increase without almost any loss of resolution compared to the conventional CDCZE analysis (data not shown). It is indicated, therefore, that the developed LVSEP-CE methods can be applied to many separation modes and many cationic analytes.

Table 5-2. SEFs of aromatic amines obtained with the LVSEP-CZE analyses.

	PVA+PAA	PAA-ran-PMPC	DODAB+POES
BA	380	750	410
NEA	290	590	390

5-4. Conclusions

Three capillary coating methods, *i.e.*, PVA+PAA coating, PAA-ran-PMPC modification, and DODAB+POES coating, were investigated to achieve the weakly positive-charged capillary surface for the successful LVSEP-CE analysis of cationic compounds. In any cases, the EOF property was shown to be suitable for the LVSEP concentration and the following separation. Finally, the LVSEP-CZE analysis of the aromatic amines was successfully performed in any capillaries with up to 750-fold sensitivity increases. Studies along this line are being in progress in the Otsuka lab, where the author found that LVSEP-MCE of cations has already been carried out successfully in the same way as in this study.

5-5. References

[1] Simpson Jr. L. S.; Quirino, P. J.; Terabe, S. *J. Chromatogr. A* **2008**, *1184*, 504–541.

[2] Sueyoshi, K.; Kitagawa, F.; Otsuka, K. *J. Sep. Sci*. **2008**, *31*, 2650–2666.

[3] Burgi, D. S.; Chien, R.-L. *Anal. Biochem.* **1992**, *202*, 306–309.

[4] Quirino, J. P.; Terabe, S. *Anal. Chem.* **1999**, *71*, 1638–1644.

[5] Timerbaev, A. R.; Hirokawa, T. *Electrophoresis* **2006**, *27*, 323–340.

[6] Britz-McKibbin, P.; Chen, D. D. Y. *Anal. Chem.* **2000**, *72*, 1242–1252.

[7] Kawai, T.; Sueyoshi, K.; Kitagawa, F.; Otsuka, K. *Anal. Chem.* **2010**, *82*, 6504–6511.

[8] Kawai, T.; Watanabe, M.; Sueyoshi, K.; Kitagawa, F.; Otsuka, K. *J. Chromatogr. A* in press.

[9] Kawai, T.; Koino, H.; Sueyoshi, K.; Kitagawa, F.; Otsuka, K. *J. Chromatogr. A* in press.

[10] Harland, G. B.; McGrath, G.; McClean S.;Smyth, W. F. *Anal. Commun.* **1997**, *34*, 9–11.

[11] Smyth, W. F.; Harland, G. B.; McClean, S.; McGrath, G.; Oxspring, D. *J. Chromatogr. A* **1997**, *772*, 161–169.

[12] Quirino, J. P.; Terabe, S. *Electrophoresis*, **2000**, *21*, 355–359.

[13] Baryla, E. N.; Lucy, A. C. *Electrophoresis*, **2001**, *22*, 52–58.

[14] Ikada, Y.; Iwata, H.; Horii, F.; Matsunaga, T.; Taniguchi, M.; Suzuki, M.; Taki, W.; Yamagata, S.; Yonekawa, Y.; Handa, H. *J. Biomed. Mater. Res.* **1981**, *15*, 697–718.

[15] Srinivasan, K.; Pohl, C.; Avdalovic, N. *Anal. Chem.* **1997**, *69*, 2798–2805.

[16] MacDonald, A. M.; Bahnasy, M. F.; Lucy, C. A. *J. Chromatogr. A* **2011**, *1218*, 178–184.

[17] Gllges, M.; Kleemlss, M. H.; Schomburg, G. *Anal. Chem.* **1994**, *66*, 2038–2046.

Chapter 6.

Hydrophobic Labeling of Amino Acids: Transient Trapping–Capillary/Microchip Electrophoresis.

6-1. Introduction

Recently, CE and microchip electrophoresis (MCE) have become popular as versatile separation techniques as a result of several advantages, e.g. a high resolution, short analysis time and low consumption of reagents/samples. In addition, various separation modes are useful for the separation of numerous kinds of samples [1–8]. Especially, electrokinetic chromatography (EKC), which is performed by adding a pseudostationary phase to a running buffer, can resolve a variety of samples by a difference in an interaction between analytes and the pseudostationary phase [4,9–14]. However, CE and MCE have a serious disadvantage of low concentration sensitivity due to a short optical pathlength (50–100 μm) and/or a small amount of the sample to be injected (~pL). To improve the concentration sensitivity, several on-line sample concentration techniques have been developed in CE and MCE [15–20]. In micellar EKC (MEKC), it is well known that sweeping developed by Terabe's group is one of the most effective concentration techniques [21,22]. In sweeping-MEKC, hundred–thousand-fold higher peaks can be easily obtained compared to a conventional MEKC analysis. The bandwidth of the focused sample zone after sweeping is defined as $l_{inj}/(k+1)$, where l_{inj} and k are the injected length of the sample zone and the retention factor, respectively. Thus, stronger interaction between the samples and micelle leads to

higher efficiency of concentration. However, the excessively strong interaction sometimes reduces the resolution based on MEKC due to a narrower separation window for highly hydrophobic analytes [4]. Moreover, a large volume injection of the sample solution (S) often compromises resolution since the effective separation length is decreased. Therefore, the high concentration efficiency was sometimes incompatible with the high resolution in the sweeping-MEKC analysis.

To improve the detectability without the unfavorable decrease in the resolution, some on-line sample concentration techniques were combined with sweeping, *e.g.*, large volume sample stacking [23], cation selective exhaustive injection [24], and dynamic pH junction [25]. In another technique, Monton *et al*. have employed mixed micelle to improve the efficiency of sweeping [26]. In the microfluidic device, the sweeping technique combined with multiple injection of S was demonstrated by a manipulation of the electric polarity [27]. These techniques could provide high sensitive analysis by suppressing the decrease in the resolution, but could not "improve" the resolution compared to the conventional CE/MCE analyses. To achieve higher sensitivity and better resolution simultaneously, Sueyoshi *et al*. developed a new sample concentration and separation technique named transient trapping (tr-trapping) in MCE [28]. In tr-trapping, the micellar (M) and sample (S) solutions are successively introduced into the capillary or the separation channel filled with the background solution (BGS) without the micelle as long plugs as shown in Figure 6-1a, and then the separation voltage is applied. In the S zone, the analytes migrate toward the M zone by a fast EOF. When the analytes reach the boundary between the S and M zones (S/M boundary), they are strongly incorporated into the micelle and trapped nearby the S/M boundary due to the effect of the micellar diffusion from the M to S zones. Therefore, the analytes cannot

penetrate into the M zone and be focused on the S/M boundary as an extremely narrow band by the trap mechanism (Figure 6-1b). At the same time, the concentration of the micelle is gradually decreased upon increasing the length of the M zone due to the diffusion, the difference in the velocity of the micelle located nearby the both ends of the M zone, and difference in the electrophoretic mobility between a micelle and

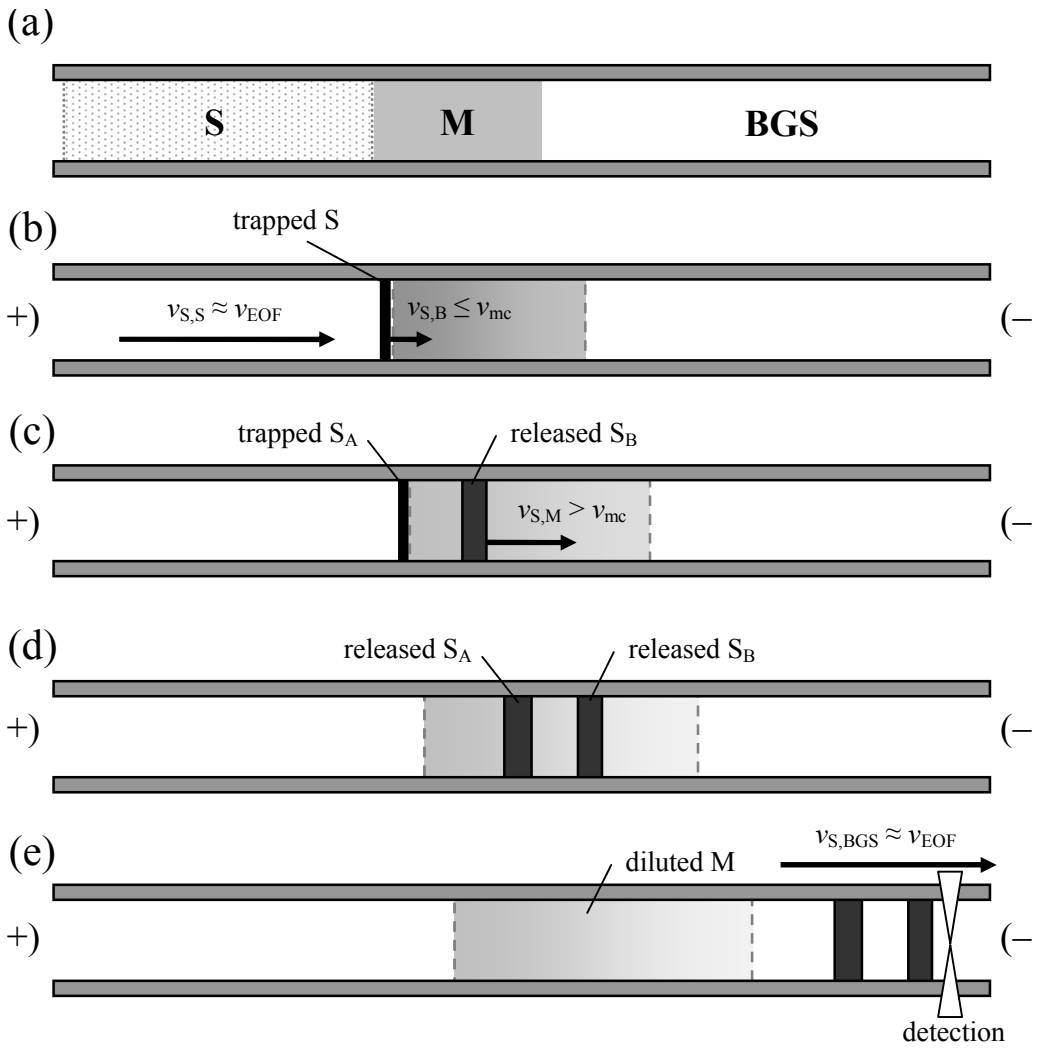

Figure 6-1. Schematics diagram of the tr-trapping. (a) initial condition, (b) concentration of analytes due to the trap mechanism, (c) separation of analytes due to the difference in the release timings of analytes, (d) separation based on MEKC and (e) detection. The symbols of $v_{S,S}$, $v_{S,M}$, $v_{S,BGS}$, and $v_{S,B}$ are the apparent velocity of the samples in the S, M, BGS and nearby the boundary between the S and M zones, respectively. The symbols of v_{mc} and v_{EOF} are the apparent velocity of the micelle and the electroosmotic velocity, respectively.

surfactant monomers [29]. As a result, the interaction between the analytes and micelle is also decreased, which allows the analytes trapped on the S/M boundary to be released into the M zone in the order of the hydrophobicity as shown in Figures 6-1c,d. Consequently, the analytes are separated by the difference in the release time. After releasing the analytes, they migrate toward the cathode as shown in Figure 6-1e. In the previous paper, it was confirmed that successive concentration and separation based on the trap-and-release mechanism resulted in not only the sensitivity enhancement but also the resolution improvement. Especially, the separation based on the release mechanism has attracted researcher's attention since highly hydrophobic analytes, which is difficult to be separated by conventional CZE and MEKC, can be resolved. However, it is still difficult to achieve both a highly effective concentration and improvement of the resolution for hydrophilic analytes since the trap mechanism require a strong interaction between the analytes and micelle. In the case of moderately hydrophobic analytes, they are once concentrated by the conventional sweeping. However, the sweeping effect should disappear after the focused bands pass through the M zone due to the desweeping effect [28] and the band broadening owing to the variation of the concentration profile of M zone [29]. Thus, the limited applicability of the tr-trapping technique should be improved to achieve a high-sensitive and high-resolution analysis.

To overcome this drawback, the author focused on the sample labeling. Generally, a derivatization by using dyes exhibiting fluorescence and UV absorption [30–32] is carried out to detect non-fluorescent or non-UV absorbance analytes. Especially, the fluorescence labeling of amino acids (AAs) was one of the important techniques for highly sensitive analyses in CE and MCE [33–34]. In this paper, the enhancement of the hydrophobicity by the fluorescence labeling technique was studied to extend the

applicability of tr-trapping-MEKC. To investigate the effect of the labeling on the tr-trapping, several AAs and fluorescent reagents reacting with amino groups were selected. The concentration and separation of the labeled AAs in tr-trapping-MEKC were demonstrated to evaluate the validity of the hydrophobic labeling in CE and MCE.

6-2. Experimental Section

Chemical and Reagents

Fluorescein isothiocyanate (FITC) was purchased from Sigma-Aldrich (Tokyo, Japan), succinimidyl esters of Alexa Fluor 488, and 6-((4,4-difluoro-5,7-dimethyl-4-bora-3a,4a-diaza-s-indacene-3-propionyl)-amino) hexanoic acid (BODIPY FL-X) were purchased from Molecular Probes (Eugene, OR, USA), 2'-methoxybenzenazo-2-naphthol (Sudan R) was purchased from Tokyo Chemical Industry (Tokyo, Japan), methanol, dimethyl sulfoxide (DMSO), AAs and sodium dodecyl sulfate (SDS) were purchased from Nacalai Tesque (Kyoto, Japan). All reagents were of analytical or HPLC grade. All of the solutions were filtered through a 0.45 μm-pore membrane filter prior to use. The BGS and M were prepared with a mixing/dilution of the 200 mM phosphate (pH 7.2 and 5.0) and 0.5 M SDS stock solutions. The detailed experimental conditions are listed in the figure captions. The Ss were prepared by the dilution of stock solutions of labeled AAs with the BGS in CZE, sweeping- and tr-trapping-MEKC and with M in MEKC.

Apparatus

CE experiments were performed on a P/ACE MDQ system (Beckman Coulter,

Fullerton, CA, USA). Detection was carried out by UV absorbance (220 nm) for native phenylalanine (Phe) and laser-induced fluorescence (LIF, excitation/emission, 488/532 nm) for labeled AAs. A fused-silica capillary (50 μm id and 375 μm od) was purchased from Polymicro (Phoenix, AZ, USA). In MCE, the originally fabricated quartz microchip with a 5 way cross injector (5-way cross chip) was used [28]. The MCE analysis was carried out on the microscope combined with a PC-controlled high-voltage source and the LIF detection scheme as previously reported [28, 35].

Fluorescence Derivatization

To evaluate the effect of the labeling, the excess amounts of AAs were mixed with fluorescent dyes for a suppression of the interference from the free and decomposed dyes. Each AA was individually labeled with fluorescent dyes as given in the following procedure. Experimentally, 1 mM fluorescent labeling reagent in DMSO was mixed with nine times volume of 10 mM each AA in 150 mM Na_2CO_3 (pH 8.5), and then the mixtures were put in dark with stirring at room temperature. The labeling reaction was sufficiently accomplished after 12 h stirring, and the obtained solutions were defined to 0.1 mM labeled AA stocks. Before the CE and MCE analyses, the stock solutions of the labeled AAs were mixed and diluted with an appropriate amount of the BGS or M.

Procedure

In tr-trapping-MEKC, the M and S solutions were successively introduced into the capillary filled with the BGS containing no micelle. The separation voltage of 20 kV was then applied to the both end of the capillary. Native Phe and the labeled AAs were detected with UV absorbance and LIF, respectively.

In tr-trapping-microchip MEKC (tr-trapping-MCMEKC), a 5 way cross microchip was employed as described in a previous paper [28]. Briefly, the whole channels were filled with the BGS. The sample and micellar reservoirs were then filled with the S and M solutions, respectively. The BGS was also poured into the sample waste, buffer waste and BGS reservoirs. By applying the programmed voltages to the reservoirs, the M and S solutions were successively introduced into the separation channel. In the case of conventional methods, S was introduced into the separation channel filled with M by the gated/pinched injection (PI) methods for the MCMEKC with/without sweeping, respectively [36, 37]. The analytes were detected at the 24 mm from the 5 way cross injector by the LIF scheme (excitation/emission wavelength, 488/516 nm).

6-3. Results and Discussion

Effect of Labeling on Tr-Trapping

Generally, the fluorescent derivatization of the non-fluorescent species is conducted to detect by the sensitive LIF scheme. In this study, the fluorescent derivatization of AAs was also carried out to enhance the hydrophobicity of these hydrophilic analytes. In this paper, commercially available three fluorescent dyes, FITC, succinimidyl esters of Alexa Fluor 488 and BODIPY FL-X, were used as the labeling reagents. Among three dyes, FITC was selected as the contrast since fluorescein, which was the main body of FITC, was not incorporated into the SDS micelle in the preliminary study (data was not shown). The chemical structures of the dyes are shown in Figure 6-2. In the case of the FITC labeling of alanine (Ala), the interaction between FITC-Ala and the SDS micelle was not observed since FITC has a hydrophilic hydroxyl

group and anionic carboxyl group at pH 7.0. Under the tr-trapping condition, therefore, FITC-Ala could not be trapped due to the low hydrophobicity and it was detected as the rectangular peak meaning the unfocused sample zone. On the other hand, Alexa-Ala was well concentrated under the same condition at the injection time of M and S ($t_{inj,M}$ and $t_{inj,S}$) of 30 and 180 s, respectively, nevertheless the Alexa dye was also hydrophilic similar to FITC due to the negative charges owing to one carboxyl and two sulfonic acid groups. In the previous paper [28], sulforhodamine B and sulforhodamine 101, which

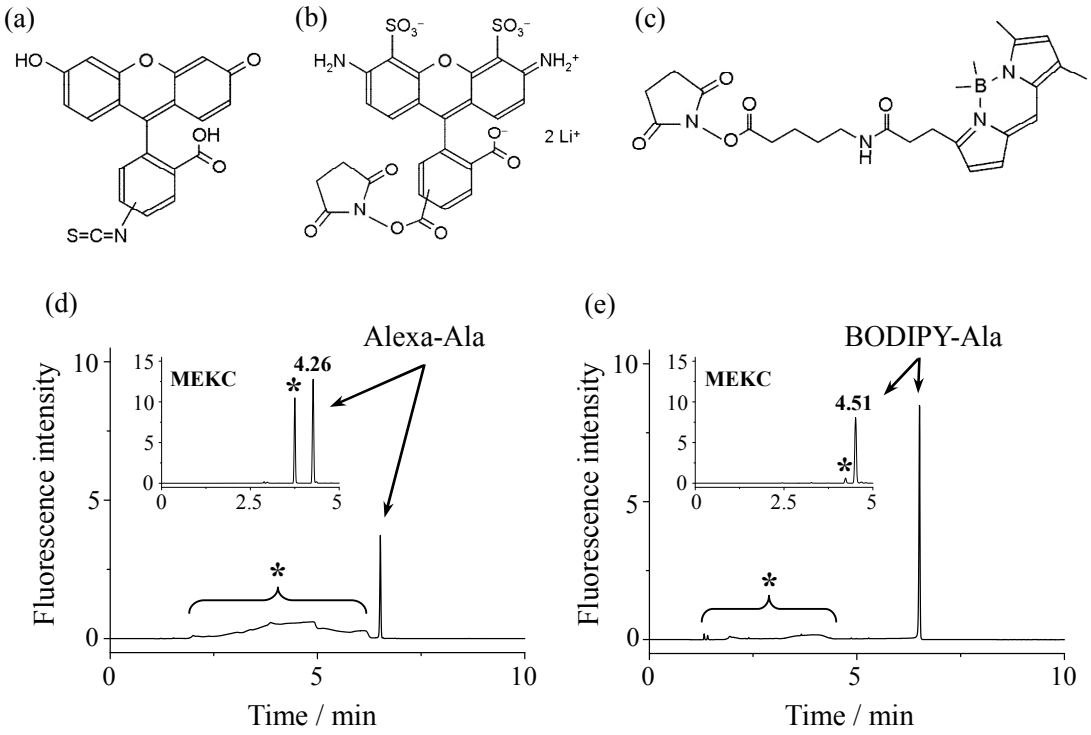

Figure 6-2. Chemical structures of (a) fluorescein isothiocyanate, (b) Alexa Fluor 488, succinimidyl ester (c) BODIPY FL-X, succinimidyl ester and electropherograms obtained with the tr-trapping-MEKC analyses of (d) Alexa- and (e) BODIPY-Ala. Total/effective length, 40/30 cm. BGS, 34 mM phosphate buffer (pH 7.0); M, 100 mM SDS in 10 mM phosphate buffer; S, 1 nM (d) Alexa- and (e) BODIPY-labeled Ala in BGS; conductivity of solutions, 4.0 mS/cm; $t_{inj,M}$, 30 s; $t_{inj,S}$, 180 s. *, free and decomposed dyes. Inserts show the conventional MEKC using the M solution as the running buffer. S, 100 nM labeled Ala in the M; $t_{inj,S}$, 5 s in MEKC.

have similar structures having sulfonic acid groups and a xanthene body with a delocalized positive charge, were also highly incorporated into the SDS micelle and well concentrated under the tr-trapping condition. These results indicate that the strong interaction between these dyes and SDS micelle was mainly based on the electrostatic interaction due to the positively charged xanthene body. In the tr-trapping analysis of BODIPY-Ala, a sharp peak was also observed as depicted in Figure 6-2e because of the hydrophobicity of the BODIPY dye that was almost neutral under the experimental condition. As for these two labeling methods, the BODIPY-labeling gave the higher and smaller peaks of free dyes and decomposed components than those obtained by the Alexa-labeling as shown in Figure 6-2d and 6-2e. To evaluate the concentration efficiency of tr-trapping for these analytes, the sensitivity enhancement factor (SEF) was calculated by the following equation:

$$\mathrm{SEF} = \frac{C_{\mathrm{normal}}}{C_{\mathrm{conc}}} \times \frac{h_{\mathrm{conc}}}{h_{\mathrm{normal}}} \qquad (6\text{-}1)$$

where C and h are the concentration and peak height of the analytes, the subscripts “conc” and “normal” mean the values obtained with and without the concentration techniques, respectively. The SEF values for Alexa- and BODIPY-Ala were calculated to be 29 and 105 compared to the conventional MEKC, respectively. Under the tr-trapping condition shown in Figures 6-2d,e, both the labeled AAs were detected as the trapped peak. There are a lot of micelles around the labeled AAs under the tr-trapping condition as same as the conventional MEKC, suggesting that the variation of the quantum yields could be negligible at least in this SEF comparison. Thus, the lower SEF of Alexa-Ala was mainly due to hydrophilicity and the negative charges of sulfonic acid groups in the Alexa dye. Thus, it was clarified that the BODIPY-labeling

was superior to the Alexa-labeling in the tr-trapping analysis because of the higher hydrophobicity, higher concentration efficiency and less signal of the free/decomposed dyes. In the remaining experiments, therefore, the BODIPY dye was selected as the labeling reagent.

To elucidate the effect of the BODIPY labeling on tr-trapping, Phe and BODIPY-Phe were analyzed under the tr-trapping-MEKC condition employing UV absorbance and LIF detection schemes, respectively. When the native Phe was injected into the capillary for 450 s after the partial injection of the M plug for 60 s, a broad and rectangular peak was detected as shown in Figure 6-3a. This demonstrated that the long sample plug could not be concentrated since the hydrophobicity of the native Phe was too low to be trapped around the S/M boundary. In contrast, an extremely sharp peak of BODIPY-Phe was observed as shown in Figure 6-3b, indicating that the hydrophobicity of Phe was well enhanced by the labeling as enough to be trapped.

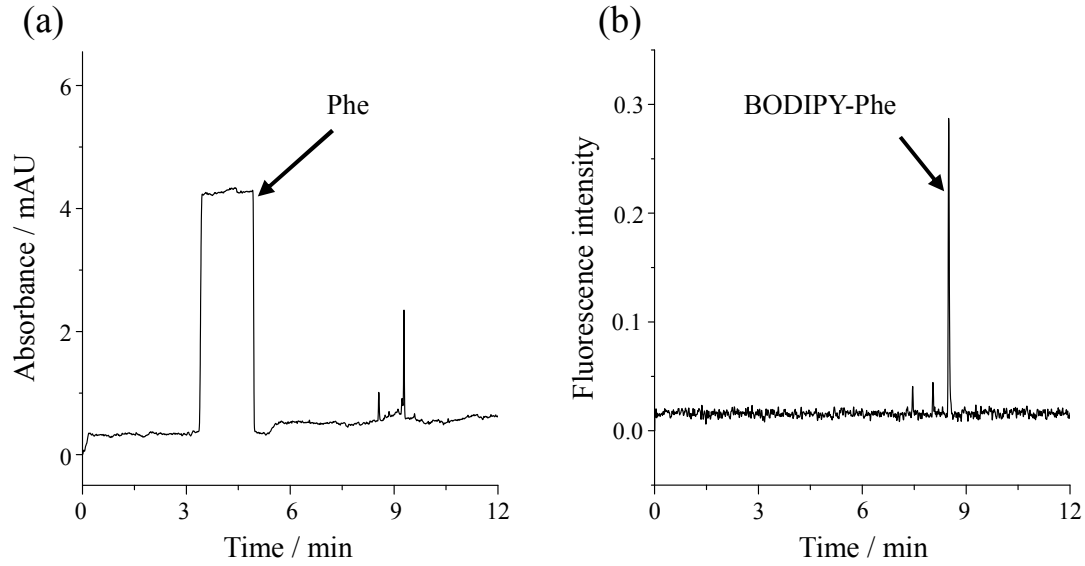

Figure 6-3. Tr-trapping-MEKC analyses of (a) unlabeled and (b) BODIPY-Phe employing UV and LIF detection, respectively. Total/effective length, 40/30 cm. BGS, 34 mM phosphate buffer (pH 5.0); M, 25 mM SDS in 29 mM phosphate buffer (pH 5.0); $t_{inj,M}$, 180 s; $t_{inj,S}$, 450 s. Concentration of S, (a) 100 μM and (b) 50 pM.

For further investigation of the hydrophobic labeling, various AAs were also labeled with the BODIPY dye and their retention factors under the MEKC condition were estimated. As a result, the *k* value of Phe was increased from 0.1 to 23 by the BODIPY labeling. The *k* values of other native AAs could not be estimated since they were not detected by the UV absorbance detector. On the other hand, the *k* values of neutral AAs labeled with the BODIPY dye were calculated 16–20, which were larger than the estimated threshold *k* (4.1) to trap on the S/M boundary under the experimental condition 28. Therefore, the hydrophobic labeling using the BODIPY dye allowed the hydrophilic analytes to be concentrated by tr-trapping and detected by LIF.

Concentration and Separation of AAs in CE

To estimate the effect of the hydrophobic labeling on the concentration and separation efficiencies in the tr-trapping technique, four neutral AAs, leusine (Leu), isoluesine (Ile), valine (Val) and Phe were derivatized with the BODIPY dye and analyzed by CZE, MEKC, sweeping-MEKC and tr-trapping-MEKC. Under the CZE condition, these labeled AAs could not be separated as shown in Figure 6-4a due to their closely resembled electrophoretic mobilities from −1.16 to −1.22 × 10^{-4} $cm^2V^{-1}s^{-1}$. These negative values of the neutral AAs labeled with the BODIPY dyes meant that the positively charged amino groups were consumed by the labeling. In MEKC, the electrophoretic mobility of the anionic micelle was comparable to the electroosmotic mobility under the experimental condition. Since the apparent velocity of the labeled AAs became very slow due to the strong interaction with the micelle, they could not be detected within 30 min. When sweeping-MEKC was carried out at the $t_{inj,S}$ of 450 s, the decrease in the effective length from ca. 60 to 40 cm allowed the analytes to reach

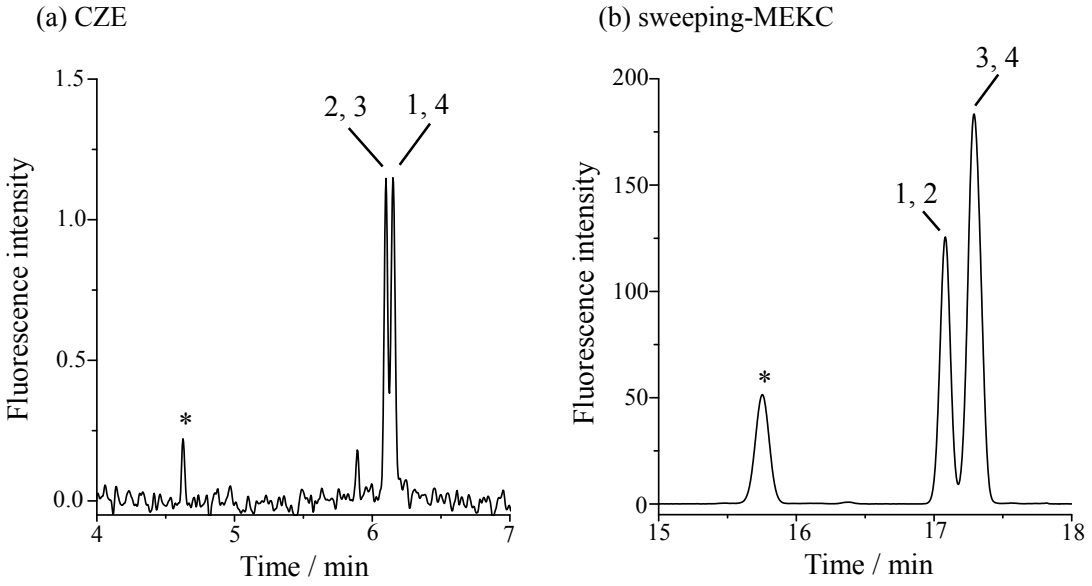

Figure 6-4. CZE and sweeping-MEKC analyses of the labeled AAs. Total/effective length, 70/60 cm. BGS, 34 mM phosphate buffer (pH 5.2) in CZE; 25 mM SDS in 29 mM phosphate buffer/10% (v/v) methanol (pH 5.3) in sweeping-MEKC. Concentration of S, 1 nM in BGS. Conductivity of the solutions, 2.1 mS/cm. Injection time of S, (a) 5 s, (b) 450 s. Observed peaks were identified as 1, Val; 2, Ile; 3, Leu; 4, Phe; *, free and decomposed BODIPY dyes.

the detection window as shown in Figure 6-4b. However, the baseline separation of the BODIPY-AAs was not achieved because the large volume injection of S decreased the effective separation length. Consequently, it was found that sweeping-MEKC was also unsuitable for the separation of the highly hydrophobic BODIPY-AAs.

In tr-trapping-MEKC, on the other hand, these analytes could be well resolved and concentrated as shown in Figure 6-5a at $t_{inj,M}$ and $t_{inj,S}$ of 60 and 150 s, respectively. The SEF values relative to the CZE analysis were increased from 18–24 to 106–125 with increase in $t_{inj,S}$ from 150 to 450 s as shown in Figure 6-5b. In the analyses of labeled Phe in CZE and tr-trapping-MEKC, the values of the limit of detection (LOD) were estimated to be 8.0×10^{-10} and 5.0×10^{-12} M, respectively, indicating 160-times improvement of the LOD. The obtained LOD value could not be directly compared to

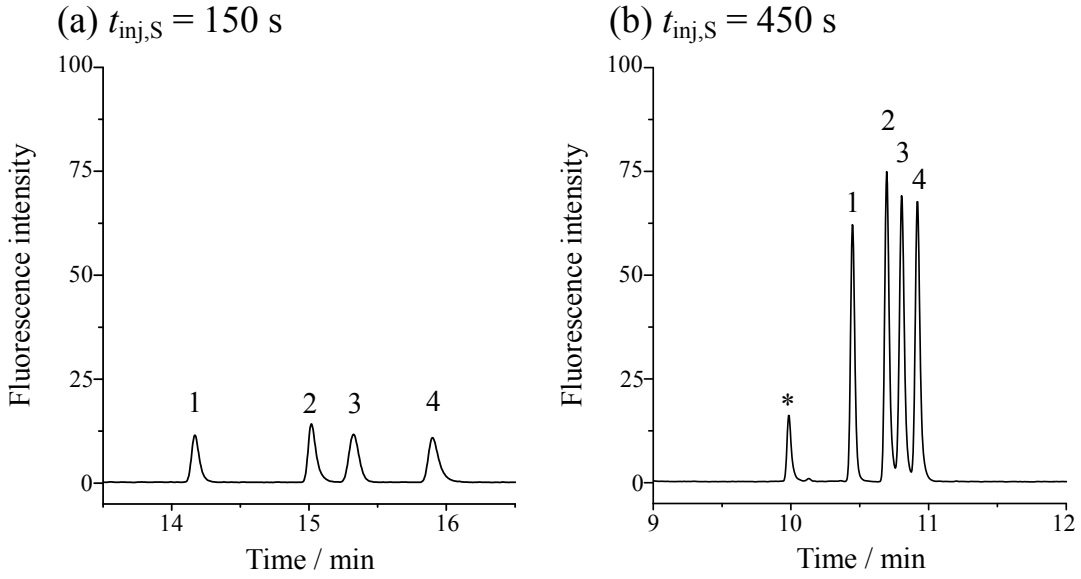

Figure 6-5. Effect of the $t_{inj,S}$ on the tr-trapping-MEKC analyses of the labeled AAs at the $t_{inj,M}$ of 60 s. Total/effective length, 70/60 cm. BGS, 34 mM phosphate buffer (pH 5.2). M, 25 mM SDS in 29 mM phosphate buffer/10% (v/v) methanol (pH 5.3). Concentration of S, 1 nM in BGS. Conductivity of the solutions, 2.1 mS/cm. Observed peaks were identified as 1, Val; 2, Ile; 3, Leu; 4, Phe; *, free and decomposed BODIPY dyes.

the previous reports [30–34] since the LOD value in the manuscript was calculated by the standards of the concentration of BODIPY dye, whereas those in the most previous reports made the concentration of AAs the standards. However, it was found that the highly sensitive analysis of labeled AAs could be demonstrated by tr-trapping-MEKC.

Table 6-1. Effect of $t_{inj,S}$ on apparent plate number and resolution in tr-trapping-MEKC.

	$N_{app} \times 10^{-5}$				R_s		
$t_{inj,S}$ / s	Val	Ile	Leu	Phe	Val–Ile	Ile–Leu	Leu–Phe
150	3.0	3.4	2.0	2.1	8.2	2.6	4.1
300	4.3	4.3	3.8	3.4	7.4	1.8	3.9
450	5.6	5.2	4.5	4.8	4.3	1.7	1.8

To confirm the separation performance in tr-trapping-MEKC, the variation of the resolution (R_s) and apparent plate number (N_{app}) were calculated with changing $t_{inj,S}$. As a result, the R_s was decreased upon increase in $t_{inj,S}$, whereas the N_{app} was increased as shown in Table 6-1. In the tr-trapping analysis, the trapped analytes are first separated by the release mechanism nearby the S/M boundary, and then resolved on the basis of MEKC in the M zone. After leaving the M zone, analyte migrates in the BGS zone based on CZE. Among these different separation mechanisms, the effect of the release mechanism was independent of the variation of the $t_{inj,S}$ reported in the previous paper [28]. The separation on the basis of CZE in the BGS zone was also not effective under the experimental condition as shown in Figure 6-4a. Hence, it was supposed that this variation of the separation efficiencies was due to the migration of the analytes in the M zone. In the previous reports on tr-trapping- and partial filling-MEKC [28,29], it was indicated that the concentration profile of micelle became trapezoidal or triangular due to a difference in the electrophoretic mobilities between micelle and other anionic species in the BGS and M zones. The concentrations of micelle and electric field in the M zone decreased gradually toward the cathode, resulting in the difference in the effective velocity of the sample molecules located in the cathodic/anodic side of the S zone. This decrease in concentration profile of M could generate the band broadening of the concentrated S zones migrating in the M zone. Thus, it was indicated that the increase in N_{app} upon increase in $t_{inj,S}$ was caused by the decrease in the band broadening in the M zone due to the decrease in the effective length. In other words, it was suggested that the analytes were detected in the M zone under the experimental condition. However, the gradient of the micellar concentration also provides the effective separation of the hydrophobic analytes in the M zone by a further extension of

the difference in the effective migration velocity of the analytes. Therefore, the better R_s was observed at $t_{inj,S}$ of 150 s than 450 s in spite of the broader peaks. Consequently, the observed effects of the injected length of S indicate that the separation based on MEKC under the micellar concentration gradient also played an important roll in tr-trapping-MEKC.

Application to MCE

The other labeled AAs, BODIPY-labeled lysine (Lys) and histidine (His), were also analyzed by MCE to realize a further high-performance electrophoretic analysis. The electropherograms obtained in conventional, sweeping- and tr-trapping-MCMEKC

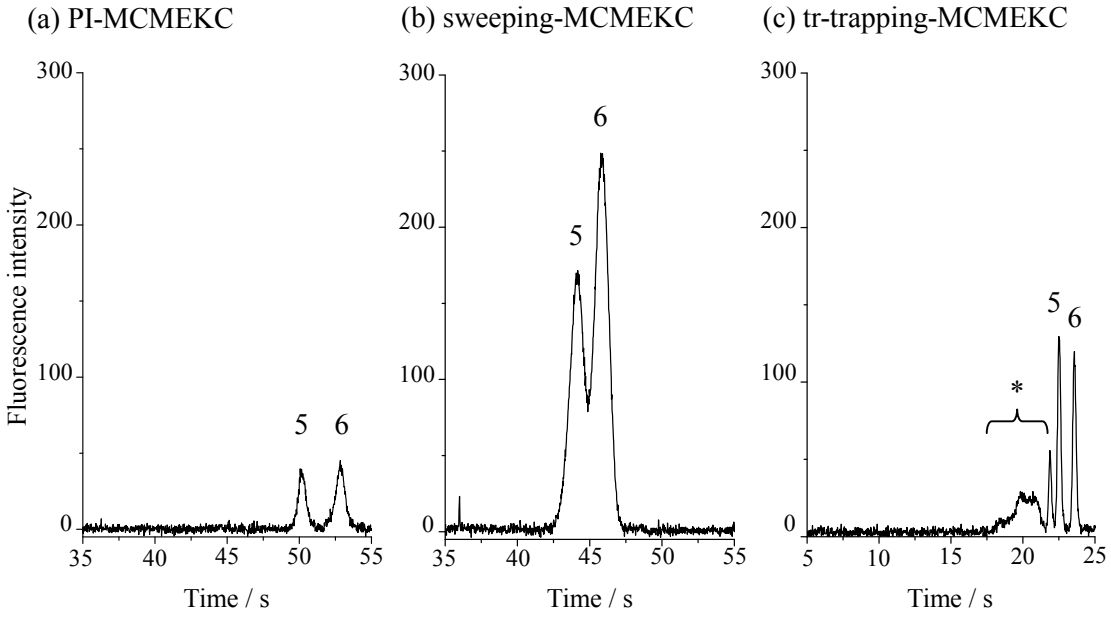

Figure 6-6. Electropherograms obtained with (a) PI-MCMEKC, (b) sweeping-MCMEKC at the $t_{inj,S}$ of 4.0 s, and (c) tr-trapping-MCMEKC at the $t_{inj,M}$ and $t_{inj,S}$ of 5.0 and 4.0 s, respectively. BGS, 30 mM phosphate buffer (pH 7.2) /10% (v/v) methanol; M, 25 mM SDS in 22 mM phosphate buffer (pH 7.2)/10% (v/v) methanol; S, (a) 500 nM Lys and His prepared with M, (b) and (c) 25 nM BODIPY-Lys and His prepared with BGS. Conductivity of the solutions, 3.2 mS/cm. Observed peaks were identified as 5, Lys; 6, His; *, free and decomposed BODIPY dyes.

are shown in Figure 6-6. The estimated R_s and N_{app} are summarized in Table 6-2. When BODIPY-Lys and His were analyzed by the conventional PI-MCMEKC, a baseline separation was achieved as shown in Figure 6-6a. In sweeping-MCMEKC (Figure 6-6b), the highest peaks were observed within 50 s. However, the observed peaks were broadened by the diffusion after finishing sweeping and not resolved completely due to both the shortened effective length and high hydrophobicity of labeled AAs. In tr-trapping-MCMEKC, on the other hand, well-resolved sharp peaks were observed within 30 s as shown in Figure 6-6c. Both N_{app} and R_s were improved relative to the conventional PI-MCMEKC, indicating that the trap-and-release mechanism provided a suppression of the band broadening and a highly effective separation by the difference in the release time [28]. With regard to the concentration effect, the SEFs for BODIPY-His and Lys in tr-trapping-MCMEKC were calculated to be 34 and 66, respectively. Furthermore, the SEF values for BODIPY-His and Lys were increased from 13 and 23 to 80 and 150, respectively, with increase in $t_{inj,S}$ from 1.0 to 10 s and maintaining acceptable R_s. Although the SEFs in sweeping-MCMEKC were higher than those in tr-trapping, the longer effective length was required for the baseline separation of AAs in sweeping-MCMEKC, which was not desirable for the high-throughput analysis in MCE. Consequently, it was confirmed that the tr-trapping technique with the BODIPY labeling allowed not only CE but also MCE to perform the high-resolution and sensitive analysis of AAs with a short analysis time.

Table 6-2. Apparent plate numbers and resolution of basic AAs in MCE.

	$N_{app,Lys}$	$N_{app,His}$	R_s
PI-MCMEKC	46 000	33 000	2.5
sweeping-MCMEKC	10 000	13 000	1.0
tr-trapping-MCMEKC	56 000	57 000	2.7

6-4. Conclusion

In this study, the author demonstrated that the applicability of tr-trapping was successfully extended to hydrophilic analytes by the hydrophobic labeling with the BODIPY dye. The labeled AAs were concentrated and separated in tr-trapping-MEKC, providing the 160-fold enhancement of the LOD and the best LOD of 5.0×10^{-12} M. In the microfluidic device, the hydrophobic labeling also provided the rapid, sensitive and high-resolution analysis of AAs in tr-trapping-MCMEKC. These results indicate that the hydrophobic labeling allows hydrophilic analytes containing amino groups to be analyzed by tr-trapping-MEKC and -MCMEKC, which will contribute toward the improvement of the analytical performance of various CE analyses.

6-5. References

[1] Jorgenson, J. W.; Lukacs, K. D. *Anal. Chem.* **1981**, *53*, 1298–1302.

[2] Manz, A.; Harrison, D. J.; Verpoorte, E.; Fettinger, J. C.; Paulus, A.; Lüdi, H.; Widmer, H. M. *J. Chromatogr.* **1992**, *593*, 253–258.

[3] Tsuda, T.; Nomura, K.; Nakagawa, G. *J. Chromatogr.* **1982**, *248*, 241–247.

[4] Terabe, S.; Otsuka, K.; Ichikawa, K.; Tsuchiya, A.; Ando, T. *Anal. Chem.* **1984**, *56*, 111–113.

[5] Hjertén, S.; Zhu, M.-D. *J. Chromatogr.* **1985**, *346*, 265–270.

[6] Cohen, A. S.; Karger, B. L. *J. Chromatogr.* **1987**, *397*, 409–417.

[7] Boček, P.; Deml, M.; Janák, J. *J. Chromatogr.* **1978**, *156*, 323–326.

[8] Sahota, R. S.; Khaledi, M. G., *Anal. Chem.* **1994**, *66*, 1141–1146.

[9] Terabe, S.; Otsuka, K.; Ando, T. *Anal. Chem.* **1985**, *57*, 834–841.

[10] Heeren, F. V.; Verpoorte, E.; Manz, A.; Thormann, W. *Anal. Chem.* **1996**, *68*, 2044–2053.

[11] Copper, C. L.; Sepaniak, M. J. *Anal. Chem.* **1994**, *66*, 147–154.

[12] Kitagawa, F.; Aizawa, S.; Otsuka, K. *Anal. Sci.* **2005**, *21*, 61–65.

[13] Palmer, C. P. *Electrophoresis* **2009**, *30*, 163–168.

[14] Ryan, R.; Donegan, S.; Power, J.; Altria, K. *Electrophoresis* **2010**, *31*, 755–767.

[15] Sentellas, S.; Puignou, L.; Galceran, M. T. *J. Sep. Sci.* **2002**, *25*, 975–987.

[16] Timerbaev, A. R.; Hirokawa, T. *Electrophoresis* **2006**, *27*, 323–340.

[17] Breadmore, M. C. *Electrophoresis* **2007**, *28*, 254–281.

[18] Simpson, S. L. Jr.; Quirino, J. P.; Terabe, S. *J. Chromatogr. A* **2008**, *1184*, 504–541.

[19] Sueyoshi, K.; Kitagawa, F.; Otsuka, K. *J. Sep. Sci.* **2008**, *31*, 2650–2666.

[20] Breadmore, M. C.; Thabano, J. R. E.; Dawod, M.; Kazarian, A. A.; Quirino, J. P.; Guijt, R. M. *Electrophoresis* **2009**, *30*, 230–248.

[21] Quirino, J. P.; Terabe, S. *Science* **1998**, *282*, 465–468.

[22] Sera, Y.; Matsubara, N.; Otsuka, K.; Terabe, S. *Electrophoresis* **2001**, *22*, 3509–3513.

[23] Zhu, L.; Tu, C.; Lee, H. K. *Anal. Chem.* **2002**, *74*, 5820–5825.

[24] Quirino, J. Q.; Iwai, Y.; Otsuka, K.; Terabe, S. *Electrophoresis* **2000**, *21*, 2899–2903.

[25] Britz-McKibbin, P.; Otsuka, K.; Terabe, S. *Anal. Chem.* **2002**, *74*, 3736–3743.

[26] Monton, M. R. N.; Otuka, K.; Terabe, S. *J. Chromatogr. A* **2003**, *985*, 435–445.

[27] Liu, Y.; Foote, R. S.; Jacobson, S. C.; Ramsey, J. M. *Lab Chip* **2005**, *5*, 457–465.

[28] Sueyoshi, K.; Kitagawa, F.; Otsuka, K. *Anal. Chem.* **2008**, *80*, 1255–1262.

[29] Muijselaar, P. G.; Otsuka, K.; Terabe, S. *J. Chromatogr. A* **1998**, *802*, 3–15.

[30] Viglio, S.; Fumagalli, M.; Ferrari, F.; Iadarola, P. *Electrophoresis* **2010**, *31*, 93–104.

[31] Poinsot, V.; Rodat, A.; Gavard, P.; Feurer, B.; Couderc, F. *Electrophoresis* **2008**, *29*, 207–223.

[32] Poinsot, V.; Gavard, P.; Feurer, B.; Couderc, F. *Electrophoresis* **2010**, *31*, 105–121.

[33] Nouadje, J.; Nertz, M.; Verdeguer, P.; Couderc, F. *J. Chromatogr. A* **1995**, *717*, 335–343.

[34] Chiesl, T. M.; Chu, W. K.; Stockton, A. M.; Amashukeli, X.; Grunthaner, F.; Mathies, R. A. *Anal. Chem.* **2009**, *81*, 2537–2544.

[35] Sueyoshi, K.; Nagai, H.; Wakida, S.; Nishii, J.; Kitagawa, F.; Otsuka, K. *Meas. Sci. Technol.* **2006**, *17*, 3154–3161.

[36] Jacobson, S. C.; Hergenröder, R.; Koutny, L. B.; Warmack, R. J.; Ramsey, J. M. *Anal. Chem.* **1994**, *66*, 1107–1113.

[37] Jacobson, S. C.; Koutny, L. B.; Hergenröder, R.; Moore, A. W. Jr.; Ramsey, J. M. *Anal. Chem.* **1994**, *66*, 3472–3476.

General Conclusion and Future Perspectives

Novel applications of LVSEP have been investigated to achieve the high sensitivity, high resolution, and simple experimental procedure simultaneously in CE and MCE. The application of tr-trapping to the analysis of hydrophilic amino acids is also performed as a challenge to achieve high-speed and high-resolution analysis in CE/MCE.

In the Chapter 2, the improvement of sensitivity, simplification of channel geometry, and the elimination of the conventional complicated voltage regulation for the fluidic control were achieved by coupling LVSEP with MCE. The minimized reduction in the resolution was theoretically and experimentally studied. At least 90% of the whole channel length could be utilized for the effective separation supporting the high resolution of LVSEP-MCE. Finally, the oligosaccharide analysis by LVSEP-MCZE was carried out. Up to 2,900-fold sensitivity increases were achieved with the simplified experimental conditions in the analyses of glucose ladder and glycans obtained from bovine ribonuclease B. These results indicated the extended potential of MCE for more practical analysis requiring high sensitivity, high resolution, and high throughput.

In the Chapter 3, LVSEP was combined with CE for the high performance analysis of oligosaccharides. The practical property of LVSEP was mainly studied in this chapter, such as the limitation of conductivity of the SM, the inversion timing of the sample migration, and the reduction in the separation performance. Up to 100 μS/cm of the conductivity in the SM was acceptable for the successful LVSEP-CZE analysis, so that the sample purified through the gel filtration column could be analyzed without further dilution with low conductivity water. The inversion timing in the LVSEP-CZE analysis

was able to be distinguished by observing the timing of a drastic increase in the electric current. By correcting the detection time with subtraction by the inversion timing, the RSD of the detection time was improved to less than 0.1%. Although around 95% of the effective separation length was considered to be maintained in LVSEP-CZE, the resolution was worsened due to the band broadening mainly caused by the molecular diffusion in the concentration stage. Hence, the strategy of suppressing the diffusion such as an addition of a gel reagent into the BGS is expected to be effective to improve the resolution. By adding poly(ethyleneoxide), actually, it was found that the resolution and the peak shape were well improved. Finally, up to 770-fold sensitivity increases were achieved in the analyses of the glycans obtained from three glycoproteins, indicating the high performance of LVSEP-CZE for real oligosaccharides samples.

In the Chapter 4, the combination of LVSEP with several chiral separation modes using CDs was studied both theoretically and experimentally, not only to realize the high performance enantioseparation but also to confirm the versatile applicability of LVSEP to many separation modes in CE. The separation performance was considered theoretically by focusing on the inversion position of the sample migration. As the result, it was found that the separation performance was slightly reduced when $\mu_{ep,eff}$ in the BGS was larger than that in the SM. In the LVSEP-CDMEKC, actually, the resolution was reduced in the analysis of Arg with the most increasing $\mu_{ep,eff}$ in the BGS. In the LVSEP-CDCZE/CDEKC/CDMEKC analyses of chiral compounds, up to 1,300-fold sensitivity increases were achieved. A C_{18} SPE desalination was also shown to be useful for the sample pretreatment of LVSEP-CDCZE analysis, where ibuprofen spiked in urine was successfully analyzed without diluting sample with low conductivity water.

In the Chapter 5, the applicability of LVSEP, which had been limited to the anion

analysis, was extended to cation analyses. Since the EOF should be reversed toward the anode in the LVSEP-CE analysis of cations, slightly positive-charged surface modifiers, PVA+PAA, PAA-ran-PMPC, and DODAB+POES, were employed. In these capillaries, it was shown that the EOF toward the anode was generated, which was fundamentally slow but quite fast only in the low *I* BGS. These EOF characteristics were quite suitable for the LVSEP concentration of cationic analytes and also for the following separation stage. In all capillaries, LVSEP-CZE analyses of aromatic amines were successfully carried out with up to 750-fold sensitivity increases compared to conventional CZE.

In the Chapter 6, tr-trapping of less hydrophobic compounds were carried out by supplying the hydrophobicity to the analytes by the derivatization with a hydrophobic BODIPY dye. Hydrophilic amino acids, Leu, Ile, Val, and Phe, were successfully labeled with the BODIPY dye. The retention factors to the SDS micelle were drastically increased, indicating the successful attachment of the hydrophobicity to each analyte. By employing tr-trapping to CE, up to 125-fold sensitivity increases were achieved in the analysis of the BODIPY-labeled amino acids. In the tr-trapping-MCE analysis, up to 160-fold sensitivity improvements were also obtained within 30 s, indicating the high performance and wide applicability of tr-trapping.

The application of LVSEP significantly simplified the CE/MCE system with increasing the sensitivity without loss of the resolution. The high-performance LVSEP-MCE with the highly-simplified experimental system did not only contribute to the improvement of the MCE performance but also gave a great impact on the current MCE studies. The author believes that both the sensitivity and simplicity will soon be a big trend among the researchers studying MCE, strongly pushing the improvement of

actual utility in MCE. It was also shown that LVSEP-CE has a wide applicability for the analysis of both cations and anions in several separation modes, indicating the practical utility of LVSEP-CE for many analytes. However, the development of the "next generation" electrophoresis with high performance and simple operation has not been accomplished in terms of the following problems: an unconfirmed applicability in LVSEP-MCE, difficult integration of LVSEP with MS detection, unclear vision of LVSEP-MCE for μTAS, and limited applicability of LVSEP to ionic analytes. For the further progress in LVSEP, therefore, the author starts studies on the following four issues: extension of the applicable analytes and separation modes in LVSEP-MCE, combination of LVSEP with MS detection, integration of LVSEP-MCE with other chip functions, and development of LVSEP-like methods using different concentration mechanisms.

First, as in the Chapter 5, the analyses of both anionic and cationic compounds are carried out with several separation modes in MCE. The author considers that such the versatile applicability of LVSEP-MCE will soon be confirmed and actually contribute to many analytical fields as the high-performance and simple-operation analytical method with a simple-designed microchannel.

Second, to improve the practical utility of LVSEP-CE/MCE, the combination with MS detection is also studied. In the principle of LVSEP, the BGS in the outlet vial must be introduced into the capillary by the EOF, conflicting with the open end of the capillary outlet in the CE/MCE-MS system. Hence, the author has conceived of an idea to employ the sheath liquid as the introduced BGS in the LVSEP process. So far, the LVSEP-CE-MS analysis has been successfully performed. Studies along this line are now in progress to achieve the high performance oligosaccharide analysis with an

ability to confirm the molecular structure of the analytes.

Third, for realizing the high-performance and simple-operation μTAS, the combination of LVSEP with other functions such as the sample derivatization, purification, and another separation mode is also studied. As a fundamental study, the combination of LVSEP-MCZE with other separation modes like microchip GE (MCGE) is investigated to achieve a simple and sensitive two-dimensional separation of biomolecules such as DNA and proteins. So far, the LVSEP-MCZE-MCGE analysis of DNA has been successfully carried out. Studies on LVSEP-two-dimensional separation are now in progress to develop the simple-operation and high-performance proteomic analytical method. The combination of LVSEP with sample derivatization and purification will also be investigated in the near future.

Fourth, on the basis of the same concept of LVSEP, the author is developing another simple-operation and high-performance MCE system employing a sample concentration mechanism different from FASS. As with the relationship between HPLC and CE, MCE must have higher performance, versatility, and simplicity to supersede the conventional methods. Although simplicity and high performance have been proved in this thesis, applicability of LVSEP has been limited to ionic analytes due to its concentration mechanism, FASS. To extend the versatility, therefore, the author focuses on the development of similar concentration methods based on other concentration mechanisms like sweeping. The author anticipates that development of the analytical methods with both high performance and simple operation will be the strong trend in the μTAS researches in the near future.

In terms of tr-trapping, the applicability was extended to the hydrophilic analytes

with excellent resolution in CE/MCE, which indicated the potential not only of tr-trapping but also of all the partial filling techniques for difficult analyses requiring extremely high resolution and rapid analysis time. As in the case of LVSEP, the combinations of tr-trapping with MS detection and with several separation modes like CDEKC are also being studied to confirm further versatility of tr-trapping. Since some mechanisms of tr-trapping are still unclear, it should be also important to complete the theoretical model of tr-trapping. The author is also conceiving an idea to apply partial filling techniques to other online concentration mechanisms such as FASS and dynamic pH junction to develop wide variety of novel methods with an excellent resolution and rapid analysis time. The author believes that the new application of the partial filling techniques will lead to the development of novel analytical techniques like tr-trapping.

In conclusion, obtained findings throughout this thesis and the following studies will significantly contribute to the progress in CE/MCE for the higher performance electrophoresis with the high sensitivity, high resolution, high speed, and simple experimental system. The author believes that this thesis will be a milestone for the "next generation" high-performance microscale electrophoresis, which should contribute to the whole analytical sciences and its applicable areas including medicine, pharmacy, biology, chemistry, and agriculture.

List of Publications

Chapter 2. “Microchip Electrophoresis of Oligosaccharides Using Large-volume Sample Stacking with an Electroosmotic Flow Pump in a Single Channel”, Takayuki Kawai*; Kenji Sueyoshi; Fumihiko Kitagawa; Koji Otsuka, *Analytical Chemistry*, **2010**, *82*, 6504–6511.

Chapter 3. “Highly Sensitive Oligosaccharide Analysis in Capillary Electrophoresis Using Large-volume Sample Stacking with an Electroosmotic Flow Pump”, Takayuki Kawai*; Masato Watanabe; Kenji Sueyoshi; Fumihiko Kitagawa; Koji Otsuka, *Journal of Chromatography A*, in press.

Chapter 4. “Highly Sensitive Chiral Analysis in Capillary Electrophoresis with Large-volume Sample Stacking with an Electroosmotic Flow Pump”, Takayuki Kawai*; Hiroshi Koino; Kenji Sueyoshi; Fumihiko Kitagawa; Koji Otsuka, *Journal of Chromatography A*, in press.

Chapter 5. “Microscale Electrophoresis of Cationic Compounds in a Single Channel Using Large-volume Sample Stacking with an Electroosmotic Flow Pump”, Takayuki Kawai*; Jun Ito; Kenji Sueyoshi; Fumihiko Kitagawa; Koji Otsuka, in preparation.

Chapter 6. “Hydrophobic Labeling of Amino Acids: Transient Trapping–Capillary/Microchip Electrophoresis”, Kenji Sueyoshi*; Kota Hashiba; Takayuki Kawai; Fumihiko Kitagawa; Koji Otsuka, *Electrophoresis*, **2011**, *32*, 1233–1240.

Related Publication. “Recent Progress of On-line Sample Preconcentration Techniques in Microchip Electrophoresis”, Fumihiko Kitagawa*; Takayuki Kawai; Kenji Sueyoshi; Koji Otsuka, *Analytical Sciences*, in press.

List of Oral Presentations in International Conferences

1. “Microchip Electrophoresis of Oligosaccharides with Large-volume Sample Stacking with Electroosmotic Flow Pump in Single Channel”, Takayuki Kawai*; Kenji Sueyoshi; Fumihiko Kitagawa; Koji Otsuka, 2010 International Chemical Congress of Pacific Basin Societies (PACIFICHEM 2010), Honolulu, USA, 16 December 2010.

2. “Highly Sensitive Chiral Analysis in Capillary Electrophoresis Using Large-volume Sample Stacking with Electroosmotic Flow Pump”, Takayuki Kawai*; Jun Ito; Kenji Sueyoshi; Fumihiko Kitagawa; Koji Otsuka, 26th International Symposium on Microscale Bioseparations (MSB 2011), San Diego, USA, 3 May 2011.

3. “Highly Sensitive Chiral Analysis by Capillary Electrophoresis Using Large-volume Sample Stacking with Electroosmotic Flow Pump”, Takayuki Kawai*; Jun Ito; Kenji Sueyoshi; Fumihiko Kitagawa; Koji Otsuka, IUPAC International Congress on Analytical Sciences 2011 (ICAS2011), Kyoto, 25 May 2011.

4. “Toward 10,000-fold Sample Preconcentration Efficiency for Oligosaccharide Analysis in Capillary Electrophoresis”, Takayuki Kawai*; Masumi Ueda; Kenji Sueyoshi; Fumihiko Kitagawa; Koji Otsuka, 37th International Symposium on High Performance Liquid Phase Separations and Related Techniques (HPLC 2011 Dalian), Dalian, China, 11 October 2011.

5. “Toward 10,000-fold Sensitivity Improvement in Capillary Electrophoresis of Oligosaccharide”, Takayuki Kawai*; Masumi Ueda; Kenji Sueyoshi; Fumihiko Kitagawa; Koji Otsuka, 11th Asia-Pacific International Symposium on Microscale Separations and Analysis (APCE 2011), Hobart, Australia, 29 November 2011.

List of Awards

1. MSB 2008 Travel Grant, "Sensitivity Enhancement by Thermal Lens Microscope Detection in Electrophoretic Analysis of Sugar Chains", Takayuki Kawai*; Fumihiko Kitagawa; Koji Otsuka, 23rd International Symposium on Microscale Bioseparations (MSB 2008), Berlin, Germany, 9 March 2008.

2. HPLC 2009 Halász Award, "Highly Sensitive Analysis of Sugar Chains in Capillary Electrophoresis", Takayuki Kawai*; Fumihiko Kitagawa; Koji Otsuka, 34th International Symposium on High Performance Liquid Phase Separations and Related Techniques (HPLC 2009), Dresden, Germany, 28 June 2009.

3. Best Presentation Award for Most Incentive Study, "Sensitivity Enhancement in the Analysis of Oligosaccharides in Capillary/Microchip Electrophoresis", Takayuki Kawai*; Kenji Sueyoshi; Fumihiko Kitagawa; Koji Otsuka, ASTEM Meeting of Young Scientists and Engineers on Bioanalysis and Bioreagents, Kyoto, 10 March 2010.

4. Best Poster Award, "Highly Sensitive Chiral Analysis of Pharmaceutical Drugs in Capillary Electrophoresis", Takayuki Kawai*; Kenji Sueyoshi; Fumihiko Kitagawa; Koji Otsuka, The 4th Summer Seminar of Kinki Branch, JSAC, Osaka, 10 August 2010.

5. PACIFICHEM 2010 Student Poster Award, "Microscale Electrophoresis of Oligosaccharides Using Large-volume Sample Stacking with Electroosmotic Flow Pump", Takayuki Kawai*; Kenji Sueyoshi; Fumihiko Kitagawa; Koji Otsuka, 2010 International Chemical Congress of Pacific Basin Societies (PACIFICHEM 2010), Honolulu, USA, 16 December 2010.

6. MSB 2011 Travel Grant, “Highly Sensitive Chiral Analysis in Capillary Electrophoresis Using Large-volume Sample Stacking with Electroosmotic Flow Pump”, Takayuki Kawai*; Jun Ito; Kenji Sueyoshi; Fumihiko Kitagawa; Koji Otsuka, 26th International Symposium on Microscale Bioseparations (MSB 2011), San Diego, USA, 1 May 2011.

7. JAIMA 2011 Poster Presentation Award, “Toward 10,000-fold Sensitivity Enhancement for Oligosaccharide Analysis in Capillary Electrophoresis. 2”, Takayuki Kawai*; Masumi Ueda; Kenji Sueyoshi; Fumihiko Kitagawa; Koji Otsuka, JAIMA Discussion on Analytical Science and Technology 2011, Tokyo, 8 September 2011.

8. Outstanding Lecture Award for Young Scientists, “Toward 10,000-fold Sensitivity Enhancement in Electrophoretic Analysis of Oligosaccharides”, Takayuki Kawai*; Masumi Ueda; Kenji Sueyoshi; Fumihiko Kitagawa; Koji Otsuka, 60th Annual Meeting of JSAC, Nagoya, 14 September 2011.

9. PSC Young Scientist Lecture Award (Level 1), “Toward 10,000-fold Sample Preconcentration Efficiency for Oligosaccharide Analysis in Capillary Electrophoresis”, Takayuki Kawai*; Masumi Ueda; Kenji Sueyoshi; Fumihiko Kitagawa; Koji Otsuka, 37th International Symposium on High Performance Liquid Phase Separations and Related Techniques (HPLC 2011 Dalian), Dalian, China, 11 October 2011.

Acknowledgments

Present studies have been carried out under the supervision of Prof. Koji Otsuka in Department of Material Chemistry, Graduate School of Engineering, Kyoto University. The author would like to express his sincere gratitude to Prof. Otsuka for his invaluable advices, suggestions, and continuous encouragement throughout this study.

The author wishes to express his gratitude to Prof. Katsuhisa Tanaka and Prof. Seijiro Matsubara for their valuable comments and discussions.

Numerous helpful comments and advices were provided from Dr. Fumihiko Kitagawa and Dr. Kenji Sueyoshi in Otsuka Lab. The author wishes to express the deep and sincere appreciation for their invaluable guidance and assistance.

The author appreciates the strong support for the microchip fabrication from Dr. Shin-ichi Wakida, Dr. Yoshihide Tanaka, Dr. Hidenori Nagai, Dr. Takashi Miyado, and Ms. Nahoko Naruishi of Health Research Institute, National Institute of Advanced Industrial Science and Technology.

The author is thankful for Research Fellowships of the Japan Society for the Promotion of Science for Young Scientists.

In Otsuka Lab, the author thanks the secretary Ms. Yoko Osaka for her continuous cooperation and encouragement. The author also thanks the students, Ms. Saeko Kinami, Mr. Hiroshi Koino, Mr. Jun Ito, Mr. Masato Watanabe, Mr. Kota Hashiba, and all other members for their cooperation and friendship.

Finally, the author greatly acknowledges the invaluable supports, encouragements, and understandings from his family, Dr. Takao Kawai, Mrs. Yoko Kawai, Ms. Tomoko Kawai, and Ms. Azusa Kawai, and also from his best friends Mr. Taro Ohta and Ms. Risa Kusumoto.

Takayuki Kawai